THE DESIGN AND SYNTHESIS OF HIGH PERFORMANCE POLYOLEFINS FOR USE IN ALKALINE ANION EXCHANGE MEMBRANE FUEL CELLS

A Dissertation

Presented to the Faculty of the Graduate School

of Cornell University

In Partial Fulfillment of the Requirements for the Degree of

Doctor of Philosophy

by

Henry Aloysius Kostalik IV

August 2011

THE DESIGN AND SYNTHESIS OF HIGH PERFORMANCE POLYOLEFINS FOR USE IN ALKALINE ANION EXCHANGE MEMBRANE FUEL CELLS

Henry Aloysius Kostalik IV, Ph.D.

Cornell University 2011

Fuel cells are devices that convert the chemical energy stored in a fuel directly into electricity and have the potential to serve as a highly efficient and environmentally sustainable power generation technology for stationary and mobile applications. Within a fuel cell, the polymer electrolyte membrane serves as the ion conducting medium between the anode and cathode, making it a central, and often performance-limiting component of the fuel cell. The most common polymer electrolyte membrane fuel cells operate under acidic conditions and are therefore proton conducting. Although proton exchange membrane (PEM) fuel cells are well developed and can offer excellent performance, they rely almost exclusively on platinum, a very expensive and scarce noble metal. This dependence on platinum has severely hindered wide scale commercialization of PEM fuel cell technologies. By comparison, alkaline fuel cells that employ hydroxide conducting alkaline anion exchange membranes (AAEMs) are relatively unexplored. A major advantage of alkaline fuel cells, when compared to acidic fuel cells, is their enhanced reaction kinetics for oxygen reduction, permitting the use of less costly, non-noble metal catalysts (e.g. Ni). Therefore, high performance AAEMs could significantly advance fuel cell technologies.

We have been working to develop new polymeric materials that can serve as effective AAEMs. Prior work in this area has mainly focused on re-engineering

existing materials to access AAEMs. In contrast, we approached this problem from a synthetic perspective by designing and synthesizing materials from the ground up.

Herein, the synthesis of two separate AAEM systems that are synthesized via ring-opening metathesis polymerization are described. The first route involves the copolymerization of a tetraalkylammonium-functionalized norbornene with dicyclopentadiene. The crosslinked thin films generated are mechanically strong and exhibit exceptional methanol tolerance. The second route involves the synthesis of a solvent processable, tetraalkylammonium-functionalized polyethylene for use as an AAEM. The membranes are insoluble in both pure water and aqueous methanol but exhibit excellent solubility in a variety of other aqueous alcohols. These solubility characteristics extend the utility of this system for use as both an AAEM and ionomer electrode material from a single polymer composition. The AAEMs generated are mechanically strong and exhibit high hydroxide conductivities.

Lastly, we have developed a standardized procedure for measuring the alkaline stability of a benzyltrimethylammonium (BTMA) model compound and a BTMA functionalized polyethylene. The procedure is broadly applicable and should serve as a testing method to better understand other systems, specifically those based on novel cations. Applying this procedure should facilitate the discovery of AAEMs with increased base stability, thus enabling high temperature AAEM fuel cell operation.

BIOGRAPHICAL SKETCH

Henry Aloysius Kostalik IV was born on January 12th 1983 to parents Nancy and Hank Kostalik. Henry began his early life in Calumet City, Illinois, where his many fond memories include playing "workerman" in his backyard with Sam, the family dog. During this time, Henry rarely talked, an issue that caused his parents great concern. After a year of speech therapy and other special classes, however, Henry finally found his voice, although he still seldom spoke more than just a few sentences at a time. During these years Henry was very fortunate to have several people other than his adoring parents who took a special interest in him. Most memorable was his Grandma Doris, who often spent hours and hours playing with him, usually allowing Henry to build elaborate forts using all the cans of food and bedroom sheets to be found in her house. After four joyful years in Illinois, the family moved to Minnesota after Henry's dad, who worked for the railroad, was transferred.

Upon arriving in Minnesota Henry noticed one significant difference from his former city: lots and lots of snow! Henry adjusted quickly to Minnesota, a process that was helped greatly by his involvement in Cub Scouts and sports (football, baseball, basketball and soccer, to name a few). Even though he was still enrolled in special classes for reading and writing, he quickly learned that he was pretty good at math. After winning every multiplication minute competition while in the second grade, his teacher recommended that he be enrolled in advanced classes for math. Around this time, he started learning about science and instantly fell in love.

While in middle and high school, Henry established himself as a slightly above average student; he was only slightly above average mostly because his study habits were non-existent. This was not entirely due to laziness; he was just more interested in other pursuits, namely playing and watching sports. (Go Chicago White Sox and

Bears!). This all changed during his junior year of high school when he took his first chemistry class. Even though he found chemistry quite interesting, he didn't study and received a B- for the semester. At the start of the next semester his chemistry teacher, Mr. Trenda, pulled him aside and told him he better "stop messing around and start fucking trying." With the impetus of this R-rated piece of advice, Henry received an A+ that semester. Thanks Mr. Trenda! At this point Henry realized that school became much easier when he actually read the textbooks and from that point on he began to earn much higher grades. Two of his medical instructors in high school, Ms. Lange and Mr. Tom, were critical in mentoring him during this stage in his life, and with their assistance, he decided that he was going to pursue a career as a doctor. When the time came to apply to college, Henry applied to only one: the University of Minnesota Duluth (UMD). He was accepted during the spring of 2001!

Henry started his college career at UMD in the fall of 2001. He entered UMD as a pre-med student and due to his new study habits, he finished with the top grades in his classes more often that not. Consequently, he was awarded a full academic scholarship from the Jim Swenson family after his second year. At this time, he chose to double major in Chemistry and Biochemistry & Molecular Biology and started undergraduate research in Professor John Evans' laboratory. Overall, Henry felt quite fortunate that he was getting paid to do something that he considered to be more of a fun hobby. From this point on, Henry was torn between pursuing either a M.D/Ph.D. or a Ph.D. in Chemistry. On one fortuitous April morning during his fourth year, he woke up (after drinking copious amounts of coffee) and immediately knew that he was going to pursue a Ph.D. in Chemistry. Regardless of this decision, he still maintains the notion that he would have made a fantastic doctor. Later that summer he met Amanda "Mandy" Chial (a student in the section) while working as a quantitative

analysis laboratory teaching assistant. Unfortunately, Mandy was late to the first laboratory session and, to make matters worse, was wearing sandals. Furthermore, she was noticeably irritated when he informed her that sandals were not proper laboratory footwear (those who know Henry no doubt find his reprimand of Mandy's sandals amusing and hypocritical). Even though their first meeting was a bit frosty, they began dating later that summer (after lab was over, of course) and eventually fell in love. Henry proposed on July 12th, 2008, and they plan to marry this summer, on July 23rd, 2011. In June 2006 Henry graduated *magna cum laude* with a B.S. in Chemistry and Biochemistry & Molecular Biology with a minor in Philosophy from UMD and became the first person in his family's history to graduate from college.

In July 2006 Henry moved to Ithaca, NY to begin graduate school at Cornell University. During his first two semesters at Cornell, Henry took a number of courses with Professors Tyler McQuade, Dotsevi Y. Sogah, Peter T. Wolczanski, Geoff W. Coates and Jon T. Njardarson. He served as a teaching assistant for four semesters, starting with an Organic Chemistry lecture course and moving on to a one-semester Organic Chemistry laboratory course and finishing with a General Chemistry lecture course. In late 2006, Henry joined the research group of Professor Geoffrey W. Coates and began work on the development of alkaline anion exchange membranes. As he works toward completing his degree, he looks forward to moving back to Minnesota with Mandy and Frankie (the couple's miniature dachshund) and beginning his career as a research scientist at 3M, where he will be working on developing next generation lithium ion battery materials.

“Cogito ergo sum”

-René Descartes

ACKNOWLEDGMENTS

Earning a Ph.D. in chemistry from Cornell University would not have been possible without the love and support of so many incredible people, and for that I am extremely grateful.

I have Professor John Evans at the University of Minnesota Duluth to thank for lighting my scientific fire and passion for the discipline. I began undergraduate research with him in the spring of 2003 and continued until graduation. We worked towards synthesizing polymers for biomedical applications through the use of plasma polymerization. At some point during the many hours we spent together in class, the lab and at his home, I learned that I was able to make important scientific contributions and the patience he had with me while I came to this realization is truly remarkable. Visits back to Duluth are never complete without discussing science and life over a few pints of Brewhouse beer with John.

While at Cornell University there have been countless people who were instrumental to my success. First and foremost is my research advisor, Professor Geoff Coates. During the summer preceding my graduation from UMD, I spent many hours searching for research that appealed to me. On one lucky afternoon I came across the Coates group website, and I knew right then and there I wanted to work for Geoff. I immediately emailed him expressing my interest and was astonished when he replied within a couple of hours. The rest is history. Besides proposing to Mandy, joining Geoff's group has been the best decision of my life. Geoff's ability to combine great science with real world application is remarkable. I am grateful that he provided me the freedom to pursue my own ideas and also offered me a great deal of guidance when I needed it. Best of all, he was always there for me when I needed support, both personal and scientific. He also created an exciting environment in which to work

(what other professor lets their students sleep in his barn?) and I will dearly miss all the Coates group parties. Although I am saddened that I will no longer have the privilege of working for Geoff, I look forward to continuing our relationship.

I am also grateful to Professors Héctor Abruña and Dotsevi Sogah for taking the time to serve on my committee. I had the pleasure of learning many of the fundamental polymer chemistry principles from Professor Sogah while taking his course. Furthermore, I enjoyed serving as his teaching assistant and listening to his entertaining lectures. I was also fortunate to have the opportunity to work in collaboration with Professor Abruña on the alkaline anion exchange membrane fuel cell project. He is a source of immense knowledge and has been crucial in aiding us in developing a new research area for the Coates group. His knowledge and vision of energy technology is second to none, and the starting up of both the Cornell Fuel Cell Institute and the Energy Material Center is a source of great inspiration for me. Dr. Paul Mutolo has been a significant help throughout the course of my graduate work and was always there to guide and assist me in any way that he could. Additionally, Eric Rus was extremely helpful and is one of the smartest people I have ever met. I thoroughly enjoyed traveling with him to both Indiana and Washington D.C. and I wish him the best of luck in his future pursuits.

In the Coates group, I have had the opportunity to work with so many talented people. As members of my first year class, Bryan Whiting and Pete Widger made the graduate school transition much less painful and I was lucky to have such great roommates. Pete is a talented and driven scientist and I wish him well at E Ink. Bryan has been a great friend throughout my graduate career. Bryan's depth of knowledge in nearly every subject area known to man is unmatched by anyone I have ever met, and he's also a pretty good dancer to boot. I have no doubt he'll be a fantastic professor

and I wish him the best of luck at Trinity University. After joining the group I am thankful that Dr. Ryan Jeske and Dr. Greg Domski took the time to answer my endless questions. Once Syud "Taz" Ahmed joined the 565 crew, things became much more entertaining and we quickly became work spouses. If there were to ever be a competition for who knows the most people at Cornell, Taz would win hands down. I know neither one of us will ever forget (for different reasons, however) the day the Chicago Bears traded for Jay Cutler; what a day! In fact, I have never met anyone who had such a great, nearly photographic memory for recalling events and I know he will have a successful career at whatever he chooses to do. And then there's the enigma that is Pasquale Iacono. I have never met anyone like Pasquale in my life; there is no one else who is as hugely talented in so many different areas. From chemistry to sports to music, he is truly remarkable, and as much as it pains for me to admit, he did beat me (just barely) in the great 40-yard dash contest of 2009. I am also thankful that he regularly took us back to his hometown of Binghamton, NY, the land of cheap and plentiful Long Island Ice Teas. I am holding out hope that he and Heather decide to move to Chicago so that they can experience the best city in the world and I can have another reason to visit. I would also like to thank Angie DiCiccio who was a constant source of happiness. Additionally, Rachna Khurana is a new addition to the newly formed energy materials subgroup, and I know she will have a very successful graduate career. Dr. Brian Long has been a great source of motivation. I really appreciate him letting me bounce numerous ideas off of him and I wish him well as he moves to the University of Tennessee to begin his career as an assistant professor. Lastly, Kelly Case has been a source of great help in a number of different areas. It's too bad she's a Yankees fan, though!

Dr. Nick Robertson, Dr. Tim Clark and Dr. Kevin Noonan have been great teammates in developing the fuel cell project. When I began in the lab, Nick had just started the project and, though I didn't realize this at the time, he had a really tough task ahead of him. I am very grateful that he had the patience to train me, especially considering my many screw-ups. I have no doubt that Nick will continue to prosper at Northland College. When Tim Clark joined the group, the three of us really started to make progress. If Tim had never teamed up with us, I have no doubt that we would have had a much tougher time making progress. Tim is one of the most intelligent people that I know and was a fantastic mentor towards me in so many ways; I am fortunate that he helped me develop into the scientist that I am today. I look forward to visiting him in Toronto in the near future. When Kevin "Phosphorus" Noonan joined the group, it quickly became clear that he was a welcome addition both in and out of the lab. Initially, he started working on another project in the group, but we got to know each other quite well outside of the lab, mostly at The Chapter House, Stella's and Pixel (men!). Once he decided to join the fuel cell project, we teamed up and started working on developing increased base stable alkaline anion exchange membranes. We pushed each other (often by screaming at each other) to be the best that we could be. Needless to say, we fought a lot and had a lot of fun doing it. Overall, Kevin has been a pleasure to work with and without him we wouldn't be where we are today. Kevin is one of the most inquisitive scientists I have ever met and I think that we really complement each other quite well. I wish Kevin the best of luck at Carnegie Mellon and I look forward to visiting him.

I would also like to thank Julie Longo, a former REU student, who spent a summer working on her contributions to the project. She is incredibly bright and hard working and has a glimmering future ahead of her. I wish her the best of luck as she

starts her graduate studies at Cornell. Also, the newest member of the fuel cell team, Kristina Hugar, joins at an exciting time and I know she has the ability to move the project into the next phase.

Finally, I need to thank a number of my collaborators and funding agencies. I am especially grateful for the help given to me by Professor Lewis Fetters at Cornell. For three years, I was funded by the National Science Foundation under the IGERT fellowship and the Energy Materials Center at Cornell, for which I am very thankful. I am also grateful for the funding that I received from Sumitomo.

I am greatly indebted to my little Pop-Tart, Mandy, who had the courage to let me move halfway across the country to pursue my dreams. Life hasn't always been easy but she has always kept a positive attitude and provided me with exceptional support. I have never met such a caring person in my life and I love her more than words can express. I look forward to starting the rest of my life with her as my wife.

TABLE OF CONTENTS

LIST OF FIGURES

LIST OF SCHEMES

LIST OF TABLES

Chapter 1

A Brief Review of Fuel Cell Technology With a Focus on Alkaline Anion Exchange Membranes For Fuel Cell Applications

1.1 Introduction

As world demand for energy rapidly grows, transforming the way we generate, supply, transmit, store, and use energy will be one of the defining challenges for America and the globe in the 21st century.[1] At its core, this challenge is a scientific one and history has demonstrated that fundamentally new technologies arise through the collaboration of many different scientific disciplines. Today, many U.S. academic and industrial research programs aim to accelerate such discovery by utilizing the talents and creativity of our national scientific workforce. In a recent State of the Union Address, U.S. President Barack Obama highlighted the importance of increasing our investment in science and coined the innovation crisis that America currently faces as "our generation's Sputnik moment":

> Half a century ago, when the Soviets beat us into space with the launch of a satellite called Sputnik, we had no idea how we would beat them to the moon. The science wasn't even there yet. NASA didn't exist. But after investing in better research and education, we didn't just surpass the Soviets; we unleashed a wave of innovation that created new industries and millions of new jobs.
>
> This is our generation's Sputnik moment. Two years ago, I said that we needed to reach a level of research and development we haven't seen since the height of the Space Race. And in a few weeks, I will be sending a budget to Congress that helps us meet that goal. We'll invest in biomedical research, information technology, and especially clean energy technology an investment that will strengthen our security, protect our planet, and create countless new jobs for our people.[2]

In August 2009, the U.S. Department of Energy established 46 Energy Frontier Research Centers (EFRCs). These centers involve universities, national laboratories, nonprofit organizations and for-profit firms that were selected by scientific peer review. These integrated, multi-investigator centers conduct fundamental research focusing on several research challenges that were identified by the scientific

community. The purpose of these centers is to combine the talents and expertise of leading scientists with a setting designed to accelerate research toward meeting our critical energy challenges. The EFRCs will harness both basic and applied research in a concerted effort to establish the scientific foundation for a fundamentally new U.S. energy economy. The outcome will decisively enhance U.S. energy security and protect the global environment in the century ahead. Cornell University was designated as an EFRC and the newly established center was named the Energy Materials Center at Cornell (EMC^2). The mission of the EMC^2 is to advance the science of energy conversion and storage by understanding and exploiting fundamental properties of active materials and their interfaces with an emphasis on fuel cells and batteries.[3] This chapter exclusively focuses on fuel cell technology, specifically alkaline anion exchange membrane (AAEM) fuel cells.

1.2 History of fuel cell technology

Fuel cells are devices that convert the chemical energy stored in a fuel (e.g. hydrogen, methanol) directly into electricity and could potentially serve as a highly efficient and environmentally sustainable power generation technology.[4] Because fuel cells are electrochemical devices, they have a more efficient conversion process as chemical energy is converted directly to electrical energy. When compared to a traditional internal combustion engine (internal combustion engines are less efficient because they rely on the conversion of thermal to mechanical energy, which is limited by the Carnot cycle), a fuel cell can be two to three times more efficient with water as the only emission product when hydrogen is used as the fuel. As a result, tremendous

research efforts have been aimed towards the development of fuel cell technology for stationary and mobile applications. Despite the immense potential of fuel cells to supplant pre-existing technologies, barriers such as cost reduction, improved performance and enhanced durability remain before wide scale commercialization is realized.

The discovery of fuel cell technology can be traced back to 1839, when Sir William R. Grove carried out the inverse reaction of water electrolysis by using platinum electrodes, tubes filled with hydrogen and oxygen and sulfuric acid (Figure 1.1).[5] A fuel cell consists of three main components, an anode, a cathode and an ion conductive electrolyte. During fuel cell operation, fuel and oxidant streams are fed into the anode and cathode, respectively, with fuel oxidation occurring at the anode and oxygen reduction taking place at the cathode. Separating the fuel and oxidant

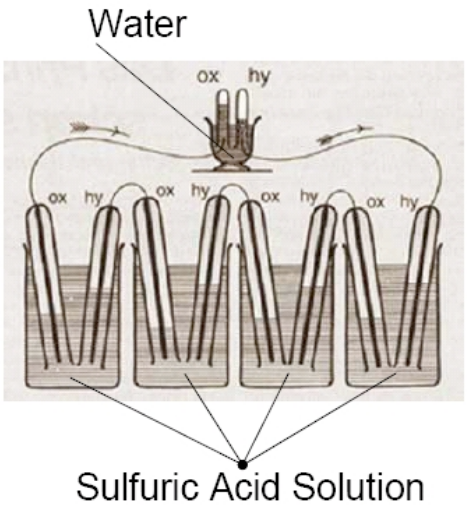

Figure 1.1. 1839 Grove fuel cell.

streams is the electrolyte, which facilitates the transport of ions between the anode and cathode. In recent years, fuel cells that use a solid polymer membrane as the electrolyte have received considerable attention due to their high efficiency, high power density and relatively low operating temperature.[6]

1.3 Proton exchange membranes for fuel cells

A high performance polymer electrolyte membrane fulfils several key requirements. It must efficiently transport ions between the anode and cathode, therefore a high ionic conductivity is required. The membrane must be electrically insulating and also act as an effective barrier toward the liquid and/or gaseous fuels. It must be chemically stable toward the oxidizing and reducing conditions within a fuel cell, in addition to being either acid or base stable. Lastly, it must be mechanically robust and maintain good dimensional stability over a broad range of temperatures and hydration states. Unfortunately, no current material fulfils all of these requirements, yet significant advances have been realized towards the ideal membrane.

The most common fuel cells, referred to as proton exchange membrane (PEM) fuel cells, operate under acidic conditions, use hydrogen as the fuel and have a solid polymer electrolyte separating the anode and cathode (Figure 1.2). The polymer electrolyte membrane serves as the ion conducting medium between the anode and cathode, and as a result is a central, and often performance-limiting component of the fuel cell.[7] PEM fuel cells were first developed by General Electric and used as a part of NASA's Gemini space program in the early 1960's. The PEM was based on a sulfonated polystyrene-divinylbenzene material, but it proved to be susceptible to

radical degradation. Nafion® a PEM, has since dominated the field due its good processability, chemical and thermal stability, and proton conductivity when properly hydrated (~110 mS/cm at 50 °C).[8,9] Nafion was discovered in 1962 by Dupont de

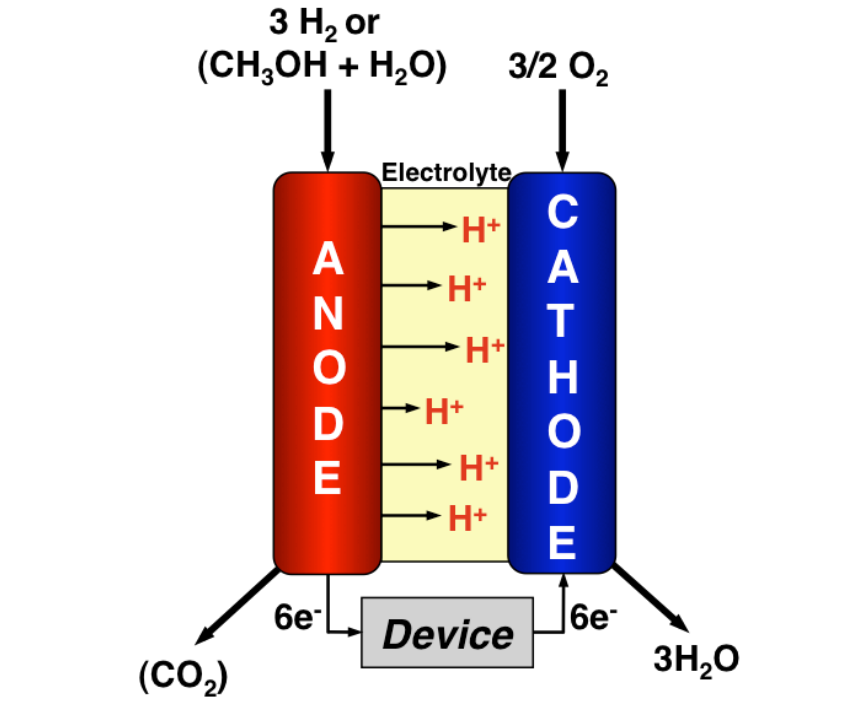

Overall:

(1) $CH_3OH + 3/2\ O_2 \rightarrow 2\ H_2O + CO_2$

(2) $3\ H_2 + 3/2\ O_2 \rightarrow 3\ H_2O$

Figure 1.2. Schematic for a polymer electrolyte fuel cell operating under acidic conditions.

Nemours and consists of a hydrophobic polytetrafluoroethylene backbone and hydrophilic perfluoroether side chains terminated by a sulfonic acid groups (Figure 1.3).[10] It is prepared by the free radical polymerization of tetrafluoroethylene and perfluorinated sulfonyl fluoride, followed by hydrolysis.[11] Although PEM fuel cells

offer excellent performance, they rely almost exclusively on platinum, a very expensive and scarce noble metal.[12] The reliance of PEM fuel cell technologies on platinum is perhaps the most significant hurdle to wide scale commercialization. Consequently, there has been increased interest in fuel cells operating under alkaline conditions.

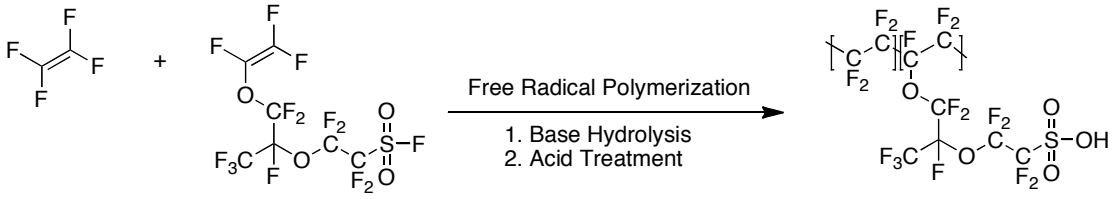

Figure 1.3. Synthesis of Nafion.

1.4 Alkaline fuel cells

A major advantage of alkaline fuel cells (AFCs), relative to acidic fuel cells, is their enhanced reaction kinetics for oxygen reduction permitting the use of less costly, non-noble metal catalysts (e.g. Ni)[13,14] AFC's use an aqueous solution of potassium hydroxide as the electrolyte, with typical concentrations of about 30%. In fact, alkaline fuel cells that use a liquid electrolyte are the best performing fuel cells that are operable below 200 ºC and were used by NASA for their Gemini and Apollo programs. Figure 1.4 shows the chemistry that occurs within an alkaline fuel cell. In this case, hydroxide ions are shuttled through the electrolyte from the cathode to the anode (opposite to the direction of the PEM fuel cell shown in Figure 1.2). Although the anode and cathode half reactions differ between alkaline and acidic operating conditions, the overall reactions are the same for both systems. Unfortunately, a main

limitation of AFCs is that the presence of carbon dioxide in either the fuel or oxidant can lead to the formation of insoluble carbonate species (hydroxide reacts with carbon dioxide forming potassium carbonate/bicarbonate) causing degrading fuel cell performance. The subsequent precipitation of potassium carbonate/bicarbonate can cause blockages between the anode and cathode while also mechanically disrupting and/or destroying the active layers. As a result, this has often limited AFCs to applications in which pure oxygen can be supplied.

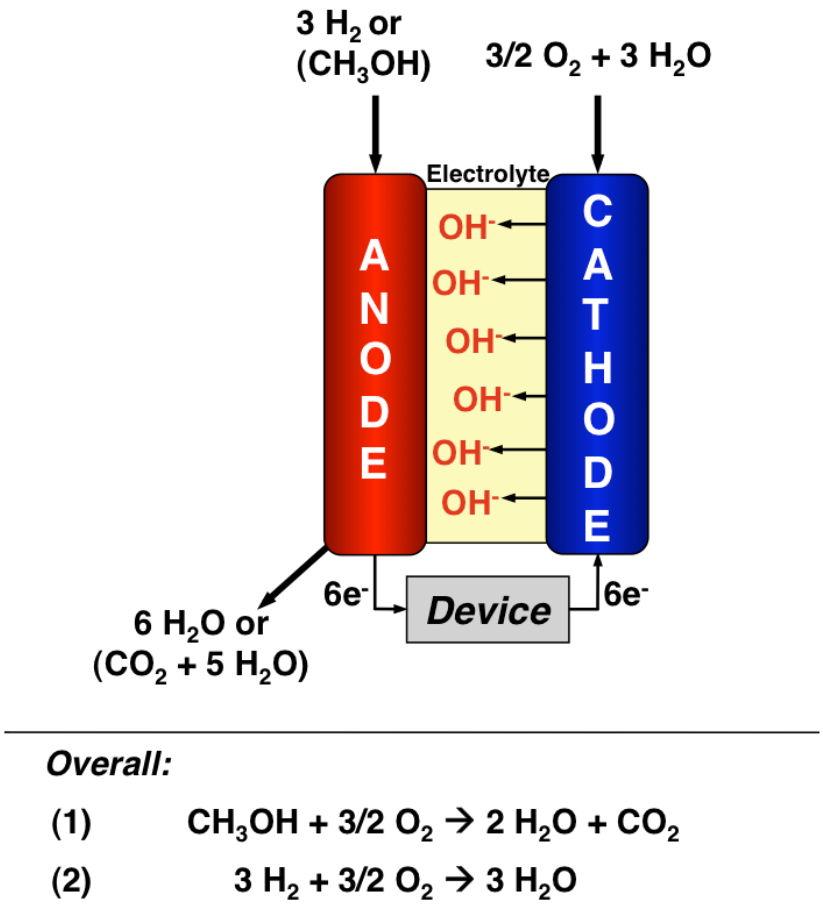

Figure 1.4. Schematic for a polymer electrolyte fuel cell operating under alkaline conditions.

1.5 Alkaline anion exchange membranes for fuel cells

As a result, there is now considerable interest in hydroxide conducting polymer electrolyte membranes, also known as AAEMs, for fuel cells operating under basic conditions.[15,16,17,18,19,20,21,22,23,24,25] Materials that have the cation covalently attached to a polymer backbone hold great promise as AAEMs because their cations cannot aggregate with anions to form a crystal lattice (Figure 1.5). Therefore, this approach enables fuel cell operation under alkaline conditions in the presence of carbon

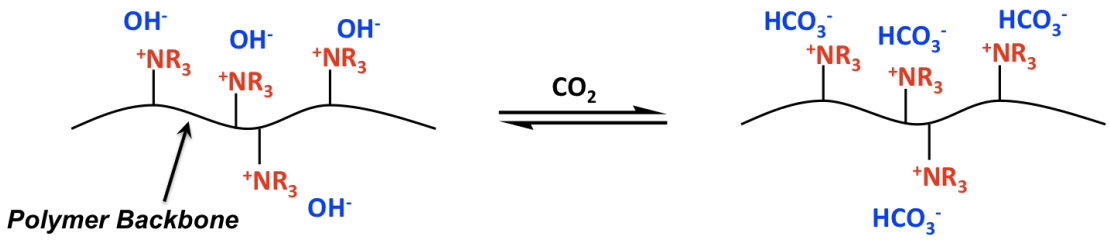

Figure 1.5. AAEMs prevent the precipitation of carbonate salts.

dioxide.[26] Additionally, the direction of hydroxide ion conduction opposes that of methanol crossover, thereby mitigating or eliminating this process. Recent developments reported by Varcoe, Slade and co-workers have shown that radiation grafting of poly(vinylbenzyl chloride) onto mixed fluorocarbon/hydrocarbon membranes, followed by amination, yields mechanically strong AAEMs (Figure 1.6) with promising hydroxide conductivities (34 mS/cm at 50 °C).[15] Others have reported

that polysulfones can act as scaffolds for successive post polymerization modification

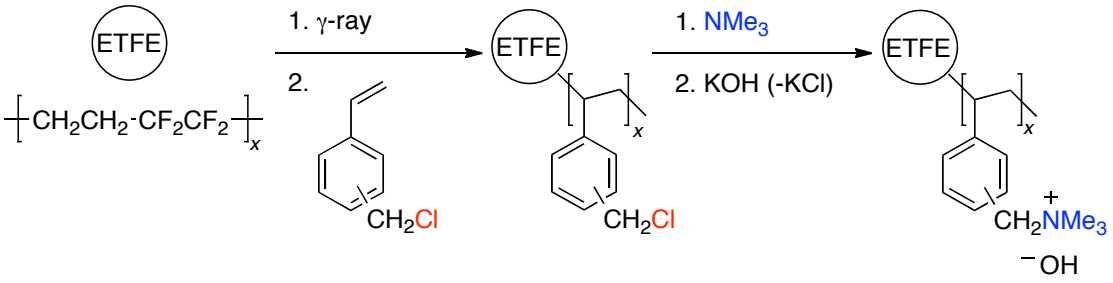

Figure 1.6. Radiation grafting of poly(vinylbenzyl chloride) onto mixed fluorocarbon/hydrocarbon membranes, followed by amination, yields mechanically strong AAEMs.[15]

reactions again yielding AAEMs (Figure 1.7) with reasonable conductivities (35 mS/cm at 30 °C).[12,16,17,18,19,20,21] Moreover, Cornelius and co-workers have shown that AAEMs based on a poly(phenylene) backbone (Figure 1.8) display impressive conductivities and alkaline stability (50 mS/cm).[22] These reports illustrate the

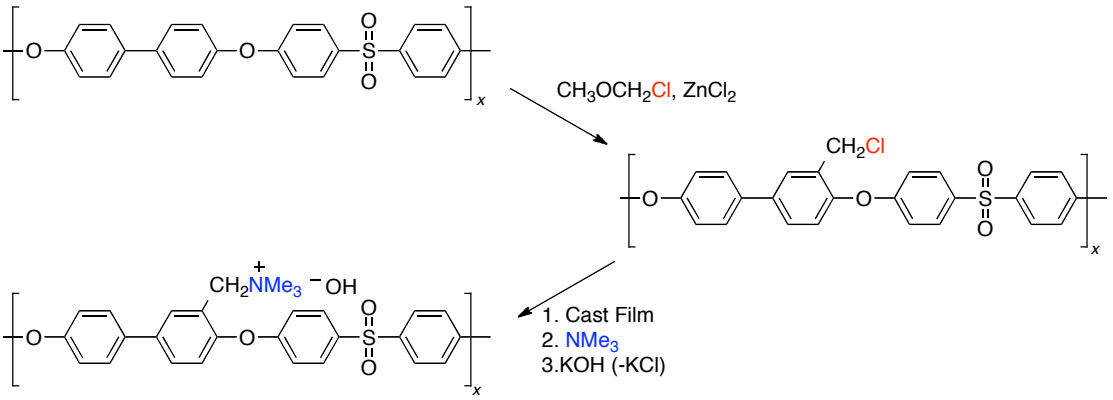

Figure 1.7. Polysulfones can act as scaffolds for successive post polymerization modification reactions yielding conductive AAEMs.[16]

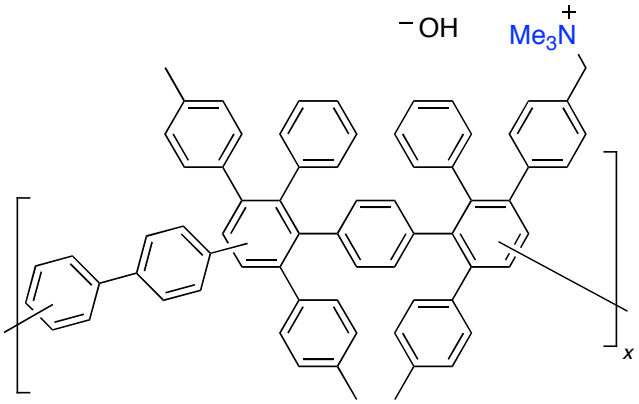

Figure 1.8. Polyphenylene-based AAEM.[22]

remarkable progress made in this area, but also reveal limitations in the synthetic approaches employed. For example, difficulty dissolving polymer samples and achieving quantitative conversions can prove challenging in postpolymerization reactions, while the use of γ irradiation and fluorinated materials may limit the utility in the case of the former. When one considers that the mobility of protons is inherently faster than that of hydroxide ions in dilute solution by a factor of 1.77,[16] it is encouraging that the aforementioned AAEMs display respectable conductivities and highlights the importance of having continuous ionic domains throughout the material to provide pathways for ionic conduction. This requirement is supported by a recent study by Schmidt-Rohr and Chen of the relationship between the conductivity and morphology of Nafion.[27] Their findings suggest that microphase separation leads to hydrophobic regions that provide mechanical support for the material and hydrophilic regions with ionic nanochannels that provide a pathway for proton conduction. While all of these systems demonstrate great promise for AAEM science and establish the feasibility of alkaline membranes, conductivity improvements are still necessary to

reach performances comparable to present PEM technologies (e.g. Nafion-117, 112 mS/cm at 50 °C). As a result, the development of new synthetic strategies (possibly those enabling crosslinking and/or block structure) toward more highly conducting AAEMs is a major research challenge.

1.5.1 Basic stability of alkaline anion exchange membranes

While the abovementioned systems represent significant progress in the development of high performance AAEMs, they rely on tetraalkylammonium (most commonly benzyltrimethylammonium (BTMA)) to coordinate and conduct hydroxide ions. Unfortunately at high pH and/or temperature, hydroxide can react with tetraalkylammonium leading to irreversible degradation by converting the cation into a neutral species. Since a neutral species can no longer coordinate hydroxide the conductivity of the AAEM will decrease, leading to decreased fuel cell performance. Due to these degradation concerns, it is generally believed that the temperature limit for tetraalkylammonium-based AAEM operation is ≤ 60 °C. As a result, a significant research objective has been the development of AAEMs based on cations that surpass the alkaline stability of tetraalkylammonium. The development of AAEMs with increased stability toward hydroxide will permit higher temperature AAEM fuel cell operation leading to increased fuel cell performance. Several promising AAEMs based on phosphonium[28,29] (Figure 1.9), guanadinium[30] (Figure 1.10), imidazolium[31,32] (Figure 1.11) and other cations[33] have recently been reported, and while these results are encouraging it remains uncertain if these systems represent an improvement upon the chemical stability of tetraalkylammonium-based AAEMs.

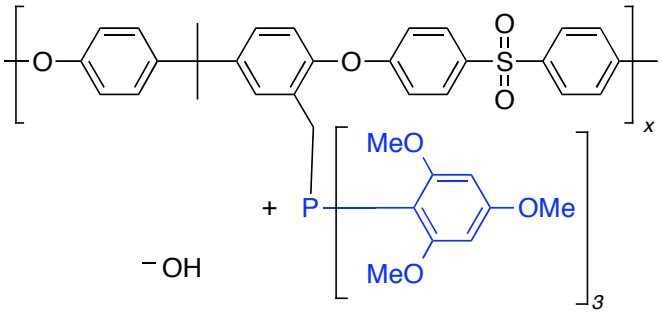

Figure 1.9. Phosphonium-based AAEM.[29]

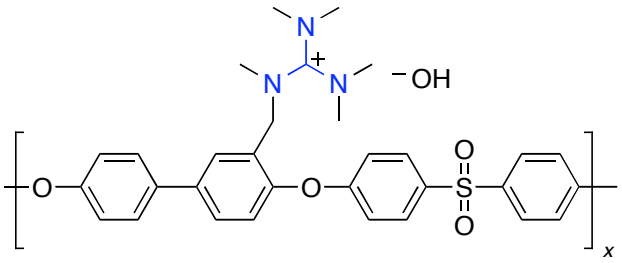

Figure 1.10. Guanadinium -based AAEM.[30]

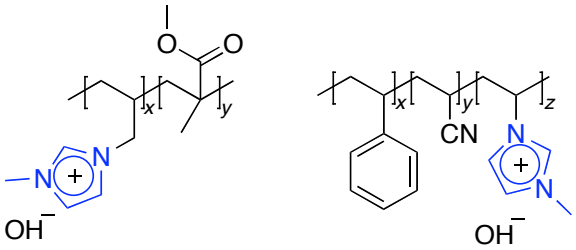

Figure 1.11. Imidazolium-based AAEMs.[31,32]

Recently, several studies investigating the stability of tetraalkylammonium under alkaline conditions have been reported. For example, Boncella and coworkers have published three reports concerning the alkaline stability of tetraalkylammonium.[34,35,36] They found that 90 % of BTMA remained in basic solution at 80 °C after 29 days (Figure 1.12). They also investigated the decomposition mechanism of tetraalkylammonium cations using both theoretical and experimental (differential scanning calorimetry, thermalgravimetric analysis and evolved gas

analysis) means. They found that ylide formation (in contrast to nucleophilic attack by hydroxide) plays a predominant role in the decomposition of tetraalklylammonium and that the solvation of hydroxide is critical to mitigate

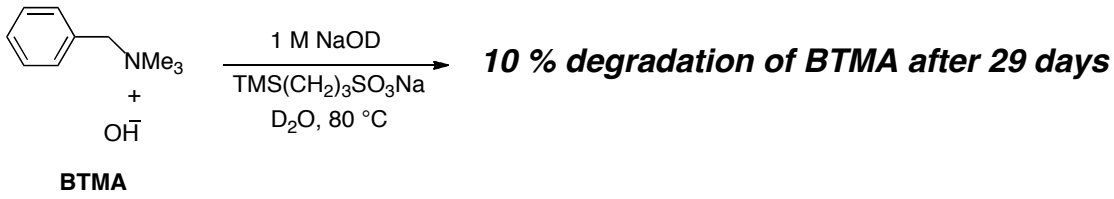

Figure 1.12. BTMA stability under studied under hydrated conditions.[34]

degradation (Figure 1.13). They surmise that solvation of the hydroxide ion greatly reduces its basisity and nucleophilicity resulting in decreased reactivity. Overall, they conclude that tetraalkylammonium-based cations show reasonable stability in alkaline media. However, they state that membrane conditions that lead to poor solvation will lead to faster degradation. Since dehydrated conditions are often associated with high temperature (≥ 80 °C) AAEM fuel cell operation, it is unclear if tetraalkylammonium-based cations are sufficiently stable for these applications. Additionally, despite the fact that these reports provide a better picture on the stability of tetramethylammonium, there is no standardized procedure to compare the stability of tetraalkylammonium to other cations (phosphonium, guanadinium, imidazolium etc.) currently being investigated for use in AAEMs. Due to the lack of a standardized procedure for assessing alkaline stability, it is difficult to ascertain the relative stability of these newly developed cations to traditional tetramethylammonium-based systems. The formation of a standardized procedure for comparing cationic stabilities would facilitate the search for more base stable AAEMs.

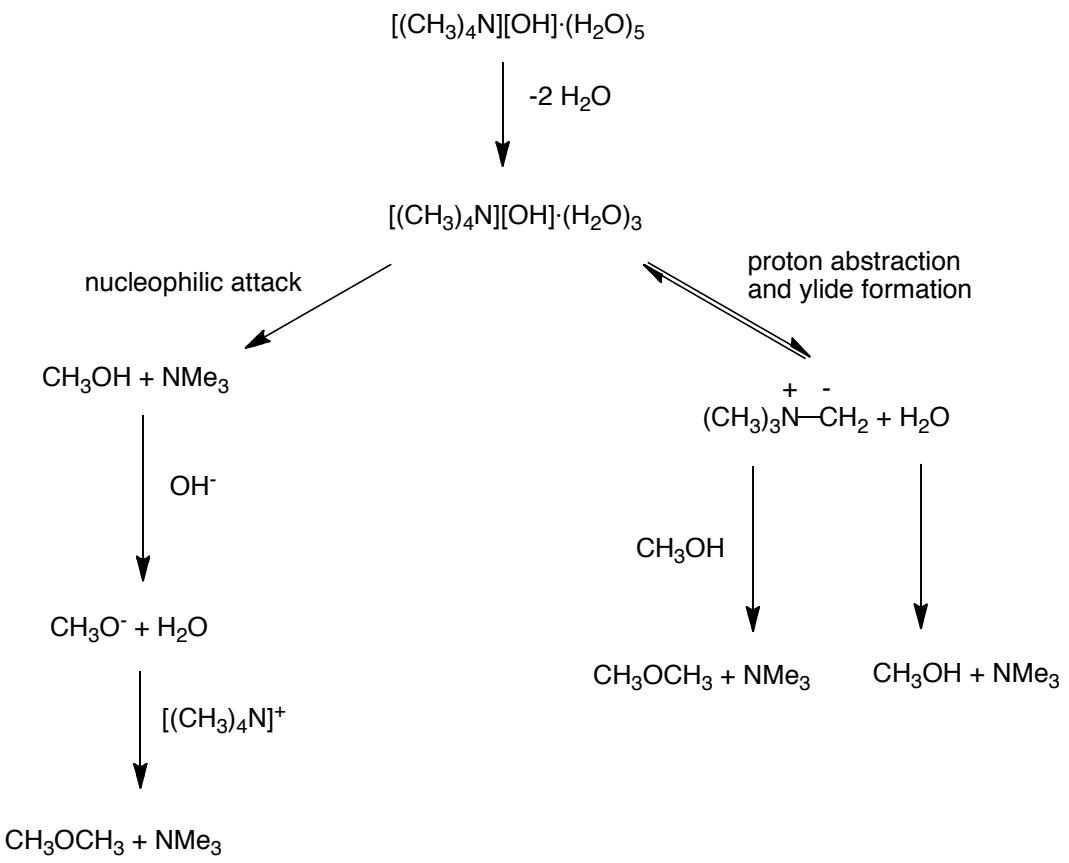

Figure 1.13. Nucleophilic vs. ylide mechanism of tetraalkylammonium degradation.[35]

1.5.2 Soluble ionomers for alkaline anion exchange membranes fuel cells

Another considerable challenge in alkaline fuel cell research is the development of an alkaline analogue of commercially available solutions of Nafion.[13] It should be noted that although Nafion technically forms dispersions, they are commonly called solutions and will be referred to as such. Nafion is insoluble in water and aqueous methanol but soluble in mixtures of other low boiling point solvents including ethanol and n-propanol. This solvent processability allows Nafion to be impregnated into the electrocatalyst layers, allowing the fabrication of a membrane electrode assembly (MEA, Figure 1.14). The MEA consists of a polymer exchange

membrane, electrocatalyst within a soluble ionomer matrix and a gas diffusion layer (GDL).[37] Typically, these components are assembled individually and then pressed together at high temperatures. The presence of ionomer in the catalyst layer facilitates ion transport from the catalyst to the membrane. In fact, MEAs that lack ionomer in the catalyst layer are generally very low performing. Examples of soluble ionomers that conduct hydroxide include Zhang and co-workers report of a highly conductive partially fluorinated polysulfone (84 mS/cm at 20 ºC) that is soluble in n-propanol; however, there is no mention of its solubility in methanol.[19] Furthermore, the membrane became gel-like when placed in water at 60 ºC. Yan and co-workers synthesized a soluble quaternary phosphonium-functionalized polysulfone for use as an alkaline ionomer electrode material that is considerably more conductive (27 mS/cm at 20 ºC)[28] than commercially available analogues (e.g., Tokuyama Co. product code: AS-4, exhibits a conductivity of 13mS/cm),[38] but unfortunately these materials are soluble in pure and aqueous methanol (50 vol% water), likely precluding the use of methanol as a fuel. Consequently the development of an ionomer that is soluble in solvents such as aqueous n-propanol but is insoluble in aqueous methanol is crucial to the fabrication of high performance AAEM MEAs.

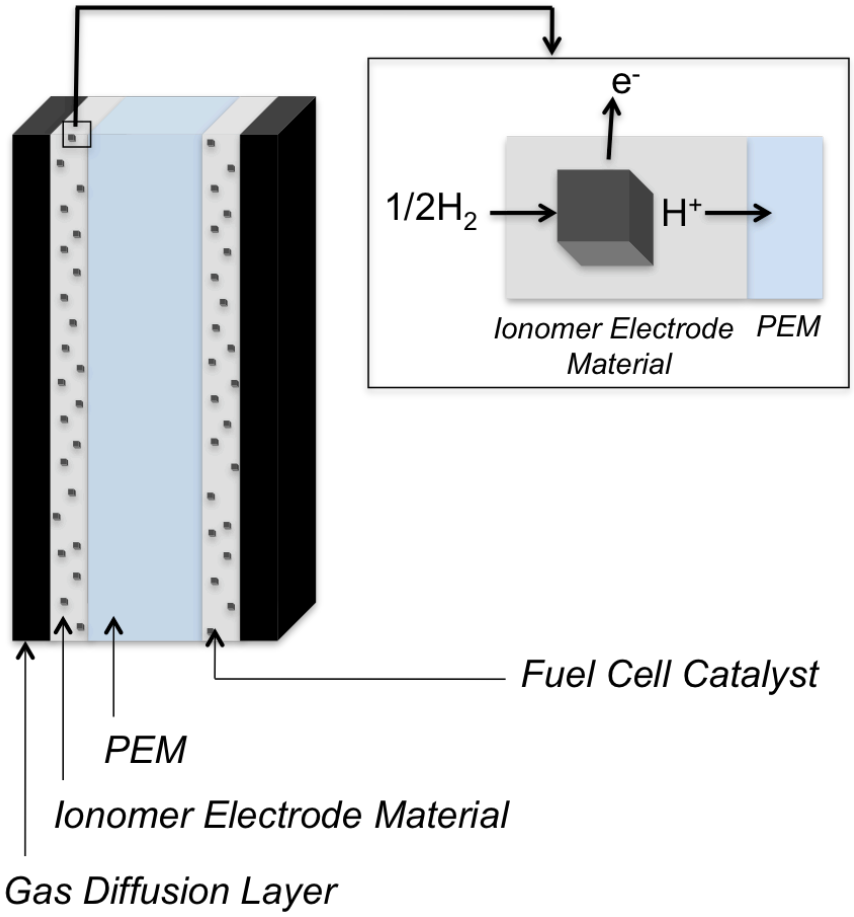

Figure 1.14. Schematic of a PEM MEA.

1.6 Conclusion and outlook

AAEM fuel cells have the potential to operate efficiently without the use of platinum at the cathode and hold great promise to one day supplant PEM fuel cell technology. However, before wide-scale commercialization of AAEM fuel cells can be realized, several significant materials research developments must be made:

(i) The development of new synthetic strategies that enable the synthesis of more highly conducting AAEMs is a significant research challenge. In

particular, materials that combine high conductivities (possibly through microphase separation) with excellent mechanical strength are desired.

(ii) The incorporation of cations, new and existing, that exhibit increased alkaline stability (relative to tetraalkylammonium) into AAEMs would enable high temperature (≥ 80 °C) fuel cell operation. This is essential for AAEM fuel cells to be considered for applications such as automotive power. Furthermore, operation at elevated temperature would reduce thermodynamic voltage losses due to the pH differences across the AAEM and improve the electrokinetics.[13]

(iii) The development of a soluble ionomer, analogues to commercially available solutions of Nafion, is crucial to the fabrication of high performance AAEM MEAs. Specifically, an ionomer that is soluble in solvents such as aqueous n-propanol (to allow simple incorporation into the catalyst layer) but is insoluble in aqueous methanol (to permit the use of methanol as a fuel) would be ideal.

If the above challenges can be met, AAEM technology has the potential to aid in societies ever increasing need for cheap, clean and reliable energy conversion sources.

References

1. DOE Energy Frontier Research Centers (EFRCs). http://www.sc.doe.gov/BES/EFRC.html (accessed Mar 20, 2011).

2. Remarks by the President in State of Union Address. http://www.whitehouse.gov/the-press-office/2011/01/25/remarks-president-state-union-address (accessed June 9, 2011).

3. The Energy Materials Center at Cornell University. http://www.emc2.cornell.edu/ (accessed June 9, 2011).

4. Appleby, A. J.; Foulkes, R. L. *Fuel Cell Handbook*, Van Nostrand Reinhold: New York, **1989**.

5. Grove, W. R. *Phil. Mag. Ser.* **1839**, *14*, 127-130.

6. Carrette, L.; Friedrich, K. A.; Stimming, U. *Fuel Cells*, **2001**, *1*, 5-39.

7. Diat, O.; Gebel, G. *Nature Mater.* **2008**, *7*, 13-14.

8. Whittingham, M. S.; Savinelli, R. F.; Zawodzinski, T. A. *Chem. Rev.* **2004**, *104*, 4243-4244.

9. Lee, C. H.; Park, H. B.; Lee, Y. M.; Lee, R. D. *Ind. Eng. Chem. Res.* **2005**, *44*, 7617-7626.

10. Grot W. G. *Macromol. Symp.* **1994**, *8*, 161.

11. Kariduraganavar, M. Y.; Nagarale, R. K.; Kittur, A. A.; Kulkarni, S. S., *Desalination* **2006**, *197*, 225-246.

12. Lu, S.; Pan, J.; Huang, A.; Zhuang, L.; Lu, J. *Proc. Natl. Acad. Sci. U. S. A.* **2008**, *105*, 20611-20614.

13. Varcoe, J. R.; Slade, R. C. T. *Fuel Cells* **2005**, *5*, 187, and references therein.

14. McLean, G. F.; Niet, T.; Prince-Richard, S.; Djilali, N. *Int. J. Hydrogen Energy* **1994**, *19*, 181-185.

15. Varcoe, J. R.; Slade, R. C. T.; Yee, E. L. H.; Poynton, S. D.; Driscoll, D. J.; Apperley, D. C. *Chem. Mater.* **2007**, *19*, 2686-2693.

16. Hibbs, M. R. Hickner, M. A.; Alam, T. M.; McIntyre, S. K.; Fujimoto, C. H.; Cornelius, C. J. *Chem. Mater.* **2008**, *20*, 2566-2573.

17. Wang, G.; Wenig, Y.; Chu, D.; Chen, R.; Xie, D. J. *J. Membr. Sci.* **2009**, *332*, 63-68.

18. Zhou, J.; Unlu, M.; Vega, J. A.; Kohl, P. A. *J. Power Sources* **2009**, *190*, 285–292.

19. Wang, J.; Zhao, Z.; Gong, F.; Li, S.; Zhang, S. *Macromolecules* **2009**, *42*, 8711–8717.

20. Yan, J.; Hickner, M. A. *Macromolecules* **2010**, *43*, 2349-2356.

21. Wang, J.; Li, S.; Zhang, S. *Macromolecules* **2010**, *43*, 3890-3896.

22. Hibbs, M. R.; Fujimoto, C. H.; Cornelius, C. J. *Macromolecules* **2009**, *42*, 8316-8321.

23. Clark, T. J.; Robertson, N. J.; Kostalik IV, H. A.; Lobkovsky, E. B.; Mutolo, P. F.; Abruña, H. D.; Coates, G. W. *J. Am. Chem. Soc.* **2009**, *131*, 12888-12889.

24. Robertson, N. J.; Kostalik IV, H. A.; Clark, T. J.; Mutolo, P. F.; Abruña, H. D.; Coates, G. W. *J. Am. Chem. Soc.* **2010**, *132*, 3400-3404.

25. Kostalik IV, H. A.; Clark, T. J.; Robertson, N. J.; Longo, J. M.; Mutolo, P. F.; Abruña, H. D.; Coates, G. W. *Macromolecules* **2010**, *43*, 7147-7150.

26. Varcoe, J. R.; Slade, R. C. T.; Yee, E. L. H. *Chem. Commun.* **2006**, 1428-1429.

27. Schmidt-Rohr, K.; Chen, Q. *Nat. Mater.* **2008**, *7*, 75–83.

28. Gu, S.; Cai, R.; Luo, T.; Chen, Z.; Sun, M.; Liu, Y.; He, G.; Yan, Y. *Angew. Chem. Int. Ed.* **2009**, *48*, 6499-6502.

29. Gu, S.; Cai, R.; Luo, T.; Jensen, K.; Contreras, C.; Yan, Y. *ChemSusChem* **2010**, *3*, 555-558.

30. Wang, J.; Li, S.; Zhang, S. *Macromolecules* **2010**, *43*, 3890-3896.

31. Guo, M.; Fang, J.; Xu, H.; Li, W.; Lu, X.; Lan, C.; Li, K.; *J. Membr. Sci.*, **2010**, *362*, 97-104.

32. Lin, B.; Qiu, L.; Yan, F. *Chem. Mater.* **2010**, *22*, 6718-6725.

33. Kong, X.; Wadhwa, K.; Verkade, J. G.; Schmidt-Rohr, K. *Macromolecules* **2009**, *42*, 1659-1664.

34. Einsla, B. R.; Chempath, S.; Pratt, L. R.; Boncella, J. M.; Rau, J.; Macomber, C.; Pivovar, B. S. *Electrochem. Soc. Trans.* **2007**, *11*, 1173-1180.

35. Macomber C. S.; Boncella, J. M.; Janicke, M.; Pivovar, B. S.; Rau, J. A. *J. Therm. Anal. Calorim.,* **2008**, *93,* 225-229.

36. Chempath, S.; Einsla, B. R.; Pratt, L. R.; Macomber, C.; Boncella, J. M.; Rau, J. A.; Pivovar, B. S. *J. Phys. Chem. C* **2008**, *112*, 3179-3182.

37. Lister, S.; McLean, G. *J. Power Sources* **2004**, *130*, 61–76.

38. Yanagi, H.; Fukuta, K. *ECS Trans.* **2008**, *16*, 257–262.

Chapter 2

A Ring Opening Metathesis Polymerization Route to Alkaline Anion Exchange Membranes: Development of Hydroxide-Conducting Thin Films from Ammonium-Functionalized Monomers

Reprinted in part with permission from the

Journal of the American Chemical Society **2009**, *131*, 12888-12889.

2.1 Introduction

A main component of a fuel cell is the polymer electrolyte, which acts as an electronically insulating barrier between the fuel and oxidant streams and simultaneously transports ions.[1] Many low temperature fuel cells (< 100°C) use an ionic polymer membrane as the electrolyte. Nafion, a proton exchange membrane (PEM), has dominated the field due to its good processability, chemical and thermal stability, and proton conductivity (when water availability is high).[1,2] However, Nafion also has some critical drawbacks including high cost of synthesis[3] along with considerable methanol crossover, when used in direct methanol fuel cells, resulting in wasted fuel and significantly decreased efficiency.[4] Despite being relatively underdeveloped, AAEM fuel cells, devices that conduct hydroxide ions, offer important benefits such as reduced methanol crossover and greatly enhanced electro kinetics. More specifically, the electro kinetics of the notoriously slow oxygen reduction reaction (ORR) at the cathode are facilitated under basic conditions. This potentially permits the use of cheaper non-noble metal catalysts (eg. Ni or Ag) making fuel cells more cost competitive.[5] Some recent AAEM developments come from Varcoe and Slade *et al*. who reported that radiation grafting of poly(vinylbenzyl chloride) onto mixed fluorocarbon/hydrocarbon membranes, followed by amination, yields mechanically strong AAEMs with promising hydroxide conductivities and low methanol permeability.[6] Others have shown that polysulfones can act as scaffolds for successive chloromethylation and amination reactions again yielding robust, conductive AAEMs.[7] Both of these reports illustrate remarkable progress made in this area, but also reveal limitations in the synthetic approaches employed. For example, difficulty dissolving polymer samples and achieving quantitative conversions can prove challenging in postpolymerization reactions, while the use of γ irradiation and

fluorinated materials may limit the utility in the case of the former. In this chapter we report on our work on the synthesis and ring opening metathesis polymerization (ROMP) of a tetraalkylammonium-functionalized norbornene with dicyclopentadiene (**DCPD**) crosslinker to yield strong, hydroxide-conducting, thin films that exhibit negligible swelling in both hot water and aqueous methanol. We targeted this route for several reasons. Firstly, olefin metathesis is an extraordinarily powerful C-C bond forming reaction and the use of air-stable Grubbs' 2nd Generation catalyst ([Ru]) enables functionalized monomers to be polymerized due to its exceptional tolerance.[8] By employing monomers with the tetraalkylammonium moiety already present, AAEM synthesis is greatly simplified because postpolymerization modifications are unnecessary and only a hydroxide exchange is required to generate the final AAEMs (Figure 2.1). A tetraalkylammonium functionalized norbornene was used as a monomer due to the large amount of ring strain associated with norbornene. It was hoped that this significant ring strain would ultimately drive the ROMP reactions toward quantitative conversions and that the norbornene polymer backbone would provide the necessary support to generate mechanically a chemically robust AAEMs. Supporting this are numerous reports that employ the ROMP of norbornene to generate mechanically strong materials.

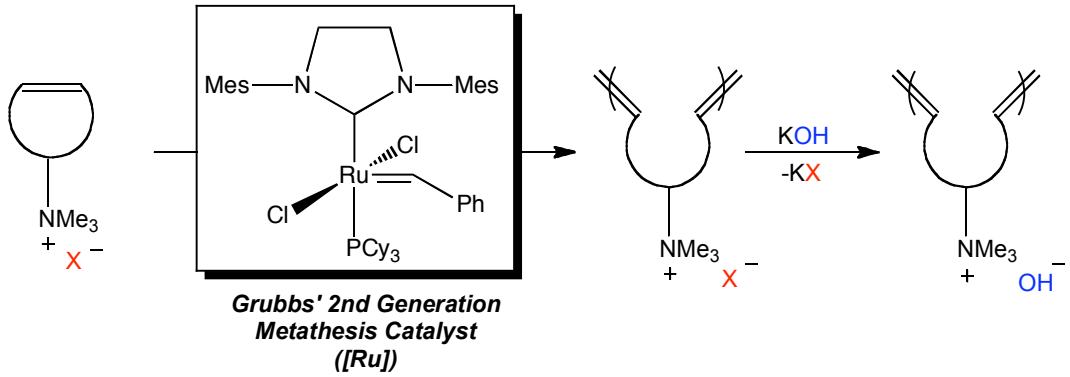

Figure 2.1. ROMP route toward AAEMs.

2.2 Results and discussion

Monomer **3** was prepared in three straightforward steps in 62% overall yield (Scheme 2.1). First, the Diels-Alder reaction between cyclopentadiene and methacrolein furnished the aldehyde norbornene derivative **2.1**, with the *exo* isomer as the major product.[9] Reductive amination of **1** with dimethylamine afforded neutral amine **2.2**, which was then alkylated with methyl iodide to give **2.3** as a white powder. Compound **2.3** can be recrystallized from chlorinated solvents or acetonitrile to afford single crystals of the *exo* isomer.

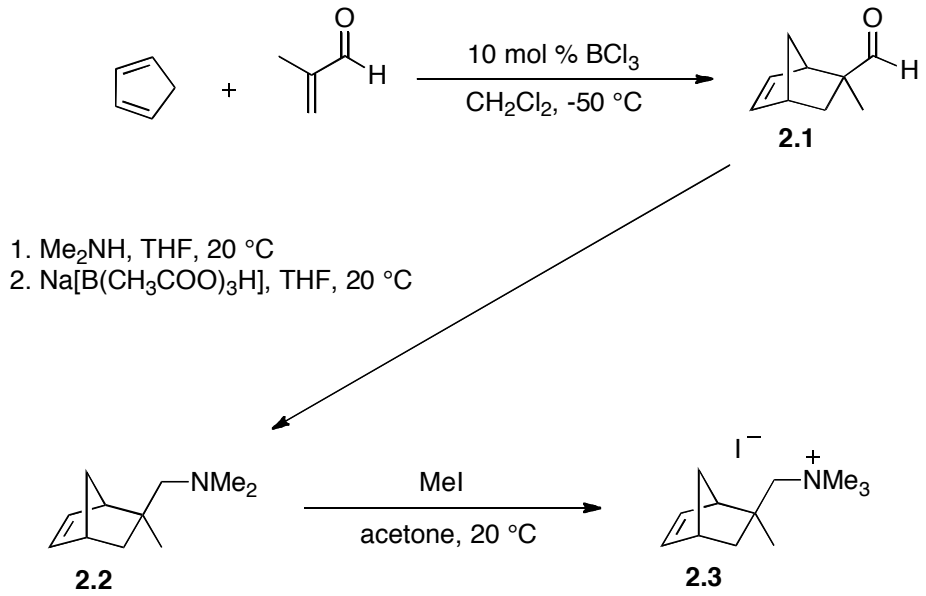

Scheme 2.1. Synthesis of an ammonium-functionalized norbornene monomer.

Notably, methacrolein was chosen as the dienophile as it produced a quarternary β-carbon atom relative to the ammonium group. This should improve the chemical stability of the ammonium ion because no β-hydrogen atoms are present, preventing Hofmann elimination degradation pathways.[10,11] Additionally,

trimethylammonium groups have exhibited good stability under alkaline conditions at elevated temperatures. Pratt, Boncella and co-workers have reported that $BnNMe_3^+$ exhibits negligible degradation in 1M sodium hydroxide at 80 °C and have recently described other possible hydroxide ion induced means of degradation with Me_4N^+ including nucleophilic substitution at a methyl subsistent and ylide formation at the nitrogen atom that must also be carefully considered.[12] Treatment of 100 equivalents of **2.3** with [Ru] in chloroform resulted in a red-brown solid precipitating from the reaction mixture after 45 minutes. Upon isolating and washing with pentane, a ^1H NMR spectrum of the light brown solid confirmed the successful formation of ionic polynorbornene. This polymer joins just a few other ionic polynorbornenes that have been previously reported.[13,14] Riande *et al*. have synthesized a polynorbornene with a pendant sulfonated phenyl group rendering the polymer ionic.[14] They then investigated the proton conductivity of membranes derived from this polymer but found that it was considerably less than Nafion owing to low water uptake.

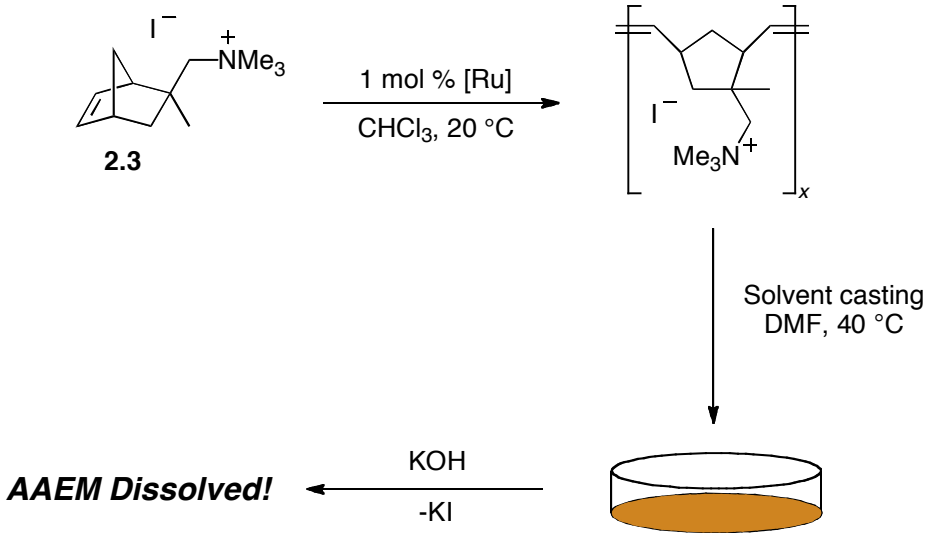

Scheme 2.2. Homopolymerization of **2.3**.

Nevertheless, intrigued by this chemistry, we solvent cast the polymer derived from **2.3**, with a view to subsequent hydroxide exchange to furnish an AAEM candidate. Unfortunately, the resultant thin films were brittle and dissolved in aqueous media (Scheme 2.2).

Hillmyer and co-workers have recently shown that robust nanoporous composites can be constructed by the [Ru] catalyzed copolymerization of **DCPD** with block copolymers containing pendant norbornene groups.[15] The mechanical strength of materials made from **DCPD** is derived from crosslinks resulting from the ring opening metathesis reaction between five-membered rings in opposing poly(**DCPD**) chains.[8a] We hypothesized that this crosslinking reaction would benefit our AAEM synthesis by making film casting easier, film properties more tunable, and would render the ionomer less likely to swell and dissolve in water or aqueous methanol. It has been noted that the presence of crosslinks in polymer films may help mitigate swelling by this increased ability to resist osmotic pressure. With this in mind, Holdcroft and DeSimone have independently described liquid polymer electrolytes that can be readily converted to solid membranes *via* UV photocrosslinking.[16] Notably, both groups report high proton conductivity, which they attribute to the increased incorporation of acidic sulfonate groups made possible by the crosslinking route without any water solubility issues. Here, thin films in the iodide form were synthesized by combining [Ru] with a chloroform solution of **2.3** and **DCPD** at room temperature (Scheme 2.3). After one minute of vigorous stirring, the orange-red homogeneous solution was transferred to a flat-bottomed, pre-heated glass Petri dish from which the solvent slowly evaporated. The film was then heated to 75°C for one

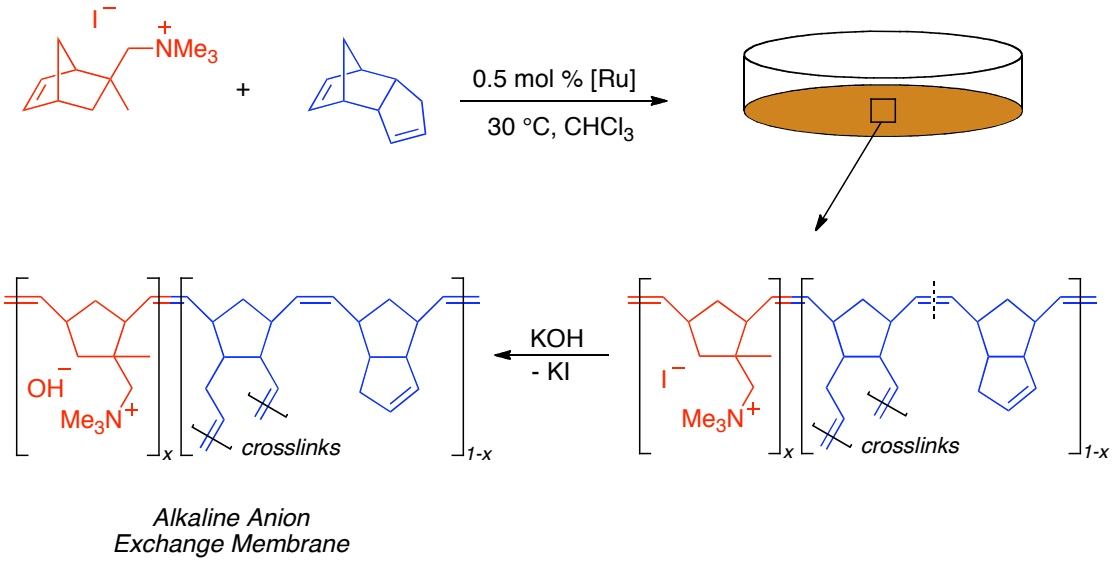

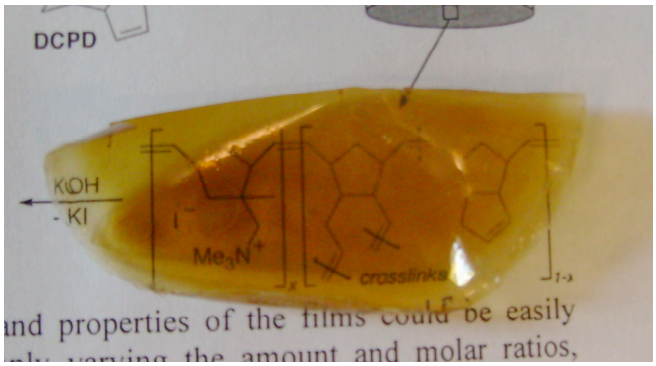

Scheme 2.3. Synthesis of a crosslinked norbornene-based AAEM.

hour, followed by facile removal from the dish. The resulting films were yellow-orange and their properties and thicknesses could be easily controlled by simply varying the amount and molar ratios of **2.3** to **DCPD**. Upon conversion to the hydroxide form, it became clear that any film with **2.3** as the major component (e.g. mol % **2.3** greater than 50%) could not be quantitatively evaluated due to significant swelling and hydrogel formation. Similarly, AAEMs comprised of considerable

amounts of **DCPD** (e.g. mol % **2.3** less than 33%) were exceptionally robust, but were not sufficiently conductive due to decreased ionicity. Overall, our studies indicated that the optimal AAEMs, with respect to mechanical integrity and hydroxide conductivity, had a mol % **2.3** of 33% or 50%.

Detailed characterization data are provided in Table 2.1. The average ion exchange capacities (IECs) for AAEM-**2.3**-33 and AAEM-**2.3**-50 samples are 1.00 and 1.35 mmol OH/g, respectively, and fall into the range observed for Nafion (0.92 mmol H^+/g for Nafion-115[17]) as well as AAEMs reported by other groups.[6,7] The theoretical IECs for AAEM-**2.3**-33 and AAEM-**2.3**-50 are 1.75 and 2.28 mmol OH-/g, respectively, and such discrepancies are commonly observed.[6,7]

It has been shown that sufficient water uptake of AAEMs is needed to form interconnected hydrated domains thereby maximizing ion conductivity, although excessive water uptake may also result in a detrimental loss of mechanical integrity due to excessive swelling. The gravimetric water uptake (WU) values of the optimized AAEMs were measured and as expected, increasing the ionic content of the AAEMs led to an increase in WU with AAEM-**2.3**-33 and AAEM-**2.3**-50 exhibiting WUs of 75 % and 258 %, respectively. These WU values exceed those of most current AAEMs, potentially leading to increased hydroxide ion conductivity; however, we were concerned that this would also result in excessive swelling.

As a result of these concerns, we also evaluated the dimensional swelling in AAEM-**2.3**-33. An ideal AAEM candidate will not swell appreciably in length, width, or thickness upon exposure to solvents contained within a fuel cell at typical operating

temperatures (50-80°C), as the integrity of the device will be compromised. Encouragingly, our results indicate that negligible swelling occurs in either water or 2 M methanol after two hours at 60°C. To further test the methanol tolerance of this material, we performed the same measurements using more concentrated aqueous methanol solutions. Indeed significant swelling (e.g. > 10%) was not observed until immersion into methanol solutions greater than 8 M. This exceptional methanol tolerance is likely attributable to the presence of the hydrocarbon **DCPD** crosslinker as the major component.

The mechanical properties of both AAEMs were investigated using tensile stress–strain measurements. AAEM-**2.3**-33 exhibited considerable tensile strength with an average 15.8 MPa of stress resulting in 7.2 % strain. This compares favorably to the non-crosslinked AAEMs reported by Varcoe and Slade which range from 45-70 % strain over 13-18 MPa.[6] The robust nature of AAEM-**2.3**-33 can be accounted for by the crosslinked **DCPD** regions. Further supporting this is the dramatic decrease in toughness observed with lower **DCPD** loadings in AAEM-**2.3**-50 samples as only 2.3 MPa was required to break samples.

The hydroxide conductivity was determined for each film composition at 20°C and 50°C to mimic fuel cell operating conditions. AAEM-**2.3**-33 has an acceptable conductivity of 14 mS/cm at room temperature that rises to 21 mS/cm at 50°C. A proportional relationship between temperature and ion conductivity is expected due to thermally promoted charge carrier mobility. Moreover, increasing the ionicity with higher loadings of **2.3** in AAEM-**2.3**-50 led to higher conductivities. At 20°C, this membrane conducts at 18 mS/cm which increases to 28 mS/cm at 50°C. This places the 1:1 thin film among the highest conducting AAEMs reported to date. For example, Cornelius and co-workers' optimized system conducts at 35 mS/cm at 30°C[7a] while

that of Varcoe and Slade has a conductivity of 34 mS/cm at 50°C.[6] Interestingly, the conductivity of AAEM-**2.3**-33 dropped dramatically from 14 mS/cm to 4 mS/cm in 24 hours at room temperature with no further decrease observed after 48 hours.

Table 2.1. AAEM characterization data.

Measurement	AAEM-**2.3**-33	AAEM-**2.3**-50
mol % **2.3**	33	50
IEC (mmol OH^-/g I^-)[a]	1.00	1.35
% Water uptake[b]	75 ± 13	258 ± 37
% swelling in water/methanol[c]	0.5	n.d.[d]
% swelling in 2 M methanol[c]	1.7	n.d.[d]
Tensile Strength at break (MPa)[e]	15.8	2.3
% Strain at break[e]	7.2	25.9
OH^- σ_{20} (mS/cm)[f]	14 ± 2	18 ± 2
OH^- σ_{50} (mS/cm)[f]	21 ± 4	28 ± 3

[a]Ion exchange capacity determined by back titration, average of 2 trials. [b]Gravimetric water uptakes of the fully hydrated membranes, average of 4 trials. [c]Three-dimensional swelling of AAEM after sitting in either 60 °C water or 2 M aqueous methanol for 2 hours, average of 2 trials. [d]Not determined due to uncontrollable curling. [e]Mechanical testing of the films in the iodide form, average of 4 trials. [f]Hydroxide conductivities of the AAEMs fully immersed in water at 20 °C and 50 °C, average of 4 trials.

Studying this process in greater detail, the conductivity of a freshly prepared AAEM-**2.3**-33 hydroxide-form sample immersed in water was monitored every 15 minutes until it remained constant (Figure 2.2, red squares). It can be clearly seen that

there is a steady decrease in hydroxide conductivity over approximately 3 hours at which time a constant value of 4 mS/cm is maintained. We hypothesized that this

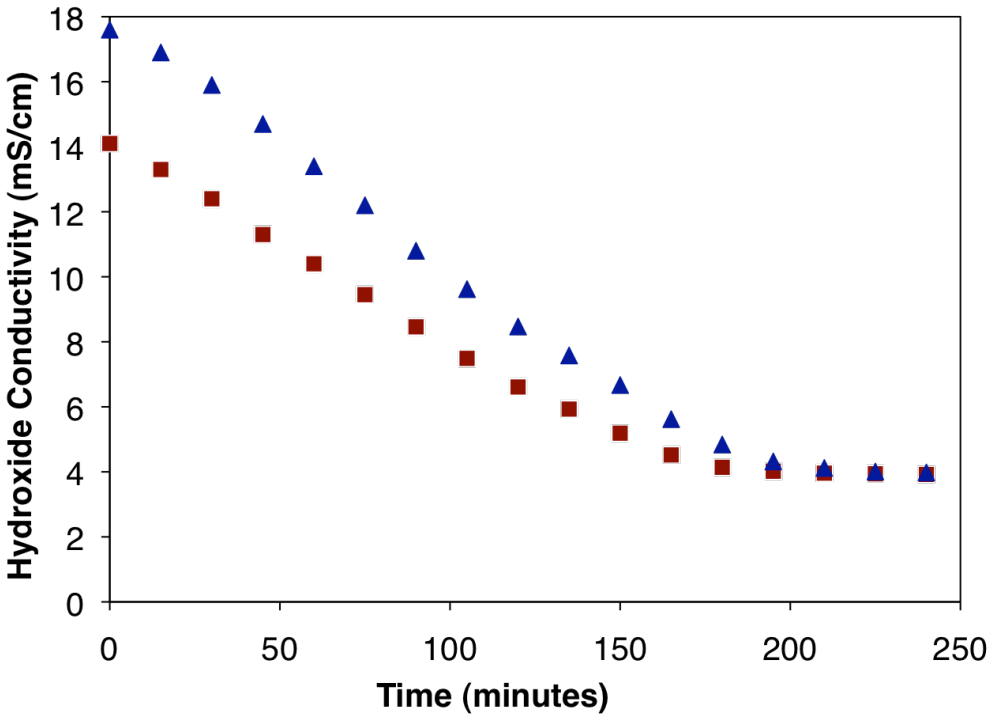

Figure 2.2. Plot of hydroxide conductivity versus time for AAEM-**2.3**-33 with non-degassed water (red squares) and degassed water (blue triangles).

could be caused by the formation of carbonate or bicarbonate species through the reaction of the hydroxide anion with dissolved carbon dioxide present in the water.[18] We prepared AAEMs with these counterions *via* anion exchange with either potassium carbonate or bicarbonate. Subsequent analysis revealed that they both conducted at ca. 4 mS/cm, acting as strong evidence for the above hypothesis. Further supporting this, using degassed water for washes following the anion exchange process and conductivity process, led to higher initial conductivity (ca. 18 mS/cm) again followed by a gradual decrease in conductivity over a similar time period to 4 mS/cm (Figure

2.2, blue triangles). This higher initial conductivity suggests carbon dioxide reacts with the AAEMs during water washes (Scheme 2.4), following ion exchange, unless degassed water is used. It also verifies the sensitivity of AAEMs in the hydroxide form towards carbonation by ambient carbon dioxide.[19] However, Varcoe and Slade have shown that carbonate formation during fuel cell operation is not detrimental to overall performance.[20] Moreover, they note that continuous regeneration of hydroxide anions occurs from the oxygen reduction reaction at the cathode.

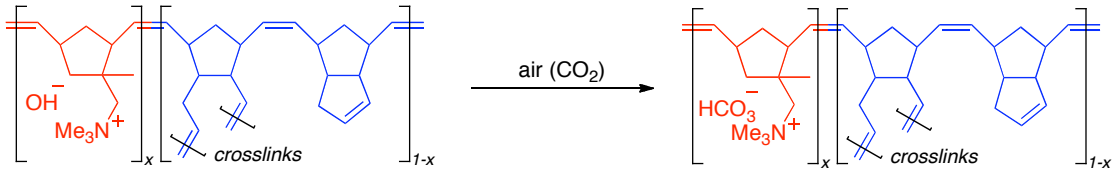

Scheme 2.4. Carbonation of AAEM.

2.3 Conclusion

In summary, we have developed a ring opening olefin metathesis route to alkaline anion exchange membranes *via* the copolymerization of a tetraalkylammonium-functionalized norbornene with dicyclopentadiene. The thin films generated are robust, exhibit good hydroxide conductivities and exceptional methanol tolerance. Future work will focus on studying the efficacy of these materials under operating conditions using in house fuel cell test stations. Additionally we are developing new materials that retain excellent mechanical properties, but display much greater hydroxide conductivity.

2.4 Experimental

2.4.1 General methods and materials

All reactions and manipulations of compounds were carried out in air unless otherwise specified. All solvents were used as received. Methacrolein, boron trichloride (1.0 M solution in dichloromethane), dimethylamine (2.0 M solution in tetrahydrofuran), sodium triacetoxyborohydride, potassium hydroxide flakes, and Grubbs 2nd Generation catalyst were purchased from Sigma-Aldrich and used as received. Dicyclopentadiene was also purchased from Sigma-Aldrich and was run through a plug of alumina prior to use. Methyl iodide and triethylamine were purchased from Acros Organics and Fisher Scientific, respectively, and used as received. Standardized hydrochloric acid (0.1014 N) and potassium hydroxide (0.1000 ± 0.0001 M) solutions were purchased from Sigma-Aldrich and Riedel-de Haën, respectively. Nafion 112 was purchased from Sigma-Aldrich and pretreated using a literature procedure.[2]

2.4.2 Small molecule characterization

^{1}H NMR spectra were recorded on Varian INOVA 400 (^{1}H, 400 MHz) or Varian INOVA 600 (^{1}H, 600 MHz) spectrometers and referenced to $CHCl_3$, 7.26 ppm or H_2O, 4.80 ppm. ^{13}C NMR spectra were recorded on a Varian INOVA 600 (^{13}C, 150 MHz) spectrometer and referenced to $CHCl_3$, 77.23 ppm.

The gradient selected HSQCAD, HMBCAD and ROESY spectra were recorded on a Varian Unity Inova (600 MHz) spectrometer operating at 599.757 MHz for ^{1}H observation using a Varian inverse ^{1}H-{^{13}C,^{15}N} triple-resonance probehead with

triple-axis gradients. NMR data were acquired with the pulse sequences supplied in Vnmrj 2.1B/Chempack 4.1 and were processed and analyzed using the MestReNova 5.3 software package (2008, Mestrelab Research S. L.). ROESY spectra were acquired using the ROESY sequence with a spectral width of 4.3 kHz. A total of 200 complex points were collected in the indirectly detected dimension with 4 scans and 0.15 s acquisition time per increment. The resulting matrices were zero filled to 1k x 1k complex data points and squared cosine window functions were applied in both dimensions prior to Fourier transformation. The multiplicity-edited adiabatic HSQC spectrum was acquired with the gHSQCAD sequence. Spectral widths were 4.3 kHz and 30 kHz in ^{1}H and ^{13}C dimensions, respectively. A total of 256 complex points were collected in the indirectly detected dimension with 2 scans and 0.15 s acquisition time per increment. The resulting matrices were zero filled to 2k x 2k complex data points and squared cosine window functions were applied in both dimensions prior to Fourier transformation. Gradient selected adiabatic HMBC spectra were acquired in phase sensitive mode with the gHMBCAD sequence optimized for 8 Hz couplings. Spectral widths were 4.3 kHz and 36.2 kHz in ^{1}H and ^{13}C dimensions, respectively. A total of 400 complex points were collected in the indirectly detected dimension with 4 scans and 1024 points per increment. The resulting matrices were zero filled to 2k x 2k complex data points and shifted sinebell window functions were applied in the ^{1}H dimension prior to Fourier transformation.

Mass spectra were acquired using a JEOL GCMate II mass spectrometer operating at 3000 resolving power for high resolution measurements in positive ion mode and an electron ionization potential of 70 eV. Samples were introduced via a GC

inlet using an Agilent HP 6890N GC equipped with a 30 m (0.25 μm i.d.) HP-5ms capillary GC column. The carrier gas was helium with a flow rate of 1 mL/min. Samples were introduced into the GC using a split/splitless injector at 230 ºC with a split ratio of 10:1.

Elemental analysis was performed by Robertson Microlit Laboratories, Inc. Madison, New Jersey.

2.4.3 AAEM characterization

Ion exchange capacities (IECs) were determined using standard back titration methods. The thin film as synthesized (in iodide form) was dried under full vacuum overnight at 50 ºC in order to completely dehydrate it and then weighed. Conversion to the hydroxide form was achieved by immersing the film in 3-60 mL portions of 1 M potassium hydroxide for 20 minutes each. Residual potassium hydroxide was washed away by immersing the membrane in 3-500 mL portions of deionized water for 20 minutes each. The AAEM was then stirred in 20 mL standardized 0.1 M $HCl_{(aq)}$ solution for 24 hours followed by titration with standardized 0.1 M $KOH_{(aq)}$ to determine the equivalence point. Control acid samples (with no AAEM present) were also titrated with standardized 0.1 M $KOH_{(aq)}$, and the difference between the volume required to titrate the control and the sample was used to calculate the amount of hydroxide ions in the membrane. This was divided by the dried mass of the membrane (*vide supra*) to give an IEC value with the units mmol OH^-/g I^-.

The in-plane hydroxide conductivity of the AAEM sample was measured by

four probe electrochemical impedance spectroscopy (EIS) using a Solartron 1280B electrochemical workstation along with ZPlot and ZView software. The conductivity cell was purchased from BekkTech LLC (Loveland, CO), and a helpful schematic and description of a similar experimental setup has been reported.[21] A strip of the thin film in iodide form (ca. 4 cm long x 0.5 mm wide) was converted to the hydroxide form by immersing it in 3-30 mL portions of 1 M potassium hydroxide for 20 minutes each. Residual potassium hydroxide was washed away by immersing the membrane in 3-60 mL portions of deionized water for 20 minutes each. Aliquots of each of these water washings were removed and analyzed by inductively coupled plasma atomic emission spectrometry (ICP-AES) for potassium ions. ICP-AES was performed by the Cornell Nutrient Analysis Laboratories, Department of Crop and Soil Sciences, Cornell University using a CIROS model from Spectro Analytical Instruments, Inc. and the EPA 6010B method. Negligible potassium ions were detected in the aqueous sample (0.047 mg/L) by the third water washing; approximately equal to that detected in deionized water (0.055 mg/L) verifying complete removal of base and preventing falsely high hydroxide conductivities. The AAEM was then clamped into the cell using a Proto 6104 torque screwdriver set to 1 inch ounce and completely immersed in Millipore water (> 18 MΩ·cm), at either 20 ºC or 50 ºC, during the measurement time. In the case of the 50 ºC measurement, the sample was allowed to equilibrate at that temperature for 1 hour. EIS was performed by imposing a small sinusoidal (AC signal) voltage, 10 mV, across the membrane sample at frequencies between 20,000 Hz and 0.1 Hz (scanning from high to low frequencies) and measuring the resultant current response. Using a Bode plot, the frequency region over which the impedance

had a constant value was checked, and the highest frequency measurement in the Nyquist plot was taken as the effective resistance of the membrane. This was then used to calculate the hydroxide conductivity by employing the following formula: $\sigma = L / Z' \cdot A$ where L is the length between sense electrodes (0.425 cm), Z' is the real impedance response at high frequency, and A is the membrane area available for hydroxide conduction (width·thickness). The dimensional measurements were performed using a digital micrometer (± 0.001 mm) purchased from Marathon Watch Company Ltd. (Richmond Hill, ON).

The hydroxide conductivity was measured for four separate AAEMs (per composition) and the precision of these measurements was evaluated. All errors are determined from sample standard deviations. Confidence intervals are at the 95 % confidence level based on the sample deviations and using the relevant student-*t* distribution (*N*-1 degrees of freedom, *N* is the number of samples tested for each membrane).

Dimensional swelling measurements were carried out in either deionized water (10 mL) or 2 M aqueous methanol solution (0.81 mL methanol in 10 mL deionized water) pre-heated to 60 ºC. Two stamp-sized pieces were cut out of an AAEM sample and their length, width and thickness measurements were recorded followed by placement of the samples in either one of the above solutions for 2 hours. At this time, the measurements were repeated and the dimensional swelling expressed as the percent difference between the two volumes.

The mechanical properties of the thin films in the iodide form were

characterized using an Instron system (model 5566) (Instron Co.,Canton, MA) using a 100 N static Lodge cell and Blue Hill software. The tensile strength of two strips from each of two wet samples were measured in the iodide form (ie four measurements total).

2.4.4 Monomer synthesis

Preparation of 2-methylbicyclo[2.2.1]hept-5-ene-2-carbaldehyde (2.1): This compound was prepared using a modified literature procedure.[9] To a solution of freshly cracked cyclopentadiene (14.0 mL, 172 mmol) in 125 mL dichloromethane at -50 ºC, methacrolein (18.5 mL, 224 mmol) and boron trichloride solution (17.0 mL, 17.0 mmol) were added sequentially under nitrogen. After these additions, stirring was commenced and the reaction allowed to proceed at -50 ºC for 90 minutes. Triethylamine (10.0 mL, 71.7 mmol) was then added *via* syringe and the reaction allowed to warm to room temperature. 125 mL of water were then added resulting in a biphasic yellow mixture, which was separated. The aqueous fraction was then extracted with 2x100 mL portions of dichloromethane, combined with the separated organic fraction and dried with magnesium sulfate. The clear, yellow solution was then dried by rotary evaporation affording 2-methylbicyclo[2.2.1]hept-5-ene-2-carbaldehyde (21.7 g, 159 mmol), as 85% *exo* aldehyde diastereomer, in 92% yield as an orange liquid which partially solidified upon standing at room temperature. The compound was generally used as is, but further purification could be carried out by distilling under full vacuum at 65 ºC resulting in the isolation of the pure aldehyde as a colorless liquid/solid. The NMR shifts closely match those in the aforementioned

literature procedure for the *exo* isomer.[9] ^{1}H NMR (400 MHz, $CDCl_3$) δ 9.65 (1H, CHO), 6.25 (1H, dd, ^{3}J = 5.6 Hz, 3.2 Hz, C*H*=CH), 6.06 (1H, dd, ^{3}J = 5.6 Hz, 2.8 Hz, CH=C*H*), 2.85 (1H, b, Bridgehead CH), 2.77 (1H, b, Bridgehead CH), 2.20 (1H, dd, ^{2}J = 12 Hz, ^{3}J = 4.0 Hz, CH_2), 1.35 (1H, m, Bridge CH), 1.25 (1H, m, Bridge CH), 0.96 (3H, s, CH_3), 0.72 (1H, d, ^{2}J = 12 Hz, CH_2). ^{13}C NMR (150 MHz, $CDCl_3$) δ 205.9, 139.7, 133.2, 54.0, 50.9, 48.6, 43.4, 34.8, 20.2.

Preparation of *N*,*N*-dimethyl-1-(2-methylbicyclo[2.2.1]hept-5-en-2-yl)methanamine (2.2): To a solution of 2-methylbicyclo[2.2.1]hept-5-ene-2-carbaldehyde (14.3 g, 105 mmol) in 150 mL of tetrahydrofuran, dimethylamine solution (68.0 mL, 136 mmol) was added and stirred at 20 ºC for 2 hours. At this time, $Na[BH(OAc)_3]$ (28.9 g, 136 mmol) was slowly added, diluted with a further 100 mL of tetrahydrofuran to loosen the slurry and stirred overnight. The reductant was quenched with 1 M aqueous potassium hydroxide (150 mL, 150 mmol) causing the reaction mixture to turn clear yellow. After 15 minutes, the solution was extracted with 3x100 mL portions of diethyl ether and dried with magnesium sulfate. The clear, yellow solution was then dried by rotary evaporation affording *N*,*N*-dimethyl-1-(2-methylbicyclo[2.2.1]hept-5-en-2-yl)methanamine (14.4 g, 87.1 mmol) in 83% yield as a yellow-orange liquid. The compound was generally used as is, but further purification could be carried out by distilling under full vacuum at 50 ºC resulting in the isolation of the pure amine as a colorless liquid. The resonances for the *exo* and *endo* isomers (*ca*. 4:1, respectively) were assigned with the aid of *g*HMBC, *g*HSQC, and ROESY experiments.

For the *exo*-isomer: ^{1}H NMR (600 MHz, $CDCl_3$) δ 6.07 (1H, dd, ^{3}J = 5.7 Hz, 2.9 Hz, C*H*=CH), 6.04 (1H, dd, ^{3}J = 5.7 Hz, 3.1 Hz, CH=C*H*), 2.71 (1H, m, Bridgehead CH), 2.47 (1H, m, Bridgehead CH), 2.39 (1H, d, ^{2}J = 13.2 Hz, $CH_2N(CH_3)_2$), 2.28 (1H, d, ^{2}J = 13.2 Hz, CH_2NMe_2), 2.26 (6H, s, $N(CH_3)_2$), 1.55 (1H, ddd, ^{2}J = 8.4 Hz, ^{3}J = 1.5 Hz, ^{3}J = 1.5 Hz, Bridge CH), 1.49 (1H, dd, ^{2}J = 11.5 Hz, ^{3}J = 3.8 Hz, CH_2), 1.30 (1H, ddd, ^{2}J = 8.4 Hz, ^{3}J = 2.7 Hz, ^{3}J = 1.8 Hz, Bridge CH), 0.89 (3H, s, CH_3), 0.78 (1H, dd, ^{2}J = 11.5 Hz, ^{3}J = 2.6 Hz, CH_2). ^{13}C NMR (150 MHz, $CDCl_3$) δ 136.9, 136.0, 71.6, 50.6, 48.4, 47.7, 43.5, 42.8, 39.7, 24.6.

For the *endo*-isomer: ^{1}H NMR (600 MHz, $CDCl_3$) δ 6.09 (1H, dd, ^{3}J = 5.6 Hz, 2.9 Hz, C*H*=CH), 6.05 (1H, m, CH=C*H*), 2.69 (1H, m, Bridgehead CH), 2.43 (1H, m, Bridgehead CH), 2.18 (6H, s, $N(CH_3)_2$), 2.13 (1H, d, ^{2}J = 12.8 Hz, $CH_2N(CH_3)_2$), 1.91 (1H, d, ^{2}J = 12.8 Hz, CH_2NMe_2), 1.58 (1H, ddd, ^{2}J = 8.4 Hz, ^{3}J = 1.5 Hz, ^{3}J = 1.5 Hz, Bridge CH), 1.41 (1H, dd, ^{2}J = 11.5 Hz, ^{3}J = 3.8 Hz, CH_2), 1.32 (1H, m, Bridge CH), 1.21 (3H, s, CH_3), 0.86 (1H, dd, ^{2}J = 11.5 Hz, ^{3}J = 2.6 Hz, CH_2). ^{13}C NMR (150 MHz, $CDCl_3$) δ 136.3, 135.5, 69.7, 52.4, 47.8, 47.5, 42.9, 42.1, 40.6, 26.3.

HRMS EI (*m*/*z*): calc. for $C_{11}H_{19}N$, 165.1517; found, 165.1522.

Preparation of *N*,*N*,*N*-trimethyl-1-(2-methylbicyclo[2.2.1]hept-5-en-2-yl)methanaminium iodide (2.3): To a solution of *N*,*N*-dimethyl-1-(2-methylbicyclo[2.2.1]hept-5-en-2-yl)methanamine (12.5 g, 75.6 mmol) in 125 mL acetone, methyl iodide (7.1 mL, 114 mmol) was added dropwise and stirred at 20 ºC with the formation of a white precipitate occurring after 2 minutes. After stirring for 16 hours to ensure complete reaction, 100 mL *n*-pentane was added to the reaction

mixture and filtered. The white powder was washed with 3-100 mL portions of *n*-pentane, isolated and dried under vacuum affording **2.3** (18.5 g, 60.2 mmol) in 80% yield. Compound **2.3** can be recrystallized from hot dichloromethane, chloroform, or acetonitrile, at 4 ºC yielding single crystals as the *exo* isomer exclusively. ^{1}H NMR (600 MHz, $CDCl_3$) δ 6.19 (1H, dd, ^{3}J = 6.0 Hz, 3.0 Hz, C*H*=CH), 6.05 (1H, dd, ^{3}J = 6.0 Hz, 3.0 Hz, CH=C*H*), 3.88 (2H, m, CH_2N$(CH_3)_2$), 3.55 (9H, s, N$(CH_3)_3$), 2.90 (1H, b, Bridgehead CH), 2.67 (1H, b, Bridgehead CH), 2.09 (1H, dd, ^{2}J = 12.0 Hz, ^{3}J = 4.2 Hz, CH_2), 1.85 (1H, d, ^{2}J = 9.0 Hz, Bridge CH), 1.43 (1H, d, ^{2}J = 9.0 Hz, Bridge CH), 1.17 (3H, s, CH_3), 0.96 (1H, dd, ^{2}J = 12.0 Hz, ^{3}J = 3.0 Hz, CH_2). ^{13}C NMR (150 MHz, $CDCl_3$) δ 138.2, 134.8, 77.6, 56.2, 52.4, 48.4, 44.4, 43.3, 40.4, 25.8. Anal. calc. for $C_{12}H_{22}NI$: C, 46.92; H, 7.22; N, 4.56. Anal. found: C, 47.18; H, 7.33; N, 4.55.

2.4.5 AAEM synthesis and characterization

Control Measurements of Nafion 112: The average proton conductivity values measured for four samples at 20 ºC and 50 ºC were 75 ± 2 mS/cm and 112 ± 3 mS/cm, respectively. The average tensile stress and strain at maximum loads measured for two samples were 31.5 MPa at 194%. The percent dimensional swelling measurements of two stamp-sized samples in 60 ºC deionized water and 2 M aqueous methanol were 1.0 % and 2.2 %, respectively.

Preparation of AAEM-2.3-33

To a solution of **1** (0.053 g, 0.17 mmol) and dicyclopentadiene (0.046 g, 0.35 mmol) in 2.0 mL chloroform, a solution of Grubbs' 2nd Generation catalyst (0.0030 g, 0.0035

mmol) in 0.6 mL chloroform was added and stirred for 1 minute at 20 ºC. At this time, the orange reaction mixture was deposited onto a flat glass Petri dish sitting on a hot plate pre-heated to a surface temperature of ca. 30 ºC with a thin metal plate separating the two in order to ensure uniform heating. Within a fumehood, a round glass cover with a volume of 550 mL and a diameter of 7 cm and a Kontes valve affixed at the top to control the rate of solvent evaporation was placed over the Petri dish to prevent drafts yielding even films (Figure 2.3). The reaction mixture solidified after 120-150 minutes, at which time the cover was removed and the surface temperature increased to ca. 75 ºC for 1 hour to ensure all volatiles were removed. The sample was then cooled, and deionized water added to the Petri dish in order to ease removal of the film.

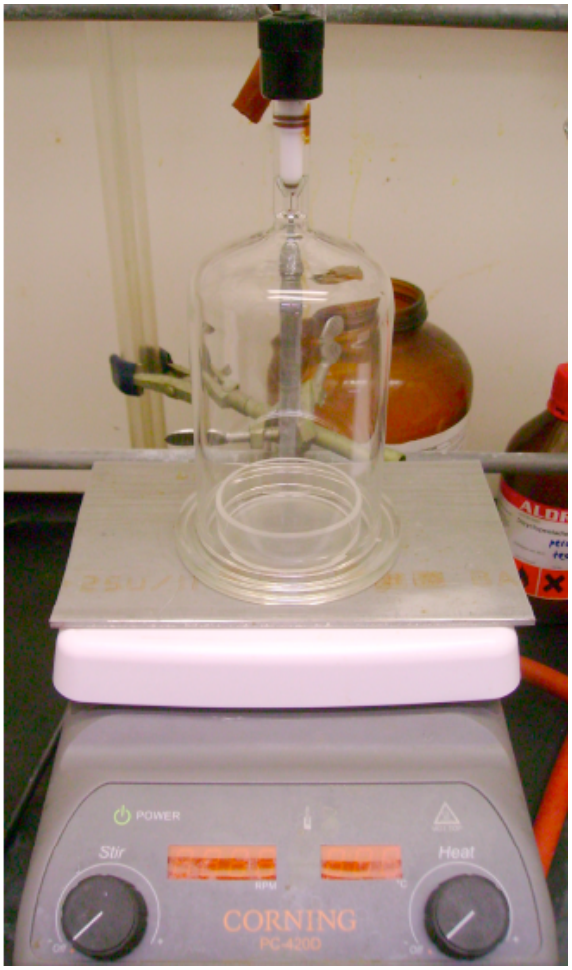

Figure 2.3. Photograph depicting the experimental setup for AAEM preparation.

The measured IEC for two separate AAEMs was 0.96 and 1.04 mmol OH^-/g giving an average value of 1.0 mmol OH^-/g. The average hydroxide conductivity values measured for four separate AAEMs at 20 ºC and 50 ºC were 14 ± 2 mS/cm and 21 ± 4 mS/cm, respectively.

The percent dimensional swelling measurements were:

Sample 1 (2 M methanol): 2.2 %

Sample 1 (deionized water): 0 %

Sample 2 (2 M methanol): 1.1 %

Sample 2 (deionized water): 1.1 %

Average: 1.7 % (methanol), 0.55 % (deionized water)

A single dimensional swelling experiment employing four stamp-sized pieces from the same AAEM sample was also performed as a means of determining the maximum concentration of aqueous methanol the membrane could tolerate (e.g. percent swelling less than 10 %) at 60 ºC. The four pieces, in the hydroxide form, were measured as above and immersed in pre-heated solutions of 4 M, 6 M, 8M and 10 M aqueous methanol. After two hours, the samples' dimensions were re-measured giving percent swelling values of 3.7 %, 3.7 %, 5.4 % and 20.7 %, respectively.

The average tensile stress and strain at break measurements for four thin films were 16 ± 6 MPa and 7.2 ± 3 %, respectively.

Preparation of AAEM-2.3-50

To a solution of **1** (0.070 g, 0.23 mmol) and dicyclopentadiene (0.030 g, 0.23 mmol) in 2.0 mL chloroform, a solution of Grubbs' 2nd Generation catalyst (0.0019 g, 0.0022 mmol) in 0.3 mL chloroform was added and stirred for 1 minute at 20 ºC. At this time, the orange reaction mixture was deposited onto a flat glass dish, and the AAEM generated as above.

The measured IEC for two separate AAEMs was 1.39 and 1.31 mmol OH^-/g giving an average value of 1.35 mmol OH^-/g. The average hydroxide conductivity

values measured for four separate AAEMs at 20 ºC and 50 ºC were 18.2 ± 2.1 mS/cm and 27.9 ± 3.4 mS/cm, respectively.

The average tensile stress and strain at break measurements for four thin films were 2.3 ± 0.5 MPa and 26 ± 3 %, respectively.

2.4.6 Single-crystal x-ray crystallography

Crystals of **1** were transferred from a crystallization vessel onto a microscope slide in a drop of viscous organic oil. Using a nylon loop, a suitable single crystal was chosen and mounted on a Bruker X8 APEX II diffractometer (MoK_α radiation) and cooled to 0 ºC. Data collection and reduction were done using Bruker APEX2[22] and SAINT+[23] software packages. An empirical absorption correction was applied with SADABS.[24] Structure was solved by direct methods and refined on F^2 by full matrix least-squares techniques using SHELXTL[25] software package. All non-hydrogen atoms were refined anisotropically. Hydrogen atoms were added to the model in their geometrically ideal positions. Colorless plate like crystals belong to a monoclinic P2(1)/c space group. The sample size was 0.30x0.20x0.05 mm^3. Overall 16041 reflections were collected, 4203 of which were unique (R_{int} = 0.0264); with 3393 'strong' reflections ($F_o > 4\sigma F_o$). Final R_1 = 3.22 %. Crystallographic data (excluding structure factors) have been deposited with the Cambridge Crystallographic Data Center. Copies of the data can be obtained free of charge on application to CCDC, 12 Union Road, Cambridge CB2 1EZ, UK (fax: (+44)1223-336-033; email:

deposit@ccdc.cam.ac.uk).

APPENDIX

Table 2.2. Crystal data and structure refinement for **2.3**.

Identification code	tjc2	
Empirical formula	C_{13} H_{24} Cl_2 I N	
Formula weight	392.13	
Temperature	273(2) K	
Wavelength	0.71073 Å	
Crystal system	Monoclinic	
Space group	P2(1)/c	
Unit cell dimensions	a = 11.1922(6) Å	α= 90°.
	b = 7.8529(4) Å	β= 103.138(3)°.
	c = 19.6551(10) Å	γ = 90°.
Volume	1682.29(15) $Å^3$	
Z	4	
Density (calculated)	1.548 Mg/m^3	
Absorption coefficient	2.204 mm^{-1}	
F(000)	784	
Crystal size	0.30 x 0.20 x 0.05 mm^3	
Theta range for data collection	1.87 to 28.44°.	
Index ranges	-14<=h<=15, -10<=k<=6, -26<=l<=25	
Reflections collected	15249	
Independent reflections	4203 [R(int) = 0.0264]	

Table 2.2. (Continued)

Completeness to theta = 28.44°	99.0 %
Absorption correction	Semi-empirical from equivalents
Max. and min. transmission	0.8978 and 0.5577
Refinement method	Full-matrix least-squares on F^2
Data / restraints / parameters	4203 / 0 / 166
Goodness-of-fit on F^2	0.999
Final R indices [I>2sigma(I)]	R1 = 0.0322, wR2 = 0.0822
R indices (all data)	R1 = 0.0429, wR2 = 0.0893
Largest diff. peak and hole	0.910 and -0.597 e.Å^{-3}

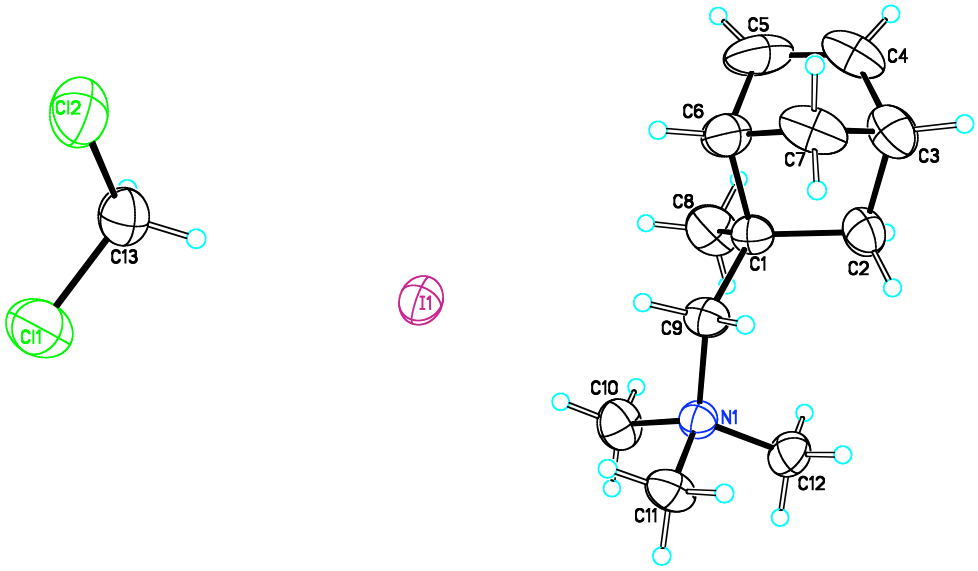

Figure 2.4. ORTEP drawing of **1** with thermal ellipsoids drawn at the 40% probability level.

Table 2.3. Atomic coordinates (x 10^4) and equivalent isotropic displacement parameters ($Å^2$x 10^3) for **2.3**. U(eq) is defined as one third of the trace of the orthogonalized U^{ij} tensor.

	x	y	z	U(eq)
I(1)	5719(1)	7211(1)	1226(1)	48(1)
Cl(1)	8612(1)	4247(2)	183(1)	98(1)
Cl(2)	7288(1)	1548(1)	717(1)	84(1)
N(1)	3773(2)	12228(2)	1455(1)	37(1)
C(1)	1813(2)	10307(3)	1464(1)	40(1)
C(2)	1132(2)	11125(4)	1966(2)	54(1)
C(3)	630(3)	9586(4)	2320(2)	65(1)
C(4)	-265(3)	8677(5)	1778(2)	73(1)
C(5)	317(4)	7926(5)	1358(2)	85(1)
C(6)	1665(3)	8325(4)	1622(2)	63(1)
C(7)	1720(3)	8399(5)	2396(2)	71(1)
C(8)	1217(3)	10701(5)	694(1)	68(1)
C(9)	3208(2)	10590(3)	1654(1)	42(1)
C(10)	3807(3)	12275(4)	698(1)	57(1)
C(11)	5082(2)	12222(4)	1858(1)	50(1)
C(12)	3178(3)	13790(3)	1644(2)	52(1)
C(13)	7221(3)	3577(4)	354(2)	70(1)

Table 2.3. Bond lengths [Å] and angles [°] for **1**.

Cl(1)-C(13)	1.747(3)
Cl(2)-C(13)	1.741(4)
N(1)-C(12)	1.483(3)
N(1)-C(10)	1.498(3)
N(1)-C(11)	1.499(3)
N(1)-C(9)	1.523(3)
C(1)-C(2)	1.520(4)
C(1)-C(9)	1.537(3)
C(1)-C(8)	1.540(3)
C(1)-C(6)	1.603(4)
C(2)-C(3)	1.561(4)
C(3)-C(4)	1.470(5)
C(3)-C(7)	1.516(5)
C(4)-C(5)	1.303(6)
C(5)-C(6)	1.512(5)
C(6)-C(7)	1.509(5)
C(12)-N(1)-C(10)	110.1(2)
C(12)-N(1)-C(11)	108.1(2)
C(10)-N(1)-C(11)	106.4(2)
C(12)-N(1)-C(9)	113.4(2)

Table 2.3. (Continued).

C(10)-N(1)-C(9)	112.5(2)
C(11)-N(1)-C(9)	105.94(18)
C(2)-C(1)-C(9)	114.3(2)
C(2)-C(1)-C(8)	112.6(2)
C(9)-C(1)-C(8)	113.5(2)
C(2)-C(1)-C(6)	101.3(2)
C(9)-C(1)-C(6)	103.75(19)
C(8)-C(1)-C(6)	110.2(2)
C(1)-C(2)-C(3)	104.2(2)
C(4)-C(3)-C(7)	100.0(3)
C(4)-C(3)-C(2)	108.0(3)
C(7)-C(3)-C(2)	99.0(2)
C(5)-C(4)-C(3)	108.8(3)
C(4)-C(5)-C(6)	107.0(3)
C(5)-C(6)-C(7)	99.4(3)
C(5)-C(6)-C(1)	105.9(3)
C(7)-C(6)-C(1)	100.1(3)
C(3)-C(7)-C(6)	94.4(2)
N(1)-C(9)-C(1)	121.21(19)
Cl(1)-C(13)-Cl(2)	113.44(18)

Table 2.4. Anisotropic displacement parameters ($Å^2 x\ 10^3$) for **2.3**. The anisotropic displacement factor exponent takes the form: $-2\pi^2[h^2 a^{*2} U^{11} + ... + 2\ h\ k\ a^*\ b^*\ U^{12}]$

	U^{11}	U^{22}	U^{33}	U^{23}	U^{13}	U^{12}
I(1)	59(1)	43(1)	44(1)	-1(1)	17(1)	3(1)
Cl(1)	72(1)	85(1)	141(1)	10(1)	33(1)	-6(1)
Cl(2)	109(1)	73(1)	83(1)	15(1)	48(1)	17(1)
N(1)	39(1)	34(1)	37(1)	1(1)	10(1)	-1(1)
C(1)	35(1)	40(1)	43(1)	3(1)	4(1)	1(1)
C(2)	48(1)	59(2)	60(2)	1(1)	20(1)	6(1)
C(3)	64(2)	71(2)	63(2)	12(2)	25(1)	2(2)
C(4)	45(1)	88(2)	85(2)	28(2)	15(1)	-11(2)
C(5)	101(3)	67(2)	77(2)	-5(2)	-1(2)	-42(2)
C(6)	54(1)	49(2)	89(2)	-12(2)	21(1)	-8(1)
C(7)	51(2)	78(2)	80(2)	27(2)	7(1)	-12(2)
C(8)	54(2)	99(3)	45(1)	-1(2)	0(1)	-11(2)
C(9)	37(1)	37(1)	50(1)	8(1)	7(1)	1(1)
C(10)	63(2)	72(2)	37(1)	4(1)	12(1)	2(1)
C(11)	39(1)	61(2)	48(1)	5(1)	7(1)	-9(1)
C(12)	63(2)	38(1)	60(2)	-2(1)	21(1)	4(1)

Table 2.4. (Continued)

	U^{11}	U^{22}	U^{33}	U^{23}	U^{13}	U^{12}
C(13)	63(2)	62(2)	88(2)	2(2)	24(2)	10(2)

Table 2.5. Hydrogen coordinates (x 10^4) and isotropic displacement parameters ($Å^2$x 10^3) for **2.3**.

	x	y	z	U(eq)
H(2A)	466	11836	1717	65
H(2B)	1682	11814	2311	65
H(3A)	365	9842	2751	77
H(4A)	-1108	8643	1741	87
H(5A)	-31	7270	970	102
H(6A)	2243	7548	1474	76
H(7A)	1582	7300	2590	85
H(7B)	2476	8899	2661	85
H(8A)	359	10432	601	102

Table 2.5. (Continued).

	x	y	z	U(eq)
H(8B)	1604	10030	397	102
H(8C)	1318	11888	604	102
H(9B)	3450(20)	10540(30)	2131(13)	40(7)
H(9A)	3630(30)	9740(40)	1484(16)	74(10)
H(10A)	2986	12354	418	86
H(10B)	4186	11254	579	86
H(10C)	4272	13246	611	86
H(11A)	5494	13212	1737	75
H(11B)	5484	11216	1744	75
H(11C)	5108	12234	2349	75
H(12A)	3609	14774	1535	79
H(12B)	3200	13777	2135	79
H(12C)	2341	13831	1384	79
H(13A)	6598	3588	-79	84
H(13B)	6974	4380	671	84

References

1. (a) Appleby, A. J.; Foulkes, R. L. *Fuel Cell Handbook*; Van NostrandReinhold: New York, 1989. (b) Whittingham, M. S.; Savinelli, R. F.;Zawodzinski, T. A.; *Chem. Rev*. **2004**, *104*, 4243-4244.

2. Lee, C. H.; Park, H. B.; Lee, Y. M.; Lee, R. D. *Ind. Eng. Chem. Res*.**2005**, *44*, 7617-7626.

3. Gil, M.; Ji, X.; Li, X.; Na, H.; Hampsey, J. E.; Lu, Y. *J. Membr. Sci*.**2004**, *234*, 75-81.

4. Thomas, S. C.; Ren, X.; Gottesfeld, S.; Zelenay, P. *Electrochim. Acta*. **2002**, *47*, 3741-3748.

5. Varcoe, J. R.; Slade, R. C. T. *Fuel Cells* **2005**, *5*, 187-200 and references therein.

6. Varcoe, J. R.; Slade, R. C. T.; Yee, E. L. H.; Poynton, S. D.; Driscoll, D.J.; Apperley, D. C. *Chem. Mater*. **2007**, *19*, 2686-2693.

7. (a) Hibbs, M. R.; Hickner, M. A.; Alam, T. M.; McIntyre, S. K.; Fujimoto, C. H.; Cornelius, C. J. *Chem. Mater*. **2008**, *20*, 2566-2573. (b) Wang, G.; Weng, Y.; Chu, D.; Chen, R.; Xie, D. *J. Membr. Sci*. **2009** *332*, 63-68. (c) Zhou, J.; Unlu, M.; Vega, J. A.; Kohl, P. A. *J. Power Sources* **2009**, *190*, 285-292.

8. (a) *Handbook of Metathesis;* Grubbs. R. H., Ed.; Wiley-VCH: Weinheim, Germany, 2003. (b) Trnka, T. M.; Grubbs, R. H. *Acc. Chem. Res.* **2001**, *34*, 18-29. (c) Grubbs, R. H. *Angew. Chem. Int. Ed.* **2006**, *45*, 3760-3765.

9. Bloch, R.; Gilbert, L. *Tetrahedron* **1988**, *44*, 2523-2539. A modified procedure was used,.

10. Einsla, B. R.; Chempath, S.; Pratt, L. R.; Boncella, J. M.; Rau, J.; Macomber, C.; Pivovar, B. S. *Electrochem. Soc. Trans.* **2007**, *11*, 1173-1180.

11. Chempath, S.; Einsla, B. R.; Pratt, L. R.; Macomber, C.; Boncella, J. M.; Rau, J. A.; Pivovar, B. S. *J. Phys. Chem. C* **2008**, *112*, 3179-3182.

12. (a) Bauer, B.; Strathmann, H.; Effenberger, F. *Desalination*, **1990**, *79*, 125-164. (b) Sata, T.; Tsujimoto, M.; Yamaguchi, T.; Matsusaki, K. *J. Membr. Sci.* **1996**, *112*, 161-170.

13. (a) Lynn, D. M.; Mohr, B.; Grubbs, R. H.; *J. Am. Chem. Soc.* **1998**, *120*, 1627-1628. (b) Boyd, T. J.; Schrock, R. R. *Macromolecules* **1999**, *32*, 6608. (c) Lynn, D. M.; Mohr, B.; Grubbs, R. H.; Henling, L. M.; Day, M. W. *J. Am. Chem. Soc.* **2000**, *122*, 6601-6608. (d) Hong, S. H.; Grubbs, R. H. *J. Am. Chem. Soc.* **2006**, *128*, 3508-3509. (e) Jordan, J. P.; Grubbs, R. H. *Angew. Chem. Int. Ed.* **2007**, *46*, 5152-5155.

14. Vargas, J.; Santiago, A. A.; Tlenkopatchev, M. A.; Gaviño, R.; Laguna, M. F.; López-González, M.; Riande, E. *Macromolecules* **2007**, *40*, 563-570.

15. (a) Chen, L.; Phillip, W. A.; Cussler, E. L.; Hillmyer, M. A. *J. Am. Chem. Soc.* **2007**, *129*, 13786-13787. (b) Chen, L.; Hillmyer, M. A. *Macromolecules* **2009**, *42*, 6075-6085.

16. (a) Schmeisser, J.; Holdcroft, S.; Yu, J.; Ngo, T.; McLean, G. *Chem. Mater.* **2005**, *17*, 387-394. (b) Zhou, Z.; Dominey, R. N.; Rolland, J. P.; Maynor, B. W.; Pandya, A. A.; DeSimone, J. M. *J. Am. Chem. Soc.* **2006**, *128*, 12963-12972.

17. Silva, R. F.; De Francesco, M.; Pozio, A. *J. Power Sources* **2004**, *134*, 18-26.

18. Nguyen, M. T.; Matus, M. H.; Jackson, V. E.; Ngan, V. T.; Rustad, J. R.; Dixon, D. A. *J. Phys. Chem. A* **2008**, *112*, 10386-10398 and references therein.

19. Out of concern for this carbonation process, Varcoe and Slade have investigated the conductivities of their AAEMs in the carbonate form and reported a decrease in conductivity, relative to the hydroxide form, by a factor of 2.3 at room temperature. See Reference 6.

20. Adams, L. A.; Poynton, S. D.; Tamain, C.; Slade, R. C. T.; Varcoe, J. R.; *Chem. Sus. Chem.* **2008**, *1*, 79-81.

21. Fujimoto, C. H.; Hickner, M. A.; Cornelius, C. J.; Loy, D. A. *Macromolecules* **2005**, *38*, 5010-5016.

22. APEX2 v.1.0-22 User Manual, Bruker AXS Inc., Madison WI 53719, 2004.

23. SAINT+ v.6.02 User Manual, Bruker AXS Inc., Madison WI 53719, 1999.

24. Sheldrick, G. M. SADABS, Program for Empirical Absorption Correction of Area Detector Data, University of Göttingen, 1996.

25. Sheldrick, G. M. SHELXTL v. 5.10 Bruker AXS Inc., Madison WI 53719, 1999.

Chapter 3

Solvent Processable Tetraalkylammonium-Functionalized Polyethylene for use as an Alkaline Anion Exchange Membrane

Reprinted in part with permission from the

Macromolecules **2010** *30*, 7147-7150.

3.1 Introduction

Fuel cells are devices that convert the chemical energy stored in a fuel directly into electricity and could potentially serve as a highly efficient and environmentally sustainable power generation technology.[1] Within a fuel cell, the polymer electrolyte membrane serves as the ion conducting medium between the anode and cathode, and as a result is a central, and often performance-limiting component of the fuel cell.[2] The most common polymer electrolyte membrane fuel cells operate under acidic conditions and are therefore proton conducting. Nafion®, a PEM, has dominated the field due its good processability, chemical and thermal stability, and proton conductivity (when properly hydrated).[3,4] Although PEM fuel cells offer excellent performance, they rely almost exclusively on platinum, a very expensive and scarce noble metal.[5] A major advantage of alkaline fuel cells, relative to acidic fuel cells, is their enhanced reaction kinetics for both oxygen reduction and fuel oxidation permitting the use of less costly, non-noble metal catalysts (e.g. Ni).[6] As a result, there is now considerable interest in hydroxide conducting polymer electrolyte membranes, also known as AAEMs, for fuel cells operating under basic conditions.[7-16]

Recent developments reported by Varcoe, Slade and co-workers have shown that radiation grafting of poly(vinylbenzyl chloride) onto mixed fluorocarbon/hydrocarbon membranes, followed by amination, yields mechanically strong AAEMs with promising hydroxide conductivities.[7] Others have reported that polysulfones can act as scaffolds for successive post polymerization modification reactions again yielding conductive AAEMs.[8-13] Moreover, Cornelius and co-workers have shown that AAEMs based on a poly(phenylene) backbone display impressive

conductivities and alkaline stability.[9] We have recently reported on the synthesis of both a norbornene-based and cyclooctene-based system of crosslinked AAEMs through the ring-opening metathesis polymerization (ROMP) of tetraalkylammonium-functionalized cyclic olefins (Figure 3.1).[10,11] Due to the exceptional functional group tolerance of [Ru], this synthetic method has eliminated the need for post polymerization modification thereby allowing the facile synthesis of highly conductive

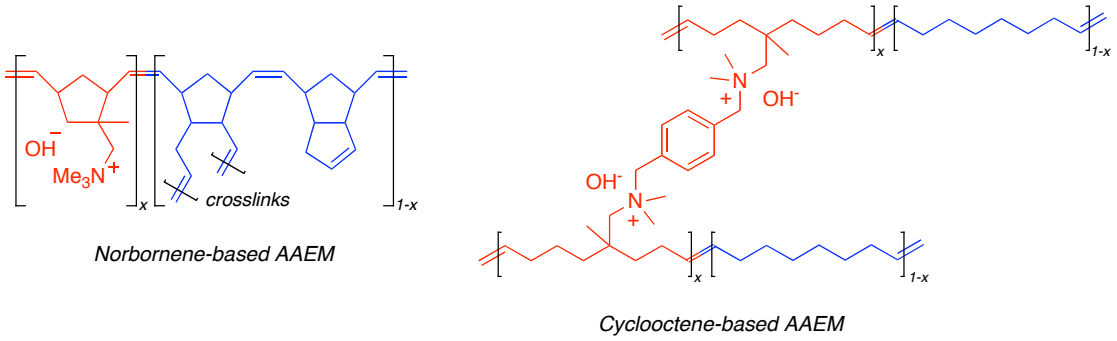

Figure 3.1. Norbornene-based and cyclooctene-based crosslinked AAEMs.

and mechanically strong AAEMs. However, due to the crosslinked nature of the AAEMs they are insoluble in all solvents, limiting their utility. Furthermore, since both systems are based on unsaturated polymer backbones they may not be sufficiently stable when exposed to the harsh oxidizing and reducing conditions of fuel cell operation. As a result, we have also been interested in developing saturated non-crosslinked copolymers that can offer benefits such as solvent processability and chemical tunability. In order to accomplish this, we propose a modified ROMP route toward fully saturated AAEMs by adding a final olefin hydrogenation step (Figure 3.2). In this chapter we report on the synthesis of highly conductive and solvent processable tetraalkylammonium-functionalized polyethylene for use as an AAEM.

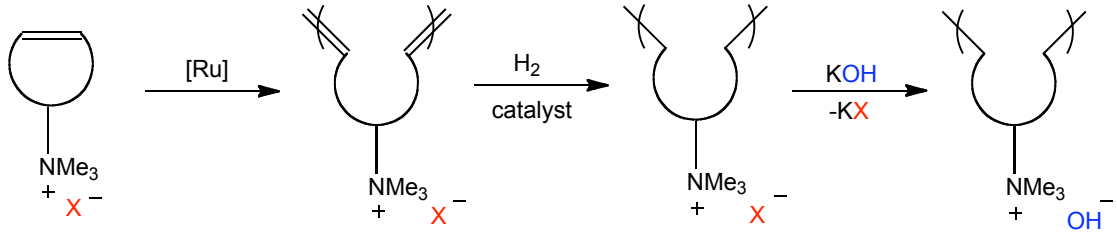

Figure 3.2. ROMP route toward fully saturated AAEMs via olefin hydrogenation.

3.2 Results and discussion

Monomer **3.6** was prepared in six steps in 39% overall yield (Scheme 3.1). First, the hydroesterification of cyclooctadidene furnished the ester cyclooctene derivative **3.1**. This was followed by the methylation of the β carbon relative to the ester furnishing **3.2**. Next, the $LiAlH_4$ reduction of the ester afforded the alcohol **3.3**, which was then oxidized via a swern oxidation giving aldehyde **3.4**. The reductive amination of **3.4** with dimethylamine provided neutral amine **3.5**, which was then alkylated with methyl iodide to give **3.6** as a white powder. The lack of β-hydrogen atoms in **3.6** prevents Hofmann elimination degradation from occurring in the hydroxide form, increasing the ammonium ion stability.[12] Additionally, trimethylammonium groups have been shown to be reasonably stable, exhibiting negligible degradation under alkaline conditions at elevated temperatures when properly hydrated.[13]

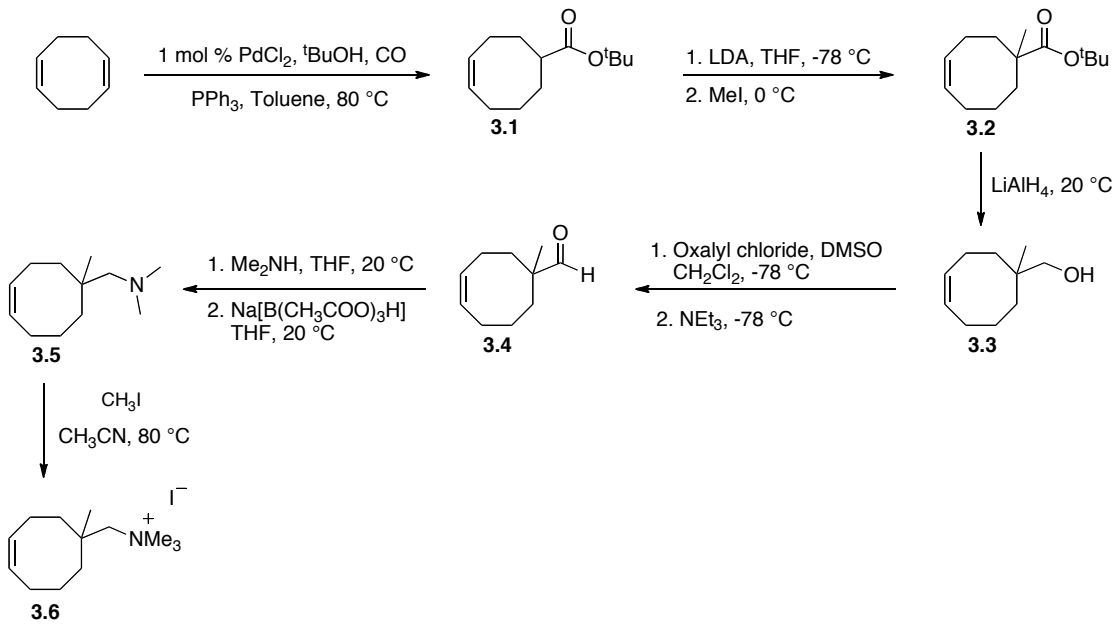

Scheme 3.1. Synthesis of an ammonium functionalized cyclooctene monomer.

We used ROMP to synthesize copolymers of varying composition by introducing [Ru] to a chloroform/methanol solution of cyclooctene (**COE**) and **3.6** at 20 °C in air (Scheme 3.2). After 1 hour the solvents and trace unreacted **COE** were removed under vacuum, and the subsequent polymer washed with chloroform to remove unreacted **3.6** with yields exceeding 90%. The relative ratio of the two monomers (determined by ^{1}H NMR spectroscopy) remains nearly constant throughout the reaction, indicative of a statistically random copolymerization. These copolymers were then cast into thin films and the iodide counterion was exchanged for a hydroxide to generate AAEMs, but unfortunately they displayed poor mechanical properties due to considerable swelling in water. Moreover, it has been previously noted that unsaturated polymers synthesized via ROMP may not be stable under ambient conditions for prolonged periods due to oxidative degradation, and this is

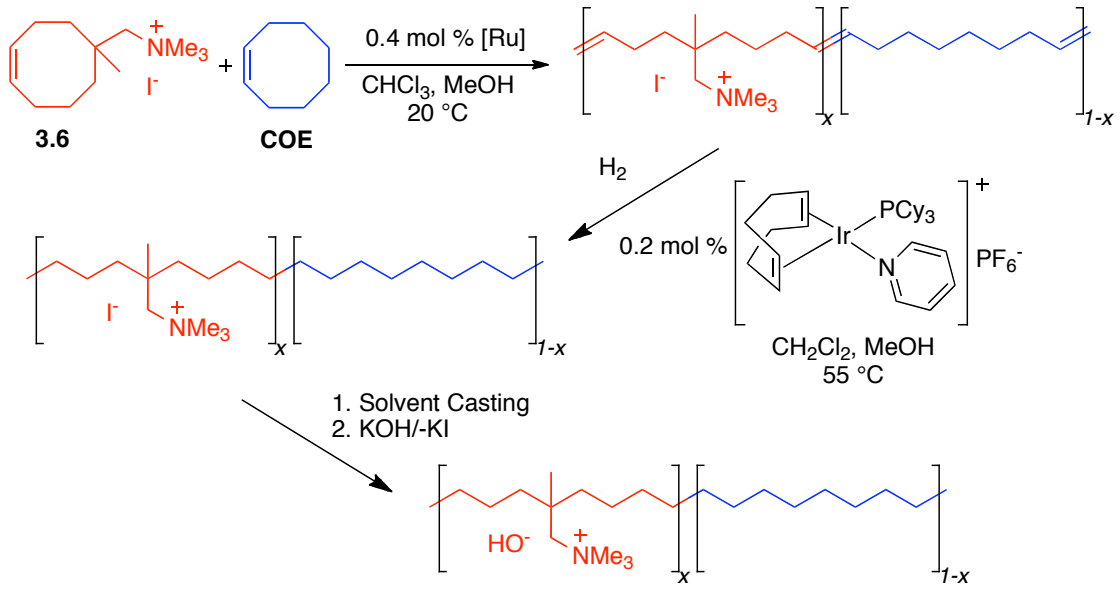

Scheme 3.2. Synthesis of a tetraalkylammonium-functionalized polyethylene.

critical as fuel cell membranes are exposed to harsh oxidizing and reducing conditions during operation.[14,15] Therefore, all the unsaturated copolymer samples were hydrogenated to produce a saturated backbone with the expectation that these concerns over stability would be eliminated. It should be noted that even though oxidative radical degradation is a concern with hydrocarbon-based PEMs, it has been shown that this degradation pathway is hindered under the highly alkaline conditions intrinsic to AAEM operation.[6,16] Preparation of the saturated copolymers was accomplished by hydrogenating the polyolefins using Crabtree's catalyst ([COD]Ir(Py)(PCy_3)]PF_6, Scheme 2.2) and hydrogen gas. Quantitative conversion was typically complete within 17 hours as confirmed by the complete disappearance of olefinic resonances in the ^{1}H NMR spectrum, effectively yielding tetraalkylammonium-functionalized polyethylene. Furthermore, it was expected that this polyethylene backbone would provide the

hydrophobic support necessary for the high ion incorporation required to maximize conductivity without the detrimental loss of mechanical stability due to swelling. Supporting this are reports in which PEMs are blended with polyethylene to provide additional mechanical support, decreased membrane swelling, and increased methanol cross over tolerance.[17,18]

The hydrogenated copolymers in the iodide form were dissolved in a chloroform/methanol cosolvent mixture and cast onto a fluoropolymer-lined metal dish preheated to 40 °C from which the volatiles were slowly evaporated. The films were removed from the dish and dried under vacuum to exhaustively remove residual solvent. Analysis of the thin films by transmission electron microscopy (TEM) revealed no microphase separation suggesting a random distribution of tetraalkylammonium ions (Figure 3.3 and 3.4).

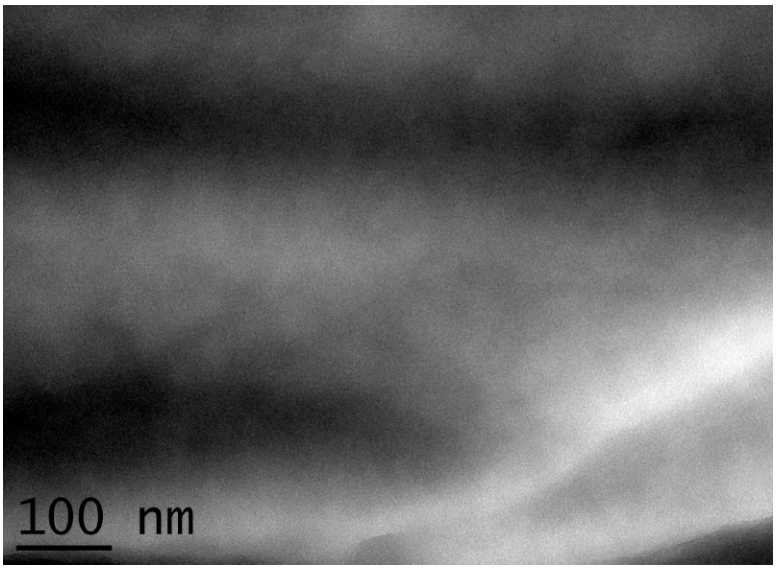

Figure 3.3. TEM image of the saturated copolymer (in iodide form) with 29 mol % **3.6**.

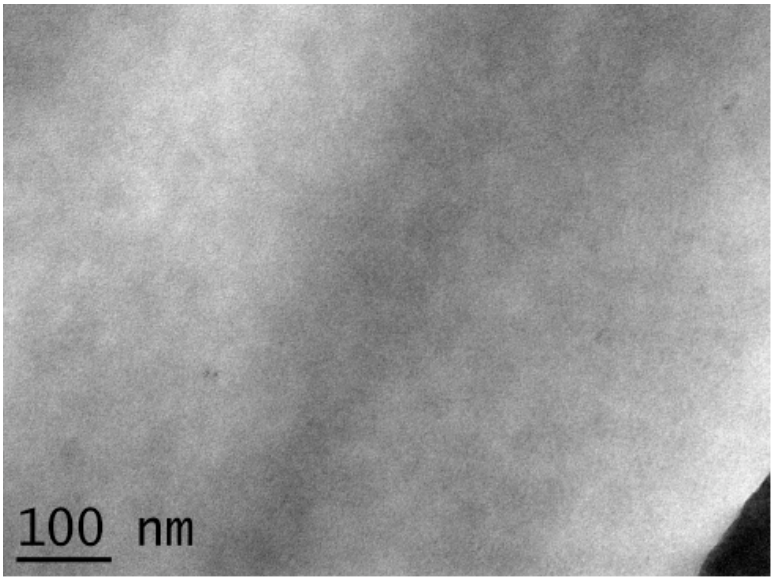

Figure 3.4. TEM image of the saturated copolymer (in iodide form) with 33 mol % **3.6**.

Ion exchange was accomplished by soaking the films in 1 M potassium hydroxide, furnishing transparent and nearly colorless AAEMs. The optimized AAEMs, with respect to mechanical properties and hydroxide ion conductivity, had 29 (AAEM-**3.6**-29) or 33 (AAEM-**3.6**-33) mol % **3.6**. Attempts to synthesize AAEMs with a higher mol % **3.6** led to materials with excessive swelling, while increasing the mol % **COE** led to decreased hydroxide conductivity. Detailed characterization data for both optimized AAEM compositions are provided in Table 3.1. Overall, the AAEMs are easily handled, exhibiting excellent flexibility and strength. Typical film thicknesses ranged from 20-50 μm, however membranes as thin as 10 μm were synthesized without any loss of mechanical integrity. Thinner AAEMs are desirable due to their decreased ionic resistance, resulting in increased fuel cell performance.

Table 3.1. AAEM characterization data.

Measurement	AAEM-**3.6**-29	AAEM-**3.6**-33
mol % **3.6** [a]	29	33
IEC (mmol OH^-/g I^-)[b]	1.29 ± 0.08	1.50 ± 0.07
% Water uptake[c]	97 ± 10	132 ± 10
Tensile Strength at break (MPa)[d]	9 ± 2	6 ± 1
% Strain at break[d]	170 ± 40	130 ± 40
OH^- σ_{20} (mS/cm)[e]	40 ± 2	48 ± 3
OH^- σ_{50} (mS/cm)[e]	59 ± 2	65 ± 3
CO_3^{2-} σ_{20} (mS/cm)[f]	12 ± 1	13 ± 1
CO_3^{2-} σ_{50} (mS/cm)[f]	29 ± 3	30 ± 2

[a]Determined by ^{1}H NMR spectroscopy. [b]Ion exchange capacity determined by back titration, average of 3 trials. [c]Gravimetric water uptakes of the fully hydrated membranes, average of 5 trials. [d]Mechanical testing of the films in the iodide form, average of 6 trials. [e]Hydroxide conductivities of the AAEMs fully immersed in degassed water at 20 °C and 50 °C, average of 4 trials. [f]Carbonate conductivities of the AAEMs fully immersed in degassed water at 20 °C and 50 °C, average of 3 trials.

A significant challenge in alkaline fuel cell research is the development of an alkaline analogue of commercially available solutions of Nafion.[6] Nafion is insoluble in water and aqueous methanol, but soluble in mixtures of other low boiling point solvents including ethanol and *n*-propanol. This solvent processability allows Nafion to be impregnated into the electrocatalyst layers producing an ionomer interface material found in high performing PEM fuel cells.[19] A critical consequence of this solvent processability is that the same polymer can be used as both the polymer electrolyte membrane and ionomer interface material. Surprisingly, the AAEMs are

completely insoluble in both pure water and aqueous methanol at 50 ˚C (50 vol. % water) allowing the use of methanol as a fuel, but exhibit excellent solubility in a variety of other aqueous alcohols (Table 3.2 and 3.3). This solvent processability (Figure 3.5) potentially extends the utility of this system for use as both a fuel cell membrane *and* ionomer interface material from a single polymer, much like Nafion.

Table 3.2. Solubility of AAEM-**3.6**-29.[a]

Solvent	50 vol% in water	Pure Solvent
Water	n.d.	–
Methanol	–	–
Ethanol	–	±
n-Propanol	+	+
Acetone	–	–
Tetrahydrofuran	–	–

[a] 5 wt% AAEM, +: soluble, –: insoluble, ± partially soluble.

Table 3.3. Solubility of AAEM-**3.6**-33.[a]

Solvent	50 vol% in water	Pure Solvent
Water	n.d.	–
Methanol	–	±
Ethanol	–	±
n-Propanol	+	+
Acetone	–	–
Tetrahydrofuran	–	–

[a] 5 wt% AAEM, +: soluble, –: insoluble, ± partially soluble.

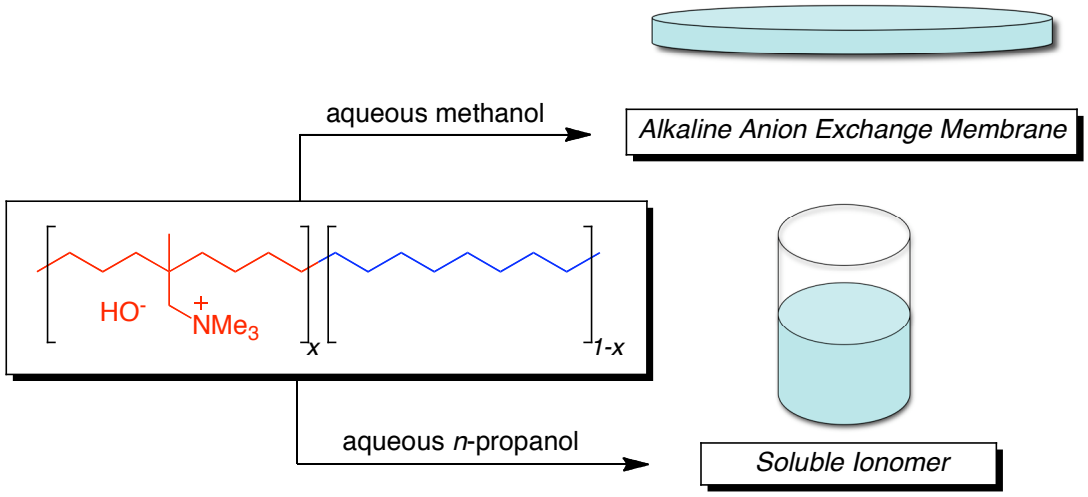

Figure 3.5. AAEM and soluble ionomer from one polymer.

The ion exchange capacities (IECs) for AAEM-**3.6**-29 and AAEM-**3.6**-33 are 1.29 and 1.50 mmol OH^-/g, respectively. These IECs are within the range of previously reported AAEMs and both commercial and non-commercial ionomer interface materials.

It has been shown that sufficient water uptake of AAEMs is needed to form interconnected hydrated domains thereby maximizing ion conductivity; however, excessive water uptake may also result in a detrimental loss of mechanical integrity.[8,10] The gravimetric water uptake (WU) values of the optimized AAEMs were measured and as expected, increasing the ionic content of the AAEMs led to an increase in WU with AAEM-**3.6**-29 and AAEM-**3.6**-33 exhibiting WUs of 97 % and 132 %, respectively. These WU values exceed those of most current AAEMs, potentially leading to increased hydroxide ion conductivity; however, we were concerned that this would also result in poor mechanical properties.

Tensile stress-strain measurements were performed in order to evaluate the mechanical properties of both samples. AAEM-**3.6**-29 had a tensile strength at break of 9 MPa at a strain of 170 %, while AAEM-**3.6**-33 sample showed a tensile strength at break of 6 MPa at a strain of 130 %. Although Varcoe, Slade and co-workers report materials that display greater tensile strength at break (13-18 MPa), they also exhibit considerably less strain at break (45-70 %).[7] Similarly, we have reported two classes of crosslinked materials that demonstrate greater tensile strength at break but also show less strain at break.[15,16] Nonetheless, this system certainly exhibits the mechanical strength required to function as a fuel cell membrane and underscores the ability of polyethylene to act as an effective hydrocarbon support.

The in-plane hydroxide conductivity for each film composition was measured at 20 °C and 50 °C. AAEM-**3.6**-29 exhibits conductivities of 39 mS/cm at 20 °C and 56 mS/cm at 50 °C. More notably, AAEM-**3.6**-33 conducts at 47 mS/cm at 20 °C and 65 mS/cm at 50 °C. By comparison, Varcoe, Slade and co-workers reported conductivities of 27 mS/cm at 20 °C and 34 mS/cm at 50 °C for their fluorinated system[7] while Cornelius and co-workers observe conductivities of 35 mS/cm at 30 °C for their polysulfone based AAEMs[8] and 50 mS/cm for their poly(phenylene) based AAEMs.[14] Moreover, we have reported a polycyclooctene-based crosslinked AAEM that has outstanding conductivities of 69 mS/cm at 20 °C and 111 mS/cm at 50 °C.[16] However, all of the above referenced AAEMs are insoluble, potentially limiting their utility strictly for use as membranes.

In order to investigate the effect of carbonation on membrane conductivity, AAEM-**3.6**-29 and AAEM-**3.6**-33 in their iodide form were converted to the carbonate

form by immersing them in 1 M potassium bicarbonate. The in-plane carbonate conductivity for each film composition was measured at 20 °C and 50 °C. AAEM-**3.6**-29 exhibits carbonate conductivities of 12 mS/cm at 20 °C and 29 mS/cm at 50 °C while AAEM-**3.6**-33 conducts at 13 mS/cm at 20 °C and 30 mS/cm at 50 °C. By comparison, Varcoe, Slade and co-workers reported carbonate conductivities of 11 mS/cm at 20 °C and 22 mS/cm at 50 °C.[7] Although these results suggest decreased ionic conductivity after carbonation, other studies suggest this is not detrimental to fuel cell performance as hydroxide anions are continuously regenerated by oxygen reduction at the cathode.[25]

As previously mentioned, a significant challenge in alkaline fuel cell research has been the development of an AAEM that is insoluble in water and aqueous methanol, but soluble in mixtures of other low boiling point solvents such as *n*-propanol (removal of a high boiling point solvent is considered difficult and unsafe in the presence of finely dispersed catalysts).[6] Zhang and co-workers have recently reported a highly conductive partially fluorinated polysulfone (84 mS/cm at 20 °C) that is soluble in *n*-propanol; however, there is no mention of its solubility in methanol.[11] Furthermore, the membrane became gel-like when placed in water at 60 °C. Yan and co-workers synthesized a soluble quaternary phosphonium-functionalized polysulfone for use as an alkaline ionomer interface material that is considerably more conductive (27 mS/cm at 20 °C) than commercially available analogues (e.g., Tokuyama Co. product code: AS-4, exhibits a conductivity of 13 mS/cm),[26] but unfortunately, these materials are soluble in pure and aqueous methanol (50 vol. % water) likely precluding the use of methanol as a fuel.[27] By comparison, the current

system displays excellent conductivities, is soluble in aqueous *n*-propanol (50 vol. % water) and is insoluble in aqueous methanol (50 vol. % water).

3.3 Conclusion

In summary, we have developed a tetraalkylammonium-functionalized polyethylene that exhibits excellent mechanical strength and high hydroxide conductivity, in addition to being solvent processable. This solvent processability extends the potential utility of this system for use as both an AAEM and ionomer interface material from a single polymer composition. Future work will focus on studying the chemical stability and performance of these materials under fuel cell operating conditions as well as synthesizing and investigating the use of novel cations.

3.4 Experimental

3.4.1 General methods and materials

All reactions and manipulations of compounds were carried out in air unless otherwise specified. Dimethylamine (2.0 M solution in tetrahydrofuran), sodium triacetoxyborohydride, potassium hydroxide, potassium bicarbonate, potassium carbonate, tert-butyl alcohol, oxalyl chloride (98%), triethylamine, *cis*-cyclooctene (95%), Grubbs' 2nd Generation catalyst (CAS Number: 246047-72-3), Crabtree's catalyst (CAS Number: 64536-78-3), standardized hydrochloric acid (0.1014 M) and standardized potassium hydroxide (0.1000 ± 0.0001 M) were purchased from Sigma-

Aldrich and used as received. Methyl iodide (99%), 1,5-cyclooctadiene (99%), *n*-butyllithium (1.6 M solution in hexanes), and lithium aluminum hydride (4.0 M solution in diethyl ether) were all purchased from Acros Organics and used as received. Diisopropylamine was purchased from Sigma-Aldrich and vacuum transferred from calcium hydride. All solvents were purchased from Sigma-Aldrich or Mallinckrodt. Tetrahydrofuran and diethyl ether were dried by passage over an alumina packed drying column glass contour. Hydrogen (99.99%) was purchased from Airgas. Palladium (II) chloride and calcium hydride were purchased from Strem Chemicals.

3.4.2 Small molecule characterization

^{1}H and ^{13}C NMR spectra were recorded on Varian MERCURY 300 (^{1}H, 300 MHz, ^{13}C, 75 MHz) or Varian INOVA 600 (^{1}H, 600 MHz, ^{13}C, 151 MHz) NMR spectrometers and referenced to C_6HD_5 (7.16 ppm), C_6D_6 (128.39 ppm), $CHCl_3$ (7.24 ppm), $CDCl_3$ (77.23 ppm), $(D_3C)_2NCHO$ (8.03 ppm) or HDO (4.80 ppm). Mass spectra were acquired using a JEOL GCMate II mass spectrometer operating at 3000 resolving power for high resolution measurements in positive ion mode and an electron ionization potential of 70 eV. Samples were introduced *via* a GC inlet using an Agilent HP 6890N GC equipped with a 30 m (0.25 μm i.d.) HP-5ms capillary GC column. The carrier gas was helium with a flow rate of 1 mL/min. Samples were introduced into the GC using a split/splitless injector at 230 °C with a split ratio of 10:1. Elemental analysis was performed by Robertson Microlit Laboratories, Inc. (Madison, NJ).

3.4.3. AAEM Characterization.

Ion exchange capacities (IECs) were determined using standard back titration methods. The thin film as synthesized (in iodide form) was dried under full vacuum overnight at 100 °C in order to completely dehydrate it and then weighed. Conversion to the hydroxide form was achieved by immersing the film in 3×60 mL portions of 1 M potassium hydroxide for 20 minutes each. Residual potassium hydroxide was washed away by immersing the membrane in 3×125 mL portions of deionized water for 20 minutes each. The AAEM was then stirred in 20 mL standardized 0.1 M $HCl_{(aq)}$ solution for 24 hours followed by titration with standardized 0.1 M $KOH_{(aq)}$ to determine the equivalence point. Control acid samples (with no AAEM present) were also titrated with standardized 0.1 M $KOH_{(aq)}$, and the difference between the volume required to titrate the control and the sample was used to calculate the amount of hydroxide ions in the membrane. This was divided by the dried mass of the membrane (*vide supra*) to give an IEC value with the units mmol OH^-/g I^-.

Water uptake was measured by the mass change between the fully hydrated and dried AAEMs. Immediately following hydroxide ion exchange, a sample was dried with a paper towel and placed in a capped vial to ensure accurate weighing. The sample was then dried at 20 °C under vacuum for 17 hours and re-weighed. The water uptake percentage value was calculated by: $WU = [(Mass_{final}-Mass_{initial})/Mass_{initial}]*100$.

The in-plane hydroxide conductivity of the AAEM sample was measured by four probe electrochemical impedance spectroscopy (EIS) using a Solartron 1280B electrochemical workstation along with ZPlot and ZView software. The conductivity

cell was purchased from BekkTech LLC (Loveland, CO), and a helpful schematic and description of a similar experimental setup has been reported.[28] A strip of the thin film in the iodide form (ca. 4 cm long × 0.5 mm wide) was converted to the hydroxide form by immersing it in 3×30 mL portions of 1 M potassium hydroxide for 20 minutes each. Residual potassium hydroxide was washed away by immersing the membrane in 3×60 mL portions of degassed deionized water for 20 minutes each. Aliquots of each of these water washings were removed and analyzed by inductively coupled plasma atomic emission spectrometry (ICP-AES) for potassium ions. ICP-AES was performed by the Cornell Nutrient Analysis Laboratories, Department of Crop and Soil Sciences, Cornell University using a CIROS model from Spectro Analytical Instruments, Inc. and the EPA 6010B method. Negligible potassium ions were detected in the aqueous sample by the third water washing; approximately equal to that detected in deionized water verifying complete removal of base and preventing falsely high hydroxide conductivities. The AAEM was then clamped into the cell using a Proto 6104 torque screwdriver set to 1 inch ounce and completely immersed in degassed Millipore water (> 18 MΩ·cm), at either 20 °C or 50 °C, during the measurement time. EIS was performed by imposing a small sinusoidal (AC signal) voltage, 10 mV, across the membrane sample at frequencies between 20,000 Hz and 0.1 Hz (scanning from high to low frequencies) and measuring the resultant current response. Using a Bode plot, the frequency region over which the impedance had a constant value was checked, and the highest frequency measurement in the Nyquist plot was taken as the effective resistance of the membrane. This was then used to calculate the hydroxide conductivity by employing the following formula: $\sigma = L / Z' \cdot A$

where L is the length between sense electrodes (0.425 cm), Z′ is the real impedance response at high frequency, and A is the membrane area available for hydroxide conduction (width·thickness). The dimensional measurements were performed using a digital micrometer (± 0.001 mm) purchased from Marathon Watch Company Ltd. (Richmond Hill, ON). The in-plane carbonate conductivity of the AAEM sample was measured and calculated using the same procedure as above except that 1 M potassium carbonate was used in place of 1 M potassium hydroxide to convert from the iodide form to the carbonate form.

The mechanical properties of the thin films in the iodide form were characterized using a Model 5566 system from Instron (Canton, MA) using a 100 N static Lodge cell and Blue Hill software. The tensile strengths of the wet samples were measured in the iodide form.

A consistent treatment of the precision of the measurements has been conducted. All errors are determined from sample standard deviations. Confidence intervals are at the 95 % confidence level based on the sample deviations and using the relevant student-*t* distribution (*N*-1 degrees of freedom, *N* is the number of samples tested for each composition).

The solubility of the AAEMs (in hydroxide form) was evaluated by immersing the washed samples in various solvents. The solutions were immediately heated and the membranes kept at 50 °C for 48 hours after which their solubility was qualitatively evaluated and is summarized in Tables S1 and S2.

For transmission electron microscopy (TEM) analysis, a piece of the sample (in iodide form) was embedded in Tissue-Tek and brought into a cryochamber at -60 °C. The samples were then ultramicrotomed on a Leica Ultracut to a thickness of ~60 nm and picked up on a 200 mesh copper TEM grid. Images were taken on an FEI Tecnai T-12 TWIN TEM.

3.4.4. Monomer synthesis

Preparation of (*Z*)-*tert*-butyl-cyclooct-4-enecarboxylate (3.1): This compound was prepared using a modified literature procedure from Wagener and co-workers.[29] *Tert*-butyl alcohol (9.80 mL, 102 mmol), 1,5-cyclooctadiene (20.0 mL, 163 mmol), toluene (9.8 mL), palladium (II) chloride (0.290 g, 1.64 mmol) and triphenylphosphine (1.71 g, 6.52 mmol) were combined in a Parr reactor equipped with an overhead stirrer and sealed. The reactor was pressurized to 800 psig carbon monoxide and then vented down to 50 psig. This process was repeated twice more to purge the reactor of air, then pressurized to 600 psig and heated to 90 °C with rapid stirring. After 12 hours, the pressure had fallen to 300 psig. It was repressurized to 600 psig and stirred for an additional 24 hours after which time it had decreased to 400 psig. It was cooled, vented and the yellow solution washed into a flask with toluene and the volatiles were removed under vacuum. The yellow solution was distilled at 75-80 °C under dynamic vacuum with the receiving flask at -78 °C yielding a colorless oil (17.7 g, 82%). The NMR shifts closely match those in the aforementioned literature procedure.[29] ^{1}H NMR (300 MHz, C_6D_6) δ 5.40-5.58 (2H, m), 2.24-2.40 (1H, m), 2.00-2.20 (2H, m), 1.70-1.95 (4H, m), 1.38-1.62 (3H, m), 1.24-1.36 (9H, s), 1.06-1.24 (1H, m). ^{13}C NMR (75

MHz, C_6D_6) δ 176.68, 130.86, 130.34, 79.39, 44.96, 32.56, 30.16, 28.52, 28.46, 26.50, 24.89. HRMS EI (*m*/*z*): calc. for $C_{13}H_{22}O_2$, 210.1620; found, 210.1621.

Synthesis of (*Z*)-*tert*-butyl-1-methylcyclooct-4-enecarboxylate (3.2): Diisopropylamine (13.9 mL, 99.2 mmol) was added to 160 mL dry tetrahydrofuran and cooled to 0 °C under flow of nitrogen. A solution of *n*-butyllithium (62 mL, 1.6 M solution in hexanes, 99 mmol) was slowly added and then stirred for 20 minutes at 0 °C yielding a pale yellow solution that was then cooled to -78 °C. A solution of compound **3.1** (19.0 g, 90.3 mmol) in 20 mL dry tetrahydrofuran was slowly added over 10 minutes *via* cannulation. The reaction mixture was stirred at -78 °C for 10 minutes and then slowly warmed to 0 °C over 30 minutes. Methyl iodide (11.3 mL, 181 mmol) was added and the reaction mixture allowed to stir for 60 minutes at 0 °C. The yellow solution was then opened to the atmosphere and 90 mL of 8 M hydrochloric acid was slowly added while the solution was still cold, followed by extraction with diethyl ether (3×200 mL). The extracts were combined, washed with saturated sodium bicarbonate (2×100 mL), saturated sodium chloride (2×100 mL) and then dried with magnesium sulfate. Removing the solvent yielded a brown oil. (19.19 g, 95%). ^{1}H NMR (300 MHz, C_6D_6) δ 5.59-5.70 (1H, m), 5.35-5.48 (1H, m), 2.19-2.40 (3H, m), 1.90-2.15 (2H, m), 1.65-1.83 (2H, m), 1.49-1.63 (1H, m), 1.35-1.49 (2H, m), 1.29-1.35 (9H, s), 1.05-1.10 (3H, s). ^{13}C NMR (75 MHz, C_6D_6) δ 176.88, 132.61, 127.21, 79.50, 46.89, 36.62, 33.41, 28.40, 28.37, 26.45, 25.74, 25.28. HRMS EI (*m*/*z*): calc. for $C_{14}H_{24}O_2$, 224.1776; found, 224.1771.

Preparation of (*Z*)-(1-methylcyclooct-4-enyl)methanol (3.3): Compound **3.2** (19.2 g, 85.6 mmol) was dissolved in 200 mL dry diethyl ether and cooled to 0 °C under a flow of nitrogen in a Schlenk adapted round bottom flask equipped with an addition funnel. Lithium aluminum hydride (24.0 mL, 96.0 mmol) was transferred to the addition funnel *via* cannulation and slowly added over 20 minutes turning the orange solution colorless. The solution was stirred at 0 °C for 2 hours and then slowly warmed to room temperature. After stirring for 20 hours at room temperature, the colorless solution was cooled back to 0 °C and 20 mL of ethyl acetate was transferred to the addition funnel and slowly added to the mixture until the solution turned cloudy. At this point the slurry was <u>*slowly*</u> poured over ~600 mL of ice with great caution and stirred overnight forming a white slurry. Concentrated hydrochloric acid was slowly added to the solution until it became homogeneous and then extracted with diethyl ether (3×200 mL). The ether extracts were washed with saturated sodium bicarbonate (200 mL) and saturated sodium chloride (200 mL). The resulting clear solution was dried with magnesium sulfate, filtered and the solvent removed *in vacuo* yielding the alcohol as a colorless oil (13.1 g, 99%). ^{1}H NMR (300 MHz, C_6D_6) δ 5.58-5.69 (1H, m), 5.37-5.49 (1H, m), 2.95-3.05 (2H, s), 1.90-2.20 (4H, m), 1.18-1.48 (7H, m), 0.75-0.81 (3H, s). ^{13}C NMR (75 MHz, C_6D_6) δ 132.95, 126.83, 72.54, 39.36, 35.57, 30.98, 25.97, 25.63, 24.91, 23.32. HRMS EI (*m/z*): calc. for $C_{10}H_{18}O$, 154.1358; found, 154.1363.

Preparation of (*Z*)-1-methylcyclooct-4-enecarbaldehyde (3.4): Prepared using a procedure adapted from Swern and coworkers;[30,31] caution, very foul-smelling reaction. Oxalyl chloride (7.88 mL, 93.1 mmol) was added to 200 mL of dichloromethane in a 500 mL round bottom flask and cooled to -78 °C. Fresh dimethyl sulfoxide (13.2 mL, 186 mmol) was slowly added over 3 minutes resulting in a large amount of gas evolution. This colorless solution was stirred for 10 minutes. A solution of compound **3.3** (13.1 g, 84.7 mmol) in 80 mL dichloromethane was added to the solution, and stirred for 20 minutes at -78 °C yielding a white solution. Addition of triethylamine (118 mL, 847 mmol) with 40 mL dichloromethane yielded a white viscous slurry. This mixture was kept at -78 °C for 10 minutes and then warmed to room temperature over 60 minutes. The slurry was washed with water (3×400 mL) and dried with magnesium sulfate. Removing the solvent afforded a yellow oil (12.1 g, 94%). ^{1}H NMR (300 MHz, C_6D_6) δ 9.10-9.13 (1H, s), 5.43-5.53 (1H, m), 5.25-5.38 (1H, q), 1.81-2.02 (4H, m), 1.70-1.81 (1H, m), 1.41-1.53 (1H, m), 1.21-1.41 (4H, m), 0.60-0.69 (3H, s). ^{13}C NMR (75 MHz, C_6D_6) δ 204.84, 132.13, 127.09, 49.14, 33.52, 29.56, 25.82, 25.33, 24.40, 22.09. HRMS EI (*m*/*z*): calc. for $C_{10}H_{16}O$, 152.1201; found, 152.1200.

Synthesis of (*Z*)-*N*,*N*-dimethyl-1-(1-methylcyclooct-4-enyl)methanamine (3.5): Dimethylamine (80 mL, 160 mmol) was directly added to compound **3.4** (12.1 g, 79.4 mmol) in a 250 mL round bottom flask forming a clear orange solution. After stirring at room temperature for 5 hours with no observable change, the solution was transferred to a large beaker with 300 mL tetrahydrofuran. Sodium

triacetoxyborohydride (25.2 g, 119 mmol) was then added with stirring, forming an orange slurry and was allowed to react for 22 hours. 400 mL diethyl ether was then added to aid clean separation of the organic and aqueous fractions. 1 M hydrochloric acid (2×200 mL) was added to protonate the amine in order to separate it from any alcohol impurities (**3.3**). After isolating the aqueous fractions, 450 mL of 1 M potassium hydroxide was added to regenerate the amine, and the solution was extracted with diethyl ether (3×150 mL). The extracts were combined, washed with water (2×200 mL) and dried with magnesium sulfate. Removing the solvent yielded a pale yellow oil (8.2 g, 57%). ^{1}H NMR (300 MHz, C_6D_6) δ 5.62-5.72 (1 H, m), 5.40-5.54 (1H, m), 2.20-2.38 (1H, m), 1.95-2.20 (9H, m), 1.85-1.95 (2H, d), 1.24-1.62 (6H, m), 1.86-1.92 (3H, s). ^{13}C NMR (75 MHz, C_6D_6) δ 133.10, 126.41, 71.38, 49.47, 40.11, 36.55, 32.47, 26.47, 25.66, 25.01, 24.79. HRMS EI (*m/z*): calc. for $C_{12}H_{23}N$, 181.1830; found, 181.1836.

Preparation of Compound 3.6: Compound **3.5** (3.00 g, 16.5 mmol) and methyl iodide (7.07 g, 49.5 mmol) were combined with 15 mL of acetonitrile in a 100 mL round bottom flask and heated to 80 °C, which briefly gave a homogeneous solution before a white precipitate formed. The reaction mixture was held at 80 °C with vigorous stirring for 19 hours and then poured into 300 mL of diethyl ether to precipitate the product and wash away unreacted organics. The solution was then filtered and the pale yellow solid washed with an additional 200 mL of diethyl ether. Drying the solid overnight under vacuum at 100 °C furnished a faint yellow powder (5.07 g, 95%). ^{1}H NMR (600 MHz, D_2O) δ 6.11-6.17 (1 H, m), 5.90-5.98 (1H, m),

3.68-3.94 (2H, m), 3.34-3.68 (9H, s), 2.47-2.82 (4H, d), 2.28-2.47 (1H, m), 1.83-2.23 (5H, m), 1.49-1.78 (3H, s). ^{13}C NMR (151 MHz, D_2O) δ 132.67, 126.40, 76.37, 56.28, 40.13, 36.72, 33.75, 25.97, 25.38, 24.14, 23.42. Anal. calc. for $C_{13}H_{26}NI$: C, 48.30; H, 8.11; N, 4.33; I, 39.26. Anal. found: C, 48.38 H, 7.97; N, 4.28; I, 39.01.

3.4.5. Polymer synthesis and characterization

Preparation of the Unsaturated Copolymer with 29 mol % 3.6: Compound **3.6** (300 mg, 0.928 mmol) and **COE** (256 mg, 2.32 mmol) were combined and dissolved in a chloroform/methanol cosolvent mixture (3 mL/0.3 mL, respectively). Grubbs' 2nd Generation catalyst (11 mg, 0.013 mmol) was added and the solution allowed to stir vigorously. After 1 hour, the cosolvent mixture and unreacted **COE** were removed under vacuum, and the resulting polymer washed with chloroform. Drying overnight under vacuum at 100 °C furnished a brown solid (501 mg, 90%). ^{1}H NMR (600 MHz, DMF-d_7) δ 5.09-5.77 (6.5 H, m), 3.32-3.91 (11H, m), 1.73-2.37 (13H, br m), 0.88-1.73 (28H, br m). ^{13}C NMR (151 MHz, CD_3Cl/ D_3COD) δ 130.15, 74.64, 56.06, 38.96, 38.39, 32.62, 32.34, 29.44, 28.77, 27.01, 26.31, 24.78, 23.15.

Hydrogenation of the Unsaturated Copolymer with 29 mol % 3.6: The unsaturated copolymer with 29 mol % **3.6** (493 mg) was dissolved in a dichloromethane/methanol cosolvent (10 mL/5.0 mL, respectively) forming a light brown solution. The polymer solution and Crabtree's catalyst (4.7 mg, 0.0058 mmol) were combined in a Parr reactor equipped with an overhead stirrer and sealed. It was pressurized to 800 psig hydrogen and then vented down to 50 psig. This process was repeated twice more to purge the reactor of air, then pressurized to 800 psig and heated to 55 °C with rapid

stirring. After 17 hours, it was cooled, vented and the swollen polymer gel dried under vacuum at 100 °C furnishing a yellow solid. (498 mg, 100%). ^{1}H NMR (600 MHz, DMF-d_7) δ 3.28-3.82 (11 H, m), 1.00-1.76 (55H, br m). ^{13}C NMR (151 MHz, CD_3Cl/ D_3COD) δ 74.67, 55.99 38.84, 29.98, 29.26, 24.69, 22.99.

Preparation of AAEM-3.6-29: The saturated copolymer with 29 mol % **3.6** (90 mg) was dissolved in a chloroform/methanol cosolvent mixture (2 mL/1 mL, respectively) forming a light yellow solution and then transferred to a preheated (40 °C) metal dish (fluoropolymer-lined, diameter of 5.25 cm and depth of 3.0 cm) on top of a hot plate covered with a metal plate to ensure uniform heating. The dish was covered with a round glass cover with a diameter of 7 cm and volume of 550 mL bearing one Kontes glass valve on top to control the rate of solvent evaporation. After one hour the cover was removed and the temperature was increased to 70 °C for another hour. Following this, water was added and the translucent film freely removed from the dish. The film was then soaked in deionized water for at least 24 hours prior to hydroxide ion exchange. The AAEM was generated as described above. To make thinner membranes the amount of polymer was scaled back accordingly.

Preparation of the Unsaturated Copolymer with 33 mol % 3.6: Compound **3.6** (350 mg, 1.08 mmol) and **COE** (237 mg, 2.16 mmol) were combined and dissolved in a chloroform/methanol cosolvent mixture (3 mL/0.4 mL, respectively). Grubbs' 2nd Generation catalyst (11 mg, 0.013 mmol) was added and the solution allowed to stir vigorously. After 1 hour, the cosolvent mixture and unreacted **COE** were removed under vacuum, and the resulting polymer washed with chloroform. Drying overnight

under vacuum at 100 °C furnished a brown solid (539 mg, 92%). ^{1}H NMR (600 MHz, DMF-d_7) δ 5.09-5.77(6 H, m), 3.32-3.91 (11H, m), 1.73-2.37 (12H, br m), 0.88-1.73 (26H, br m). ^{13}C NMR (151 MHz, $CDCl_3$/D_3COD) δ 130.18, 74.52, 55.98, 38.98, 38.26, 32.67, 32.35, 29.45, 28.78, 27.02, 26.33, 24.74, 23.17.

Hydrogenation of the Unsaturated Copolymer with 33 mol % 3.6: The unsaturated copolymer with 33 mol % **3.6** (539 mg) was dissolved in a dichloromethane/methanol cosolvent mixture (10 mL/5.0 mL, respectively) forming a light brown solution. The polymer solution and Crabtree's catalyst (4.8 mg, 0.0060 mmol) were combined in a Parr reactor equipped with an overhead stirrer and sealed. It was pressurized to 800 psig hydrogen and then vented down to 50 psig. This process was repeated twice more to purge the reactor of air, then pressurized to 800 psig and heated to 55 °C with rapid stirring. After 17 hours, it was cooled, vented and the swollen polymer gel dried under vacuum at 100 °C furnishing a yellow solid. (544 mg, 100%). ^{1}H NMR (600 MHz, DMF-d_7) δ 3.28-3.82 (11 H, m), 1.00-1.76 (49H, br m). ^{13}C NMR (151 MHz, CD_3Cl/ D_3COD) δ 75.05, 56.04 38.90, 30.05, 29.52, 24.86, 23.16.

Preparation of the AAEM-3.6-33: The saturated copolymer with 33 mol% **3.6** (90 mg) was dissolved in a chloroform/methanol cosolvent mixture (2 mL/1 mL, respectively) forming a light yellow solution and then transferred to a preheated (40 °C) metal dish (fluoropolymer-lined, diameter of 5.25 cm and depth of 3.0 cm) on top of a hot plate covered with a metal plate to ensure uniform heating. The dish was covered with a round glass cover with a diameter of 7 cm and volume of 550 mL bearing one Kontes glass valve on top to control the rate of solvent evaporation. After

one hour the cover was removed and the temperature was increased to 70 °C for another hour. Following this, water was added and the translucent film freely removed from the dish. The film was then soaked in deionized water for at least 24 hours prior to hydroxide ion exchange. The AAEM was generated as described above. To make thinner membranes the amount of polymer was scaled back accordingly.

Appendix

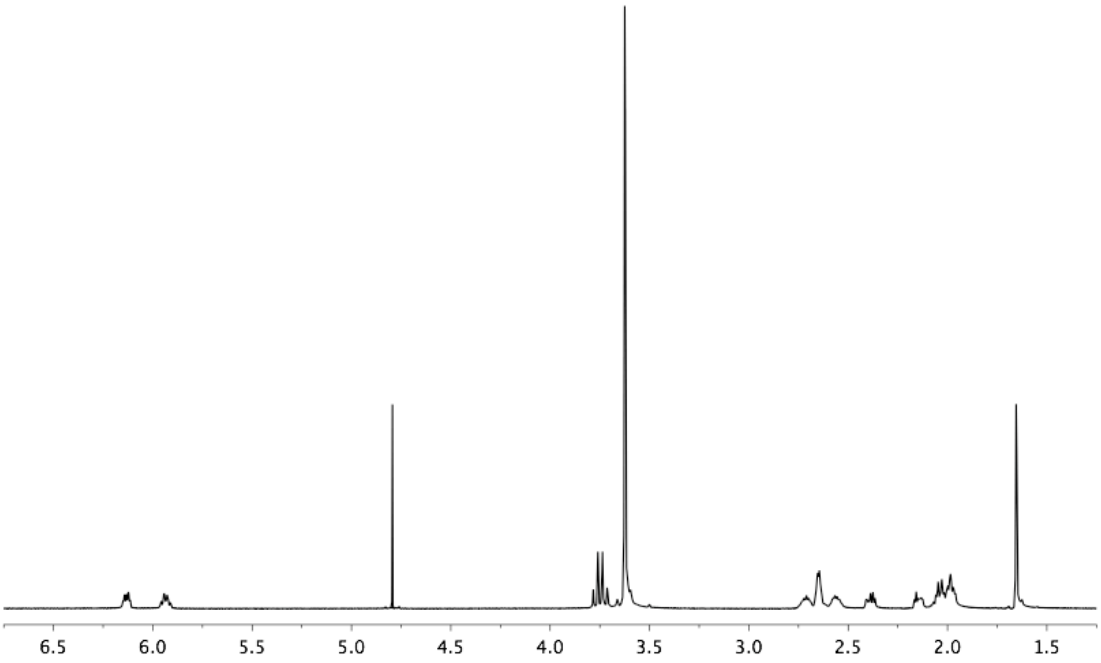

Figure 3.6. ^{1}H spectrum (600 MHz, D_2O) of compound **3.6**.

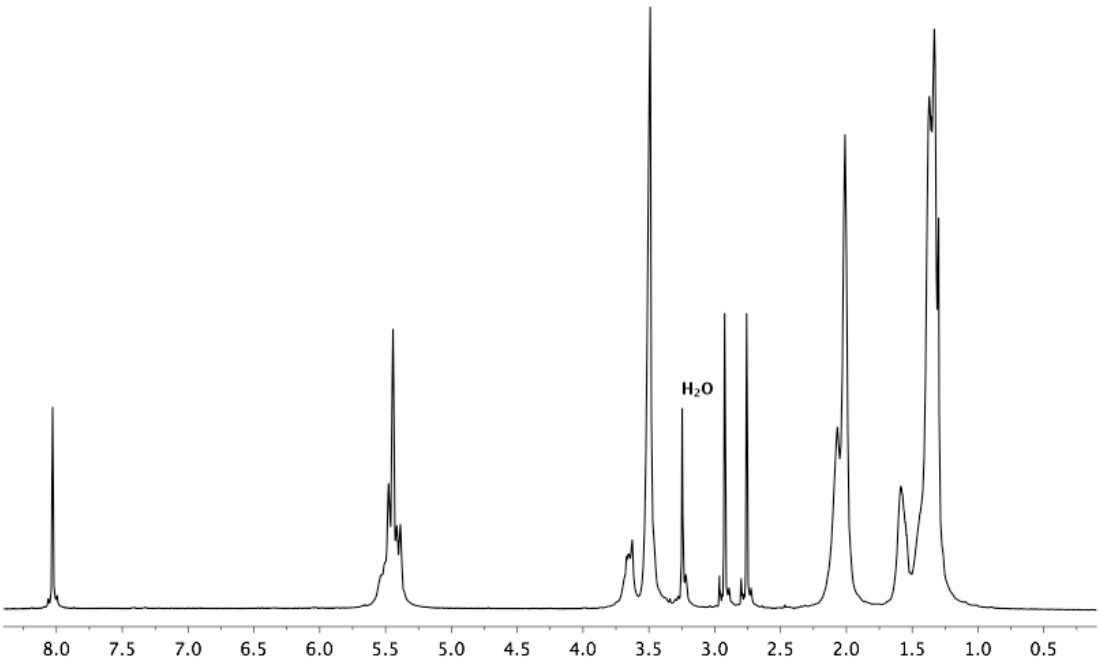

Figure 3.7. ^{1}H spectrum (600 MHz, DMF-d_7) of unsaturated copolymer (in iodide form) with 29 mol % **3.6**.

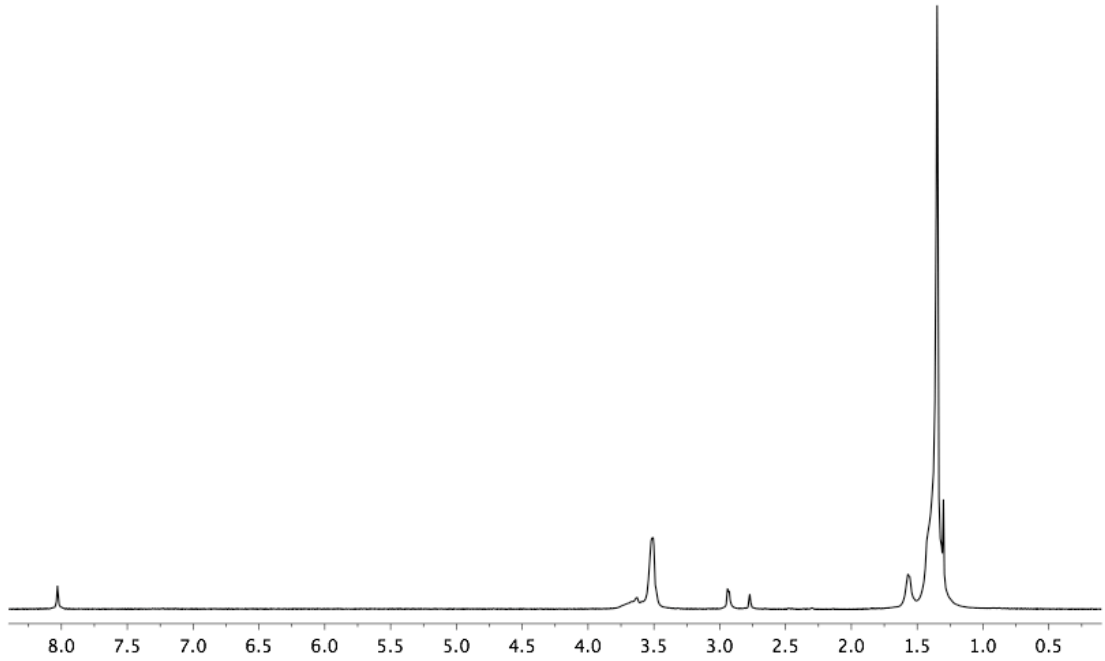

Figure 3.8. ^{1}H spectrum (600 MHz, DMF-d_7) of saturated copolymer (in iodide form) with 29 mol % **3.6**.

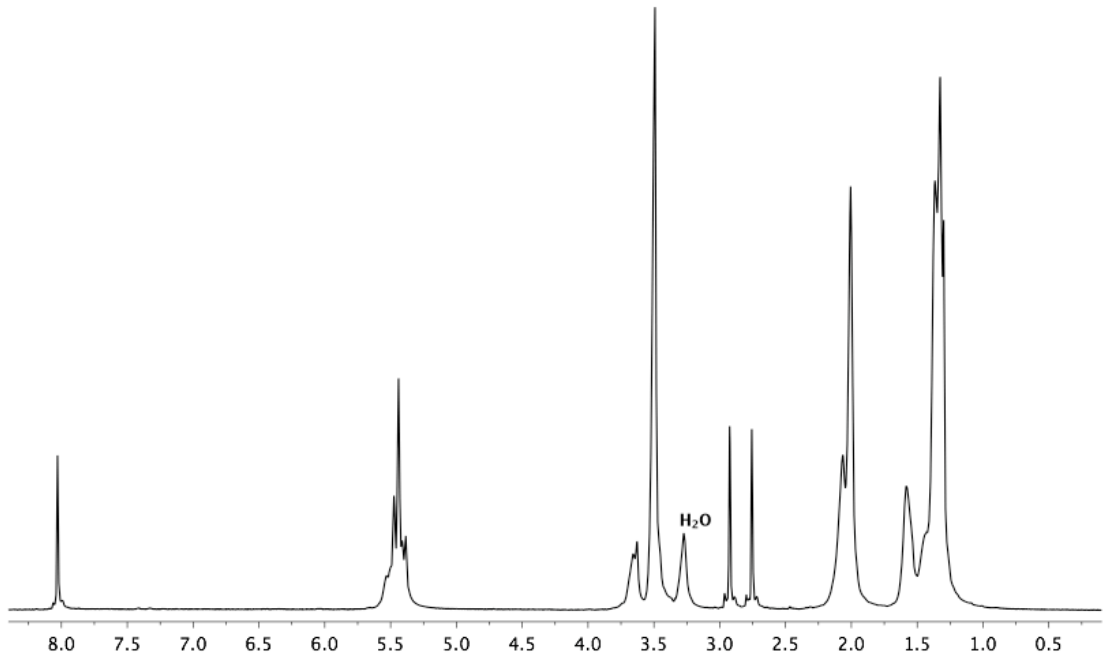

Figure 3.9. ^{1}H spectrum (600 MHz, DMF-d_7) of unsaturated copolymer (in iodide form) with 33 mol % **3.6**.

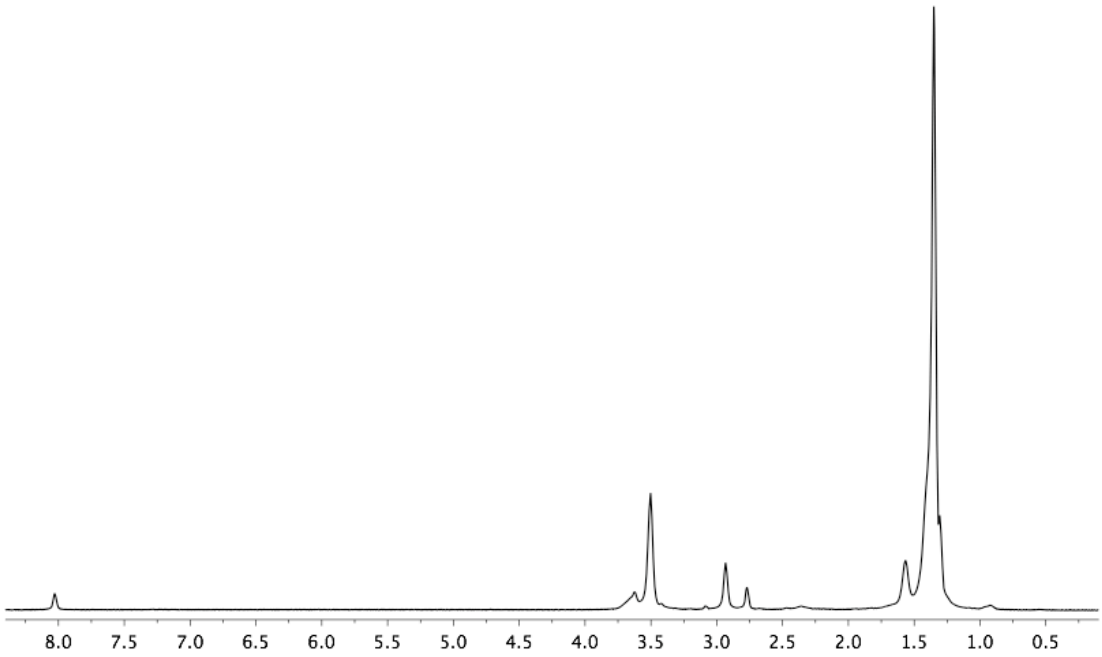

Figure 3.10. ^{1}H spectrum (600 MHz, DMF-d_7) of saturated copolymer (in iodide form) with 33 mol % **3.6**.

References

1. Appleby, A. J.; Foulkes, R. L. *Fuel Cell Handbook*, Van Nostrand Reinhold: New York, **1989**.

2. Diat, O.; Gebel, G. *Nature Mater*. **2008**, *7*, 13-14.

3. Whittingham, M. S.; Savinelli, R. F.; Zawodzinski, T. A. *Chem. Rev*. **2004**, *104*, 4243-4244.

4. Lee, C. H.; Park, H. B.; Lee, Y. M.; Lee, R. D. *Ind. Eng. Chem. Res*. **2005**, *44*, 7617-7626.

5. Lu, S.; Pan, J.; Huang, A.; Zhuang, L.; Lu, J. *Proc. Natl. Acad. Sci. U. S. A*. **2008**, *105*, 20611-20614.

6. Varcoe, J. R.; Slade, R. C. T. *Fuel Cells* **2005**, *5*, 187, and references therein.

7. Varcoe, J. R.; Slade, R. C. T.; Yee, E. L. H.; Poynton, S. D.; Driscoll, D. J.; Apperley, D. C. *Chem. Mater*. **2007**, *19*, 2686-2693.

8. Hibbs, M. R. Hickner, M. A.; Alam, T. M.; McIntyre, S. K.; Fujimoto, C. H.; Cornelius, C. J. *Chem. Mater*. **2008**, *20*, 2566-2573.

9. Wang, G.; Wenig, Y.; Chu, D.; Chen, R.; Xie, D. J. *J. Membr. Sci*. **2009**, *332*, 63-68.

10. Zhou, J.; Unlu, M.; Vega, J. A.; Kohl, P. A. *J. Power Sources* **2009**, *190*, 285–292.

11. Wang, J.; Zhao, Z.; Gong, F.; Li, S.; Zhang, S. *Macromolecules* **2009**, *42*, 8711–8717.

12. Yan, J.; Hickner, M. A. *Macromolecules* **2010**, *43*, 2349-2356.

13. Wang, J.; Li, S.; Zhang, S. *Macromolecules* **2010**, *43*, 3890-3896.

14. Hibbs, M. R.; Fujimoto, C. H.; Cornelius, C. J. *Macromolecules* **2009**, *42*, 8316-8321.

15. Clark, T. J.; Robertson, N. J.; Kostalik IV, H. A.; Lobkovsky, E. B.; Mutolo, P. F.; Abruña, H. D.; Coates, G. W. *J. Am. Chem. Soc.* **2009**, *131*, 12888-12889.

16. Robertson, N. J.; Kostalik IV, H. A.; Clark, T. J.; Mutolo, P. F.; Abruña, H. D.; Coates, G. W. *J. Am. Chem. Soc.* **2010**, *132*, 3400-3404.

17. Einsla, B. R.; Chempath, S.; Pratt, L. R.; Boncella, J. M.; Rau, J.; Macomber, C.; Pivovar, B. S. *Electrochem. Soc. Trans.* **2007**, *11*, 1173-1180.

18. Chempath, S.; Einsla, B. R.; Pratt, L. R.; Macomber, C.; Boncella, J. M.; Rau, J. A.; Pivovar, B. S. *J. Phys. Chem. C* **2008**, *112*, 3179-3182.

19. Delaude, L.; Demonceau, A.; Noels, A. F. *Macromolecules* **1999**, *32*, 2091-2103.

20. Kang, H. A.; Bronstein, H. E.; Swager, T. M. *Macromolecules* **2008**, *41*, 5540-5547.

21. Hübner, G.; Roduner, E. *J. Mater. Chem.* **1999**, *9*, 409-418.

22. Yildirim, M. H.; Stamatialis, D.; Wessling, M. *J. Membr. Sci.* **2008**, *321*, 364-372.

23. Mokrini, A.; Huneault, M. A.; Shi, Z.; Xie, Z.; Holdcroft, S. *J. Membr. Sci.* **2008**, *325*, 749-757.

24. Varcoe, J. R.; Slade, R. C. T.; Yee, E. L. H. *Chem. Commun.* **2006**, 1428-1429.

25. Adams, L. A.; Poyton, S. D.; Tamain, C.; Slade, R. C. T.; Varcoe, J. R. *Chem. Sus. Chem.* **2008,** *1*, 79-81.

26. Yanagi, H.; Fukuta, K. *ECS Trans.* **2008**, *16*, 257–262.

27. Gu, S.; Cai, R.; Luo, T.; Chen, Z.; Sun, M.; Liu, Y.; He, G.; Yan, Y. *Angew. Chem. Int. Ed.* **2009**, *48*, 6499-6502.

28. Lee, C. H; Park, H. B.; Lee, Y. M.; Lee, R. D. *Ind. Eng. Chem. Res.* **2005,** *44*, 7617-7626.

29. Lehman, S. E.; Wagener, K. B.; Baugh, L. S.; Rucker, S. P.; Schulz, D. N.; Varma-Nair, M.; Berluche, E. *Macromolecules* **2007**, *40*, 2643-2656.

30. Mancuso, A. J.; Huang, S. L.; Swern, D. *J. Org. Chem.* **1978,** *43*, 2480-2482.

31. Omura, K. Swern, D. *Tetrahedron* **1978,** *34*, 1651-1660.

Chapter 4

A Standardized Procedure for Measuring the Alkaline Stability of Polymeric Alkaline Anion Exchange Membranes

4.1 Introduction

Fuel cells are devices that convert the chemical energy stored in a fuel directly into electricity and could potentially serve as a highly efficient and environmentally sustainable power generation technology.[1] Within a fuel cell, the polymer electrolyte membrane serves as the ion conducting medium between the anode and cathode, making it a central, and often performance-limiting component of the fuel cell.[2] The most common polymer electrolyte membrane fuel cells operate under acidic conditions and are therefore proton conducting. Although proton exchange membrane (PEM) fuel cells are well developed and can offer excellent performance, they rely almost exclusively on platinum, a very expensive and scarce noble metal.[3] By comparison, alkaline fuel cells that employ hydroxide conducting membranes (alkaline anion exchange membranes, AAEMs) are relatively unexplored. A major advantage of alkaline fuel cells when compared to acidic fuel cells is their enhanced reaction kinetics for oxygen reduction, permitting the use of less costly, non-noble metal catalysts (e.g. Ni).[4,5] As a result, there is now considerable interest in hydroxide conducting polymer electrolyte membranes for fuel cells operating under basic conditions.[4,6]

Several recent advances in alkaline fuel cell research have yielded mechanically strong AAEMs with promising hydroxide conductivities.[7,8,9,10,11,12,13,14,15,16,17,18,19,20,21,22,23,24] Despite significant progress in the field of high performance AAEMs, many of these reports rely on tetraalkylammonium moieties to coordinate and conduct hydroxide ions. At high pH and/or elevated temperature, hydroxide reacts with tetraalkylammonium via several pathways leading

to irreversible degradation by converting the cation into a neutral species, limiting fuel cell performance. [25,26,27] Consequently, it is generally accepted that the temperature limit for tetraalkylammonium-based AAEM operation is ≤ 60 °C.[4] The development of AAEMs containing cations with superior alkaline stability compared to tetraalkylammonium would permit higher temperature AAEM fuel cell operation thus leading to higher performing fuel cells.[4] Several promising AAEMs based on phosphonium,[18,19] guanadinium,[20] imidazolium[21,22] and other cations[23] have been recently reported. While these results are encouraging, the level of improvement over existing systems is uncertain, as stability data are often measured under a wide range of conditions, rendering comparison impossible.

Several recent studies have investigated the stability of tetraalkylammonium ions under alkaline conditions.[25,28,29,30] For example, Boncella, Pratt, Pivovar and coworkers have published seminal studies concerning the alkaline stability of tetraalkylammonium ions under conditions relevant to fuel cells.[31,32,33,34] They found that 90 % of benzyltrimethylammonium (BTMA) remained after 29 days at 80 °C in a basic D_2O solution (1 M NaOH, [NaOD]/[BTMA] = 1).[31] They also investigated the decomposition mechanism of tetraalkylammonium cations using both theoretical and experimental (differential scanning calorimetry, thermogravimetric analysis and evolved gas analysis) methods.[32,33,34] They conclude that the pathways of tetraalkylammonium cation degradation are expected to be a combination of nucleophilic substitution and ylide formation followed by rearrangement. Shown in Figure 4.1 are the degradation pathways for BTMA. Furthermore, solvation of hydroxide with water molecules is critical to mitigate cation decomposition. Solvation

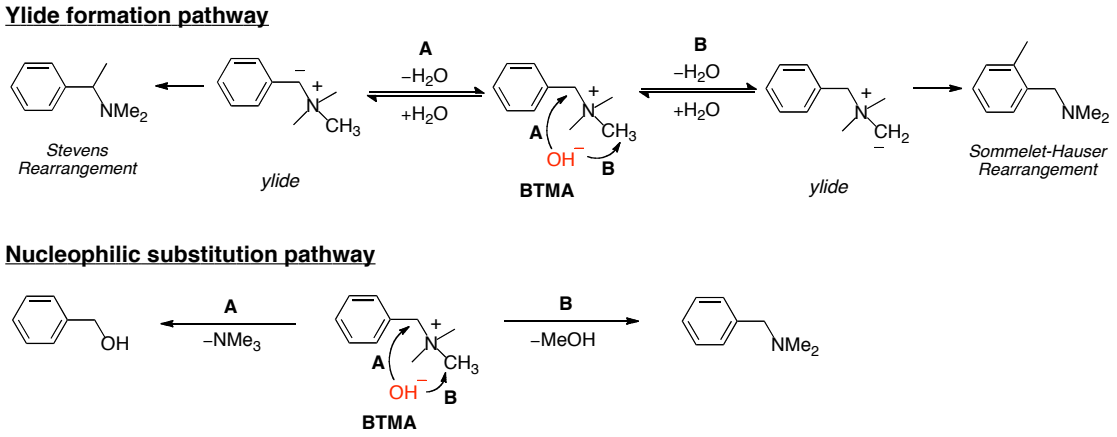

Figure 4.1. Degradation pathways of BTMA.

of the hydroxide ion greatly reduces its basicity and nucleophilicity resulting in decreased reactivity. Overall, tetraalkylammonium-based cations show reasonable stability in alkaline media; however, conditions leading to poor solvation (e.g. AAEM fuel cell operation ≥ 60 °C) will accelerate degradation. Therefore, the utility of tetraalkylammonium-based cations remains unclear in these applications. Although the reports by Boncella, Pratt, Pivovar and coworkers provides fundamental insight into the stability of tetraalkylammoniums, we believe that a set of standardized experiments which evaluate the alkaline stability of newly developed cations, would be highly valuable for the overall development of AAEM based fuel cells. Such a protocol would enable the direct comparison of tetraalkylammonium to other cations (phosphonium,[18,19] guanadinium,[20] imidazolium[21,22] and others[23]). Herein, we report a standardized procedure (Figure 4.2) used to determine the alkaline stability of a BTMA cation and a BTMA-based AAEM. This procedure can be applied to other systems, specifically those based on novel cations. As a result, we recommend this

procedure be applied to other recently developed systems to determine their alkaline stabilities *relative* to BTMA-based AAEMs. Since this procedure is dependent on a number of variables (e.g. vacuum pressure), we recommended that this protocol be reproduced in other laboratories using BTMA and BTMA-based AAEMs, prior to assessing other cations. After the results are known, they can be compared to data from other cations, and a stability assessment *relative* to BTMA can be made.

Phase 1: Determination of the Alkaline Stability of a Model Compound (C^+)

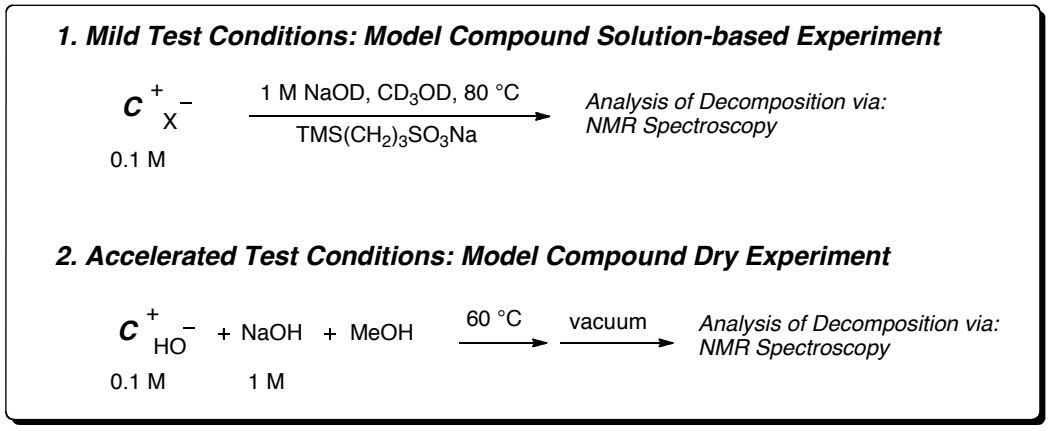

Phase 2: Determination of the Alkaline Stability of an AAEM

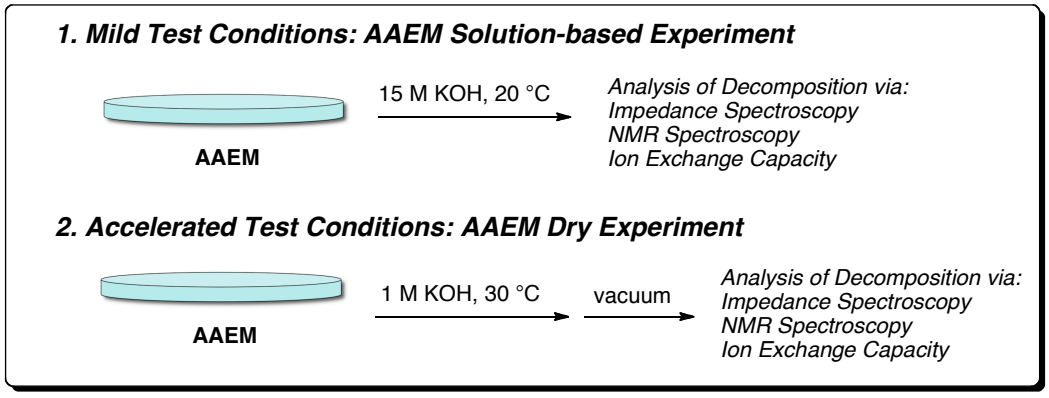

Figure 4.2. Standardized procedure for measuring alkaline stability.

4.2 Results and Discussion

Assessment of small molecule model compounds provides useful insight into the chemical reactivity of polymeric materials. BTMA-based model compounds were used for this study because they are the most commonly found cation among AAEM materials. Since various degrees of solvation may exist during fuel cell operation, two different test conditions were developed: (1) a solution phase experiment to determine the BTMA stability under alkaline conditions in methanol; and (2) an experiment in the absence of solvent to determine the effect of solvation on stability.

The solution phase experiment (Scheme 4.1) was conducted over a 20 day period and is a modified version of a procedure developed by Boncella, Pratt, Pivovar and coworkers.[31] As previously mentioned, they found that 90 % of BTMA remained after 29 days in a basic D_2O solution (1 M NaOH, [NaOD]/[BTMA] = 1) at 80 °C. We propose that replacing D_2O with CD_3OD would increase the rate of BTMA decomposition. Therefore we selected CD_3OD as the solvent for the experiment. We expected that the decreased solvating ability of methanol relative to water would increase the rate of degradation, thereby producing data more rapidly. Furthermore, since lipophilic organic cations generally exhibit enhanced solubility in methanol compared to water, this test will be broadly applicable to various polyatomic cations with little to no modification.

The reaction was performed in a sealed fluoropolymer lined vessel[35] with BTMA dissolved in a mixture of CD_3OD, 40 weight percent $NaOD/D_2O$[36] solution (1 M NaOD, [NaOD]/[BTMA] = 10) and, an internal standard ($TMS(CH_2)_3SO_3Na$). Aliquots of the reaction were removed every 4 days and analyzed by ^1H NMR

spectroscopy. The ^{1}H NMR spectra revealed several new signals attributable to three new species: trimethylamine (NMe_3), (deuteriomethoxy methyl)benzene ($PhCH_2OCD_3$) and N,N-dimethyl-1-phenylmethanamine ($PhCH_2N(CH_3)_2$) (Scheme 4.1). These products suggest that the BTMA cation is degrading primarily by nucleophilic attack at either the benzyl position or at a methyl group. Since NaOD is in equilibrium with $NaOCD_3$ there are two potential nucleophiles in the reaction mixture. Moreover, as both the deuterio methoxide and deuterio hydroxide are basic as well as nucleophilic, H/D exchange occurs at the benzylic and methyl positions. Note that when applying this procedure, great care should be taken to distinguish between H/D exchange and degradation. The mass spectra of the decomposition products confirmed deuteration had occurred, as signals corresponding to several different isotopologues were observed with the (deuteriomethoxy methyl)benzene and N,N-dimethyl-1-phenylmethanamine. Thus, under solvated conditions the primary modes of decomposition in basic media appear to be nucleophilic attack at the benzylic (pathway **A**, Scheme 4.1) or methyl positions (pathway **B**, Scheme 4.1) of the BTMA cation. Under the described conditions, ~67 % degradation is observed over 20 days (Figure 4.3). In comparison, the D_2O-based study showed only ~10 % degradation over 29 days. Therefore, BTMA degrades faster in methanol than observed under aqueous conditions, which suggests that using methanol as a fuel for a BTMA-based fuel cell may lead to shorter device lifetimes.

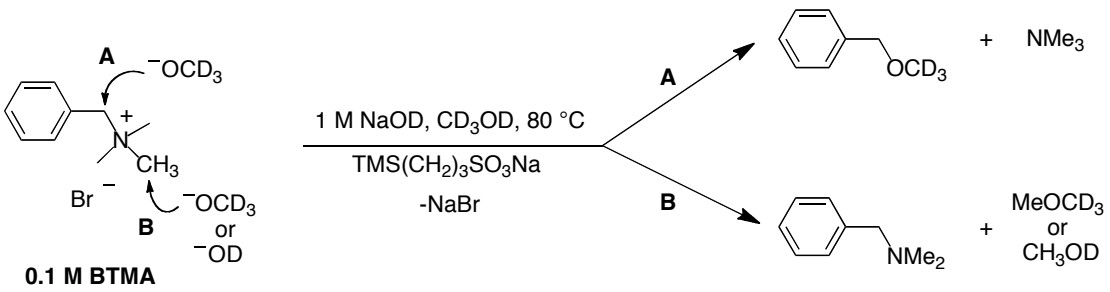

Scheme 4.1. Degradation products of BTMA after exposure to an alkaline solution.

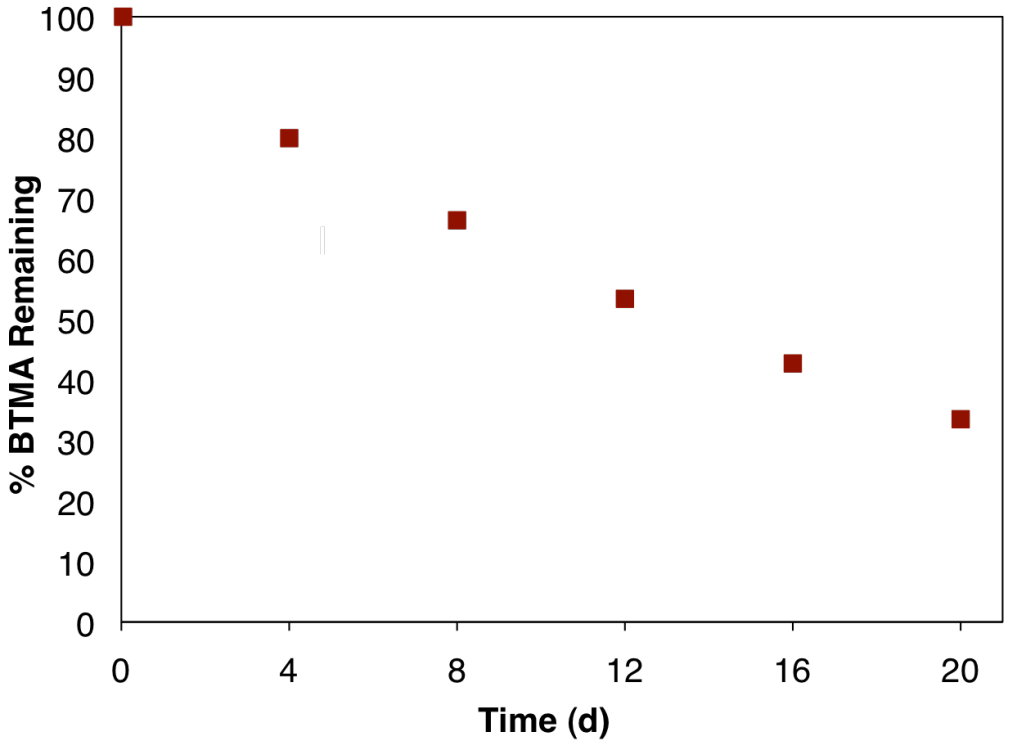

Figure 4.3. Degradation of BTMA in CD_3OD and NaOD as a function of time.

Next, the effect of solvation was investigated by studying BTMA in the absence of solvent (Scheme 4.2). Since solvation of hydroxide by protic compounds (H_2O, CH_3OH) diminishes its nucleophilicity and basicity, dry conditions should significantly enhance the degradation rate of BTMA. Initially, BTMA hydroxide[37] was dissolved in a mixture of CH_3OH and 40 weight percent $NaOH/H_2O$[38] solution (1 M

NaOH, [NaOD]/[BTMA] = 1). The flask was evacuated (350 mTorr) and the volatiles (methanol, water and degradation products) steadily removed over time, leaving only NaOH and unreacted BTMA. After predetermined time intervals, the reaction was brought to atmospheric pressure and the contents of the flask were then dissolved in a mixture of CD_3OD and D_2O, and the amount of unreacted BTMA was determined by ^1H NMR spectroscopy in combination with an internal standard. Under the described conditions, ~96 % degradation is observed after only 4 h *in vacuo* (350 mTorr) at 60 °C (Figure 4.4). It is important to note that the observed degradation rate is *extremely* dependent on a number of variables (e.g. vacuum pressure). Consequently, great care should be taken to reproduce these BTMA results in each individual laboratory in order to directly compare the stability of BTMA to other systems.

Analysis of the degradation products, which were condensed into a cooled (-196 °C) receiving flask during the course of the experiment, by ^1H NMR spectroscopy and GC-MS reveals N,N-dimethyl-1-(o-tolyl)methanamine, N,N-dimethyl-1-phenylmethanamine and (methoxymethyl)benzene are the primary products (Scheme 4.2). The presence of N,N-dimethyl-1-(o-tolyl)methanamine indicates that under the described conditions, BTMA degrades to a certain extent via ylide formation and subsequent Sommelet-Hauser rearrangement.[39] This result is consistent with Boncella, Pratt, Pivovar and coworkers findings that ylide formation was reported to play a dominant role in the decomposition of tetramethylammonium hydroxide.[31,32,33,34] Overall, anhydrous conditions promote the degradation kinetics of BTMA, as compared to the solution-based test, and can also be used as a relatively rapid

screening tool to analyze the alkaline stability of other candidate cations for AAEM materials.[40]

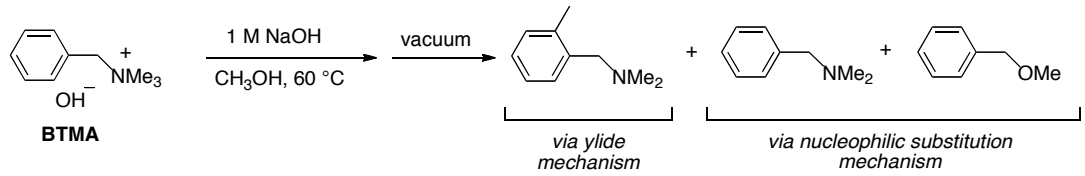

Scheme 4.2. Degradation products of BTMA after exposure to dry alkaline conditions.

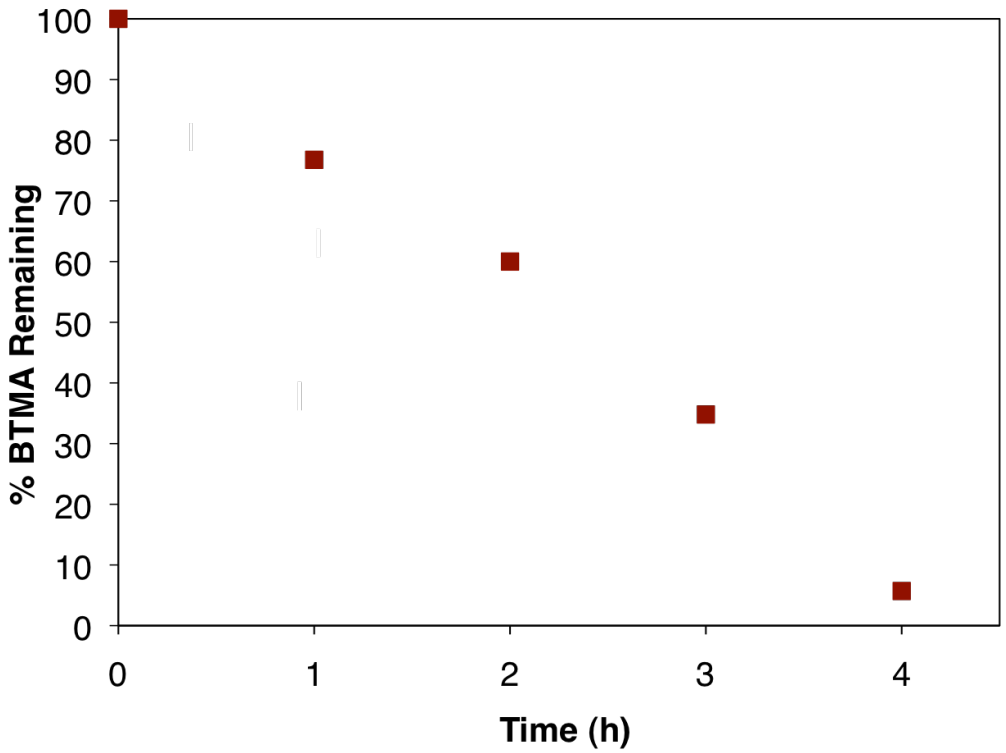

Figure 4.4. Degradation of BTMA under dry alkaline conditions as a function of time.

To fully investigate AAEM stability, analysis of the cation appended to a polymer, rather than simply a small molecule, is crucial. Note that the alkaline stability of both the cation and the polymer backbone contributes to overall AAEM

stability. Since this study is concerned primarily with cation stability, polyethylene was selected as the polymer backbone due to its chemical inertness.

Compound **4.3** was readily synthesized in two steps (Scheme 4.3) and subsequently copolymerized via ring opening metathesis polymerization (ROMP) by introducing Grubbs' 2nd Generation catalyst ([Ru]) to a chloroform solution of

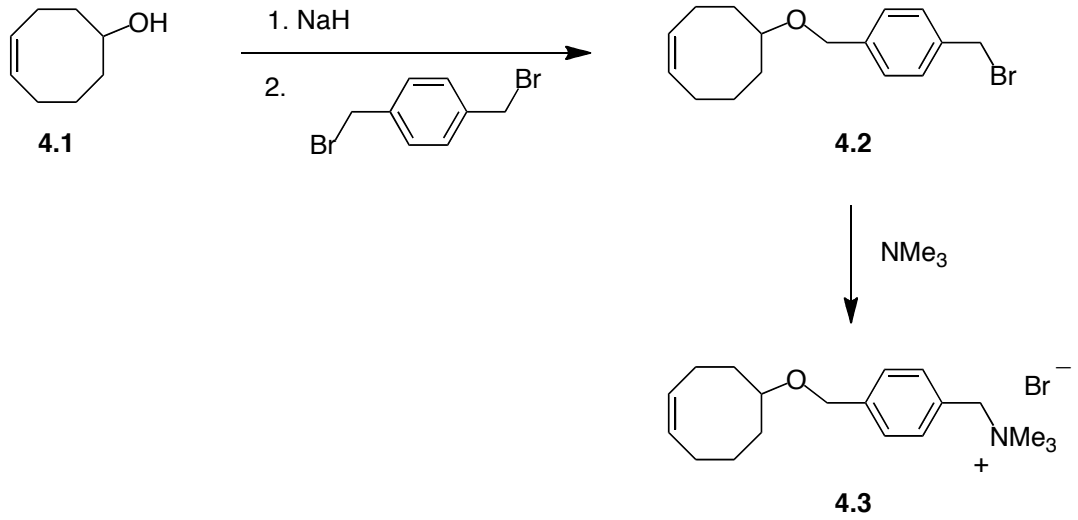

Scheme 4.3. Synthesis of a BTMA functionalized monomer.

cyclooctene (**COE**) and **4.3** at 20 °C under nitrogen (Scheme 4.4). Hydrogenation of the unsaturated BTMA functionalized polymer was accomplished using Crabtree's catalyst ([COD]Ir(Py)(PCy_3)]PF_6) and hydrogen gas. Quantitative conversion was complete within 17 h as confirmed by the complete disappearance of olefinic resonances in the ^{1}H NMR spectrum, yielding BTMA-functionalized polyethylene. The hydrogenated copolymers in the bromide form were dissolved in a chloroform/methanol cosolvent mixture and cast onto a glass dish preheated to 45 °C from which the volatiles were slowly evaporated. The exchange of bromide for

hydroxide was accomplished by soaking the films in 1 M KOH, yielding transparent and nearly colorless AAEMs.

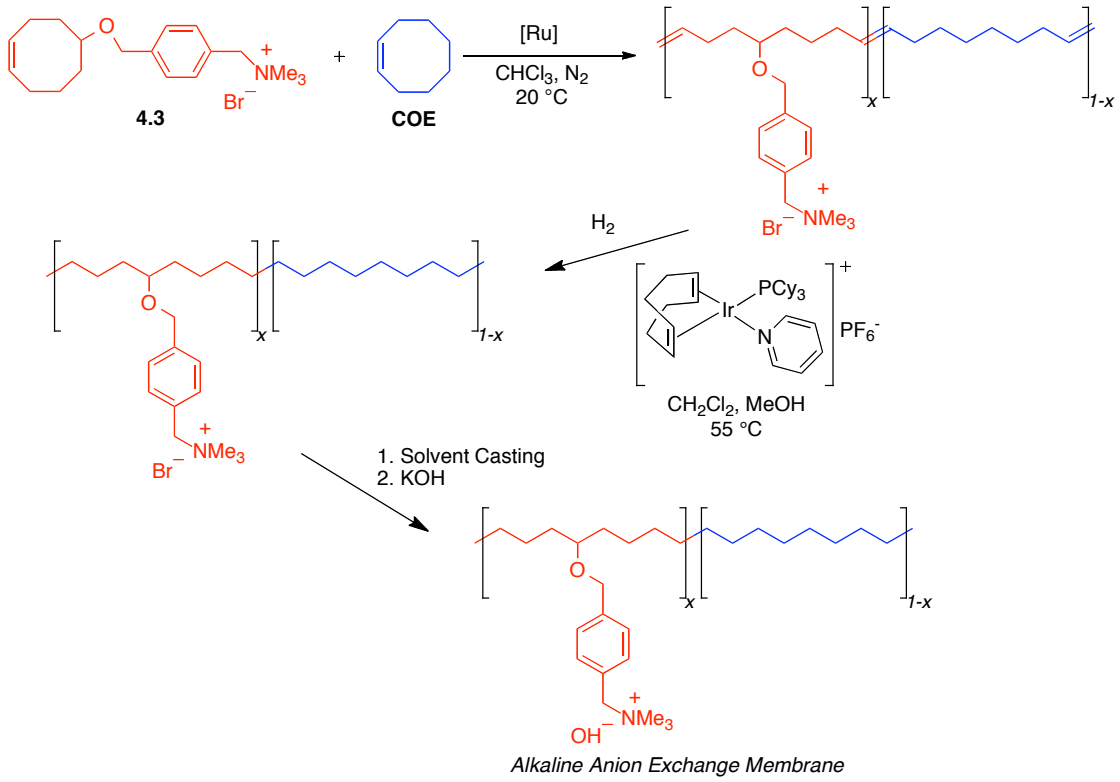

Scheme 4.4. Synthesis of a BTMA functionalized polyethylene.

Overall, the AAEMs are easily handled, exhibiting good flexibility and strength. All the AAEMs used for this study were ~50 μm in thickness. Note that when comparing two different systems, films of similar thickness should be used to eliminate possible hydration differences that may result in different degradation rates. The optimized AAEM used for further studies had 28 mol % **4.3** (AAEM-**4.3**-28). Attempts to synthesize AAEMs with a higher mol % **1** led to materials with excessive swelling, while increasing the mol % **COE** led to polymers with insufficient solubility. Detailed characterization data for AAEM-**4.3**-28 is provided in Table 4.1. The IEC, water

uptake and hydroxide conductivity values of AAEM-**4.3**-28 are within the range of previously reported AAEMs.[7-24] As a result, AAEM-**4.3**-28 is a reasonable analogue of traditional BTMA-based AAEMs.[7-24]

Table 4.1. AAEM characterization data.

Measurement	AAEM-**4.3**-28
mol % **1**[a]	28
IEC (mmol OH^-/g Br^-)[b]	1.33 ± 0.04
% Water uptake[c]	109 ± 8
OH^- σ_{20} (mS/cm)[d]	40 ± 1
OH^- σ_{50} (mS/cm)[d]	59 ± 2

[a]Determined by ^{1}H NMR spectroscopy. [b]Ion exchange capacity determined by back titration, average of 4 trials. [c]Gravimetric water uptakes of the fully hydrated membranes, average of 4 trials. [d]Hydroxide conductivities of the AAEMs fully immersed in water at 20 °C and 50 °C, average of 4 trials.

The alkaline stability of AAEM-**4.3**-28 was studied under hydrated basic conditions (Scheme 4.5) and degradation was monitored by measuring the hydroxide conductivity as a function of time. A similar method for characterizing degradation was described by Hattenbach and Kneifel.[41] Note that ^{1}H spectroscopy and/or ion exchange capacity are also suitable methods for determining decomposition. AAEM-**4.3**-28 was soaked in 1 M KOH over 1 h to assure that all bromide ions were replaced with hydroxide ions. Next, AAEM-**4.3**-28 was placed in a plastic bottle containing 15 M KOH at 20 °C. After predetermined time intervals the film was removed and soaked in deionized water for 24 h to ensure complete hydration, re-exchanged with 1 M KOH, washed with water to remove any residual base and the in-plane hydroxide

conductivity measured at 20 °C. Figure 4.5 illustrates that the membranes show no appreciable loss of conductivity over the course of 8 days. As a result, this experiment should serve as a minimum threshold of alkaline stability when examining AAEMs.

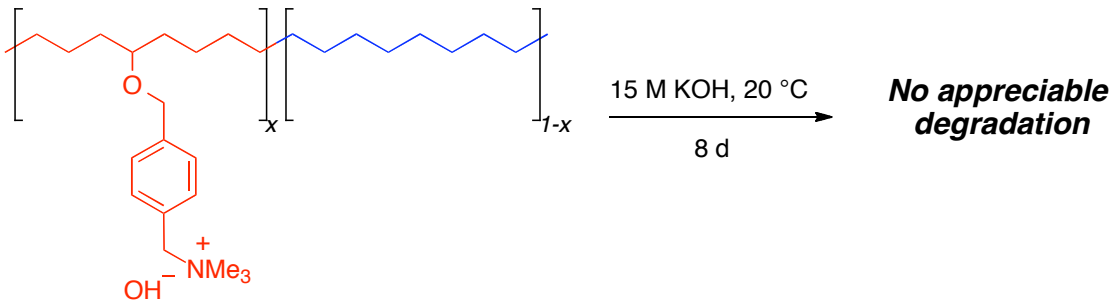

Scheme 4.5. Exposure of AAEM-**4.3**-28 to a basic alkaline solution.

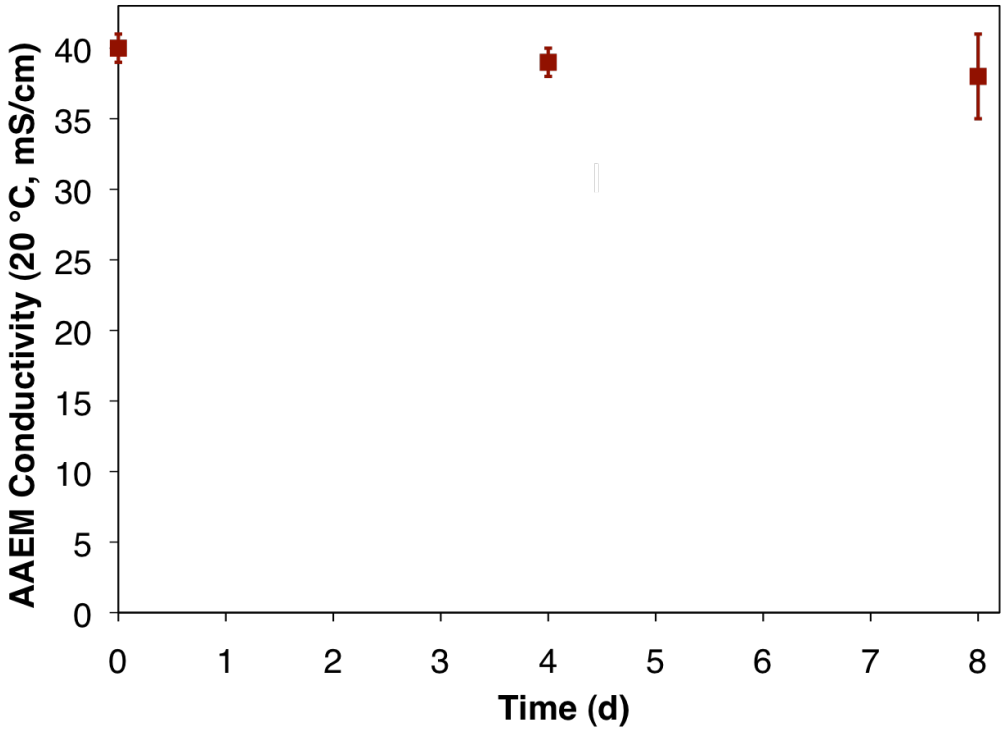

Figure 4.5. AAEM-**4.3**-28 hydroxide conductivity as a function of time when immersed in 15 M KOH at 20 °C.

Next, the alkaline stability of AAEM-**4.3**-28 was studied under dry basic conditions (Scheme 4.6) and degradation was monitored by measuring the hydroxide conductivity as a function of time. AAEM-**4.3**-28 was soaked in 1 M KOH over 1 h to assure that all bromide ions were replaced with hydroxide ions. Next, AAEM-**4.3**-28 was then removed from the 1 M KOH solution and immediately placed in a plastic bottle. The entire contents were evacuated (350 mTorr) at 30 ºC for varying amounts of time. Methanol was not used for this study in order to minimize membrane swelling. The film was then soaked in deionized water for 24 h to ensure complete hydration, re-exchanged with 1 M KOH, washed with water to remove any residual base and the in-plane hydroxide conductivity measured at 20 °C. Figure 4.6 illustrates that the membranes steadily lose conductivity as a function of time under anhydrous conditions. In fact, nearly complete loss of conductivity is observed after 4 h *in vacuo* (350 mTorr) at 30 ºC (Figure 4.6). [40]

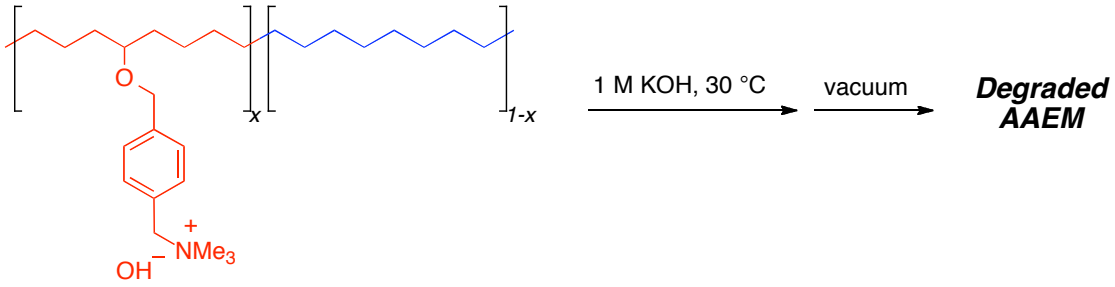

Scheme 4.6. Exposure of AAEM to dry alkaline conditions.

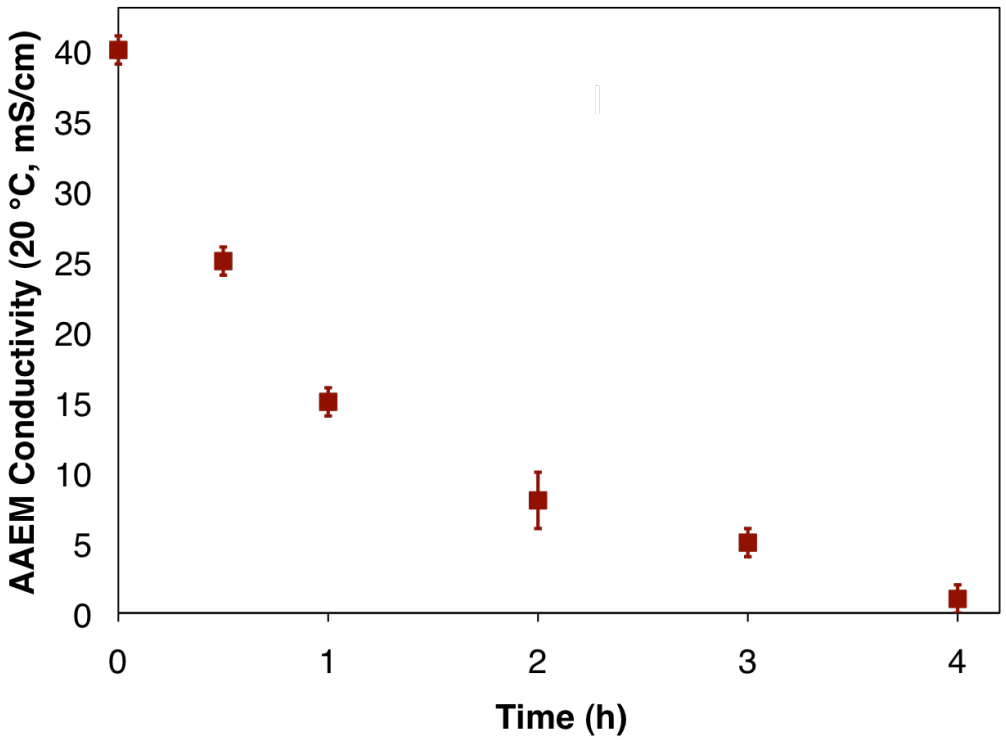

Figure 4.6. Degradation of AAEM-**4.3**-28 under dry alkaline conditions.

4.3 Conclusion

In summary, a standardized procedure used to determine the alkaline stability of BTMA and a BTMA-based AAEM was developed. In basic methanol solution at 80 °C, ~67 % degradation is observed over 20 days for BTMA. Furthermore, by using dry conditions the rate of BTMA degradation can be considerably enhanced, ~94 % degradation is observed in only 4 h *in vacuo* (350 mTorr) at 60 ºC. Lastly, a BTMA functionalized polyethylene, AAEM-**4.3**-28 was synthesized. AAEM-**4.3**-28 was tested under hydrated basic conditions and no appreciable loss of conductivity was observed after immersion in 15 M KOH for 8 days at 20 °C. Next, AAEM-**4.3**-28 was tested under basic dry conditions and nearly complete loss of conductivity was

observed in only 4 h *in vacuo* (350 mTorr) at 30 ºC. Overall, this procedure has been designed to be widely applicable to other systems, specifically those based on novel cations. The application of this procedure enables the comparison of many different systems and should facilitate the discovery of AAEMs with increased base stability. Since this procedure is designed to compare *relative* stabilities and is dependent on a number of variables (e.g. vacuum pressure), we recommended that this protocol be reproduced in other laboratories using BTMA and BTMA-based AAEMs, prior to assessing other cations. After the results are known, they can be compared to data from other cations, and a stability assessment *relative* to BTMA can be made. Future work will focus on using thermal gravimetric analysis in combination with mass spectrometry (TGA-MS) as a tool to further study the degradation of BTMA and newly developed cations.

4.4 Future outlook of AAEM technologies

AAEM fuel cells have the potential to operate efficiently without the use of platinum at the cathode and hold great promise to one day supplant PEM fuel cell technology. However, before wide-scale commercialization of AAEM fuel cells can be realized, several significant materials research developments must be made:

(i) The development of new synthetic strategies that enable the synthesis of more highly conducting AAEMs is a significant research challenge. In particular, materials that combine high conductivities (possibly through microphase separation) with excellent mechanical strength and dimensional stability are desired.

(ii) The incorporation of cations, new and existing, that exhibit increased alkaline stability (relative to tetraalkylammonium) into AAEMs would enable high temperature (≥ 80 °C) fuel cell operation. This is essential for AAEM fuel cells to be considered for applications such as automotive power. Furthermore, operation at elevated temperature would reduce thermodynamic voltage losses due to the pH differences across the AAEM and improve the electrokinetics.

(iii) The development of a soluble ionomer, analogues to commercially available solutions of Nafion, is crucial to the fabrication of high performance AAEM MEAs. Specifically, an ionomer that is soluble in solvents such as aqueous n-propanol (to allow simple incorporation into the catalyst layer) but is insoluble in aqueous methanol (to permit the use of methanol as a fuel) would be ideal.

(iv) The design and synthesis of fuel cell electrocatalysts, especially those based on cheap and abundant metals, designed specifically for operation under basic conditions is critical to achieving high performance AAEM fuel cells.

(v) The optimization of the fabrication of high performing AAEM MEAs is important to the overall development of AAEM fuel cells. In particular, tailoring the interface between the catalyst layer and AAEM will result in AAEM fuel cells with longer operating lifetimes.

(vi) The investigation into the use of other fuels such as hydrazine and ethanol may lead to improved efficiencies relative to PEM-based fuel cells. The

use of ethanol as a fuel is especially intriguing due to its widespread availability and consumer approval.

If the above challenges can be met, AAEM technology has the potential to aid in societies ever increasing need for cheap, clean and reliable energy conversion sources.

4.5 Experimental

4.5.1 General methods and materials

All reactions and manipulations of compounds were carried out in air unless otherwise specified. Benzyl bromide (98%), sodium hydride, α,α-dibromo-*p*-xylene (97%) potassium hydroxide, sodium hydroxide, potassium bicarbonate, potassium carbonate, sodium sulfate, *cis*-cyclooctene (95%), Grubbs' 2nd Generation catalyst (CAS Number: 246047-72-3), benzyltrimethylammonium hydroxide (BTMA-OH, 40 wt% in H_2O), sodium deuteroxide (40 wt% in D_2O), 3-(Trimethylsilyl)-1-propanesulfonic acid sodium salt (97%), trimethylamine solution (31-35 wt. % in ethanol, ~4.2 M), Crabtree's catalyst (CAS Number: 64536-78-3), standardized hydrochloric acid (0.1014 M) and standardized potassium hydroxide (0.1000 ± 0.0001 M) were purchased from Sigma-Aldrich and used as received. 1,5-Cyclooctadiene (99%) and lithium aluminum hydride were purchased from Acros Organics and used as received. All solvents were purchased from Sigma-Aldrich or Mallinckrodt. Tetrahydrofuran was dried by passage over an alumina packed drying column glass contour. Hydrogen (99.99%) was purchased from Airgas. 5-Hydroxy-1-cyclooctene was prepared according to a literature procedure.[42]

4.5.2 Small molecule characterization

^{1}H and ^{13}C NMR spectra were recorded on a Varian INOVA 400 (^{1}H, 400 MHz, ^{13}C, 100 MHz) or Varian INOVA 500 (^{1}H, 500 MHz, ^{13}C, 125 MHz) NMR spectrometers and referenced to CD_3OH (4.78 ppm), $CHCl_3$ (7.24 ppm), $CDCl_3$ (77.23 ppm), $(D_3C)_2NCHO$ (8.03 ppm) or HDO (4.80 ppm). Mass spectra were acquired using a JEOL GCMate II mass spectrometer operating at 3000 resolving power for high resolution measurements in positive ion mode and an electron ionization potential of 70 eV. Samples were introduced *via* a GC inlet using an Agilent HP 6890N GC equipped with a 30 m (0.25 μm i.d.) HP-5ms capillary GC column. The carrier gas was helium with a flow rate of 1 mL/min. Samples were introduced into the GC using a split/splitless injector at 230 °C with a split ratio of 10:1. Elemental analysis was performed by Robertson Microlit Laboratories, Inc. (Madison, NJ).

4.5.3. AAEM characterization

Ion exchange capacities (IECs) were determined using standard back titration methods. The thin film as synthesized (in bromide form) was dried under full vacuum overnight at 100 °C in order to completely dehydrate it and then weighed. Conversion to the hydroxide form was achieved by immersing the film in 3×60 mL portions of 1 M potassium hydroxide for 20 minutes each. Residual potassium hydroxide was washed away by immersing the membrane in 3×125 mL portions of deionized water for 20 minutes each. The AAEM was then stirred in 20 mL standardized 0.1 M $HCl_{(aq)}$ solution for 24 hours followed by titration with standardized 0.1 M $KOH_{(aq)}$ to determine the equivalence point. Control acid samples (with no AAEM present) were

also titrated with standardized 0.1 M $KOH_{(aq)}$, and the difference between the volume required to titrate the control and the sample was used to calculate the amount of hydroxide ions in the membrane. This was divided by the dried mass of the membrane (*vide supra*) to give an IEC value with the units mmol OH^-/g Br^-.

Water uptake was measured by the mass change between the fully hydrated and dried AAEMs in the bromide form. The thin film as synthesized (in bromide form) was dried under full vacuum overnight at 100 °C in order to completely dehydrate it and then weighed. Conversion to the hydroxide form was achieved by immersing the film in 3×60 mL portions of 1 M potassium hydroxide for 20 minutes each. Residual potassium hydroxide was washed away by immersing the membrane in 3×125 mL portions of deionized water for 20 minutes each. Immediately following the water wash, a sample was dried with a paper towel and placed in a capped vial to ensure accurate weighing. The water uptake percentage value was calculated by: $WU = [(Mass_{final}-Mass_{initial})/Mass_{initial}]*100$.

The in-plane hydroxide conductivity of the AAEM sample was measured by four probe electrochemical impedance spectroscopy (EIS) using a Solartron 1280B electrochemical workstation along with ZPlot and ZView software. The conductivity cell was purchased from BekkTech LLC (Loveland, CO), and a helpful schematic and description of a similar experimental setup has been reported.[43] A strip of the thin film in the bromide form (ca. 4 cm long × 0.5 mm wide) was converted to the hydroxide form by immersing it in 3×30 mL portions of 1 M potassium hydroxide for 20 minutes each. Residual potassium hydroxide was washed away by immersing the membrane in

3×60 mL portions of deionized water for 20 minutes each. The AAEM was then clamped into the cell using a Proto 6104 torque screwdriver set to 1 inch ounce and completely immersed in deionized water, at either 20 °C or 50 °C, during the measurement time. EIS was performed by imposing a small sinusoidal (AC signal) voltage, 10 mV, across the membrane sample at frequencies between 20,000 Hz and 0.1 Hz (scanning from high to low frequencies) and measuring the resultant current response. Using a Bode plot, the frequency region over which the impedance had a constant value was checked, and the highest frequency measurement at 0° phase angle in the Nyquist plot was taken as the effective resistance of the membrane. This was then used to calculate the hydroxide conductivity by employing the following formula: $\sigma = L / Z' \cdot A$ where L is the length between sense electrodes (0.425 cm), Z' is the real impedance response at high frequency, and A is the membrane area available for hydroxide conduction (width·thickness). The dimensional measurements were performed using a digital micrometer (± 0.001 mm) purchased from Marathon Watch Company Ltd. (Richmond Hill, ON).

A consistent treatment of the precision of the measurements has been conducted. All errors are determined from sample standard deviations. Confidence intervals are at the 95 % confidence level based on the sample deviations and using the relevant student-*t* distribution (*N*-1 degrees of freedom, *N* is the number of samples tested for each composition).

4.5.4. Model compound synthesis

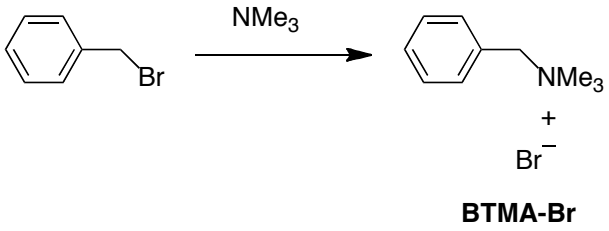

BTMA-Br

Scheme 4.7. Synthesis of BTMA-Br.

Preparation of Compound BTMA-Br: Benzyl bromide (1.20 ml, 10.0 mmol) was added to a 50 ml round bottom flask containing acetonitrile (15 ml) and the solution was stirred while trimethylamine solution (7.14 ml, 30.0 mmol) was slowly added. The mixture was stirred at 22 ºC, after 24 h the solvent was removed by a rotary evaporator. The subsequent solid was washed with tetrahydrofuran (250 ml), filtered and dried under vacuum at 100 ºC for 8 hr giving the desired product (2.14 g, 9.30 mmol, 93%) as a white solid. ^{1}H NMR (400 MHz, CD_3OD) δ 7.66-7.68 (2H, m), 7.50-7.59 (3H, m), 4.72-4.74 (2H, s), 3.20-3.22 (9H, s). ^{13}C NMR (100 MHz, $CDCl_3$) δ 134.28, 131.98, 130.37, 129.35, 70.10, 53.28. HRMS EI (*m/z*): calc. for $C_{10}H_{16}N$, 150.1283 [M+]; found, 150.1285.

4.5.5. Characterization of model compound stability

Solution Phase Experiment: BTMA-Br (230 mg, 1.00 mmol), sodium deuteroxide (40 wt% in D_2O, 1.03 g, 10.0 mmol), 3-(Trimethylsilyl)-1-propanesulfonic acid sodium salt (110 mg, 0.504 mmol) and CD_3OD (10 ml) were placed in a fluoropolymer lined vessel and heated at 80 ºC for 1 hour. After 1 hr an aliquot was

removed and analyzed by ^{1}H NMR spectroscopy. The integration of the aromatic region of BTMA relative to 3-(Trimethylsilyl)-1-propanesulfonic acid sodium salt provided the initial quantity of BTMA. Aliquots of the reaction were removed every 4 days (a series of the spectra over time are shown in Figure 4.7) and analyzed by ^{1}H NMR spectroscopy and GC-MS in order to determine the quantity of BTMA remaining and degradation products. The primary degradation products were confirmed as (methoxy deuteriomethyl)benzene and N,N-dimethyl-1-phenylmethanamine.

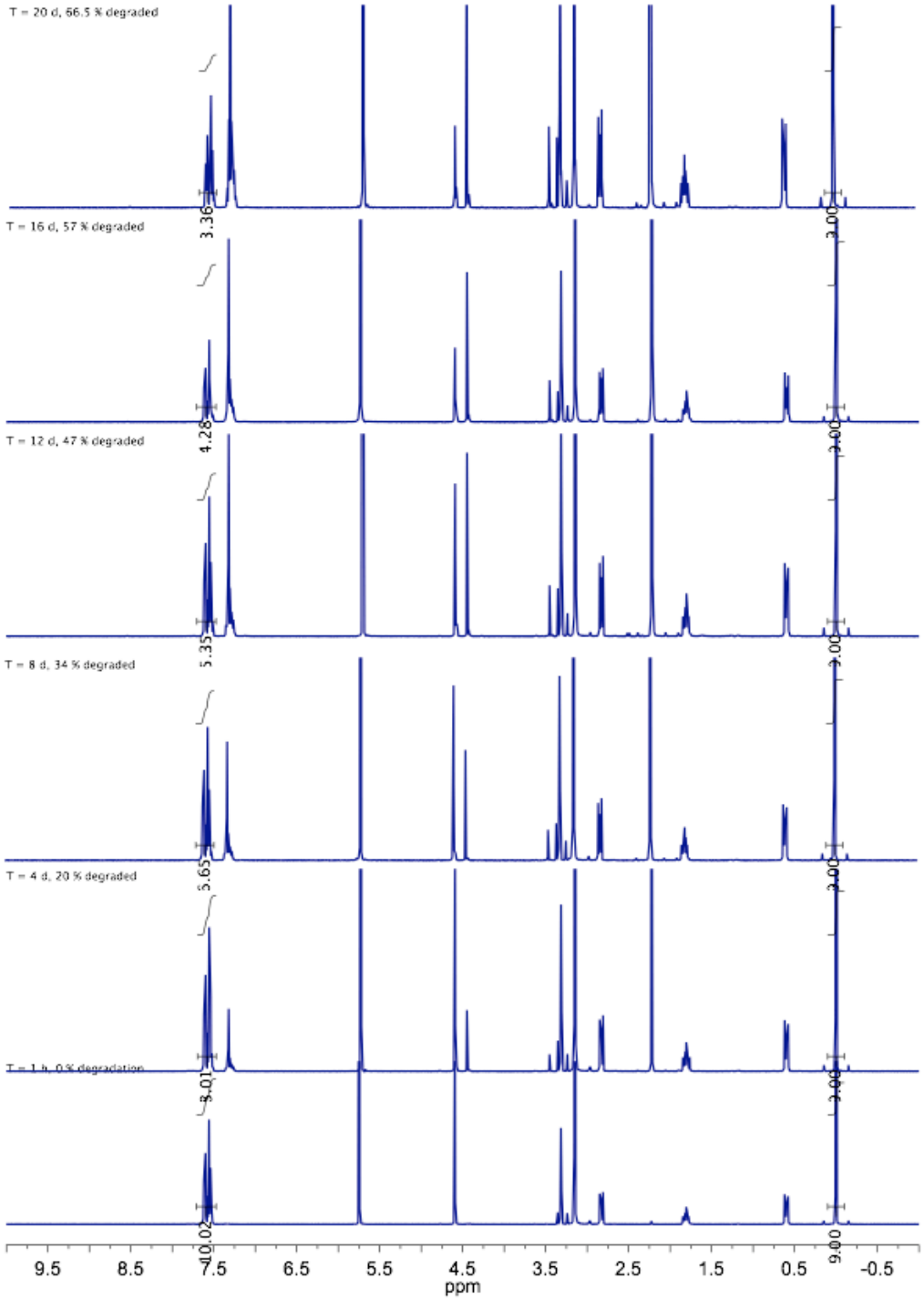

Figure 4.7. [1]H NMR spectra during the course of the solution phase experiment.

Dry Experiment: BTMA-OH (40 wt% H_2O, 105 mg, 0.25 mmol), sodium hydroxide (40 wt% in H_2O, 250 mg, 2.50 mmol) and CH_3OH (2.3 ml) were placed in a 25 ml round bottom flask and heated at 60 ºC under vacuum (Figure 4.8). After a given time the reaction was brought to atmospheric pressure and allowed to cool at which point the contents of the round bottom flask were dissolved in CD_3OD (2.3 ml) and D_2O (0.2 ml). 3-(trimethylsilyl)-1-propanesulfonic acid sodium salt (27.3 mg, 0.125 mmol) was added and the integration of the aromatic region of BTMA relative to 3-(trimethylsilyl)-1-propanesulfonic acid sodium salt provided the quantity of BTMA remaining. The experiment was carried out twice and the results averaged. A series of sample spectra are shown below (Figure 4.6). The non volatile degradation products were condensed by a liquid nitrogen cooled vessel during the course of the experiment and analyzed by ^1H NMR spectroscopy and GC-MS. The ^1H NMR and GC-MS spectra are consistent with N,N-dimethyl-1-(o-tolyl)methanamine, N,N-dimethyl-1-phenylethanamine and (methoxymethyl)benzeneby as the primary products and correspond to know literature values.[44,45,46]

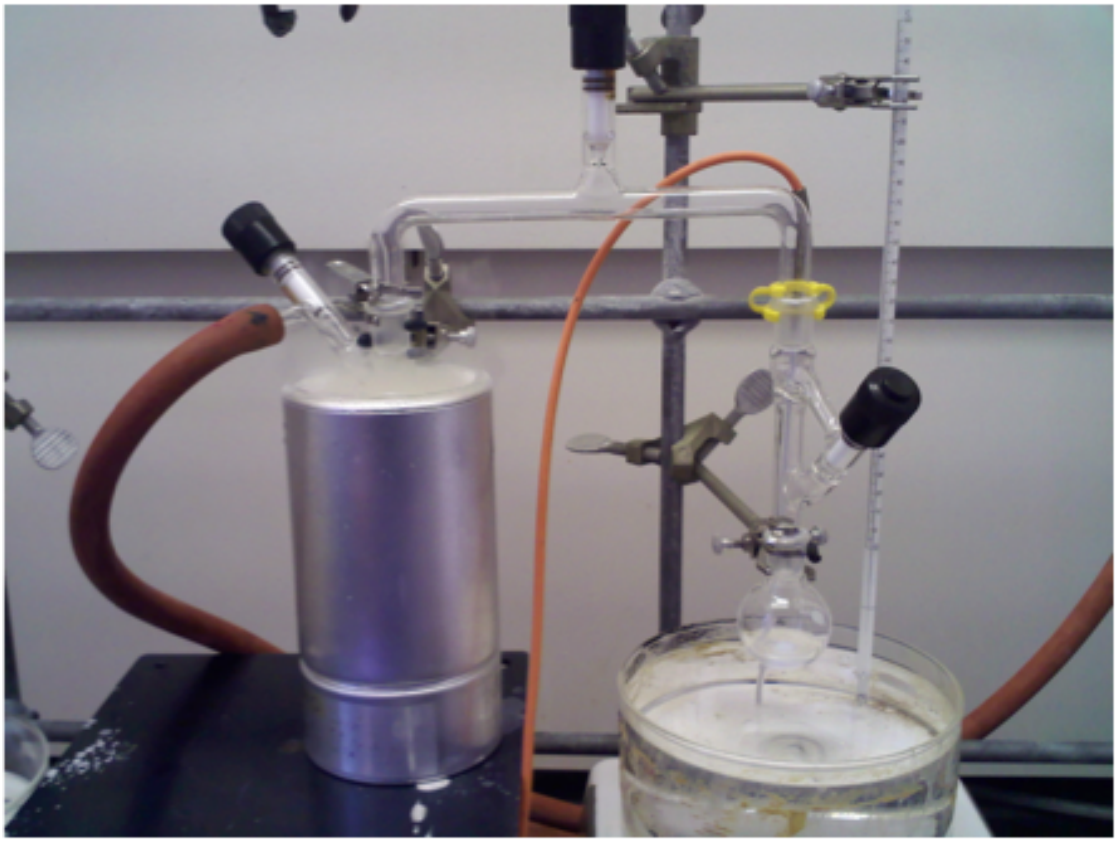

Figure 4.8. Photograph depicting the experimental setup for AAEM preparation.

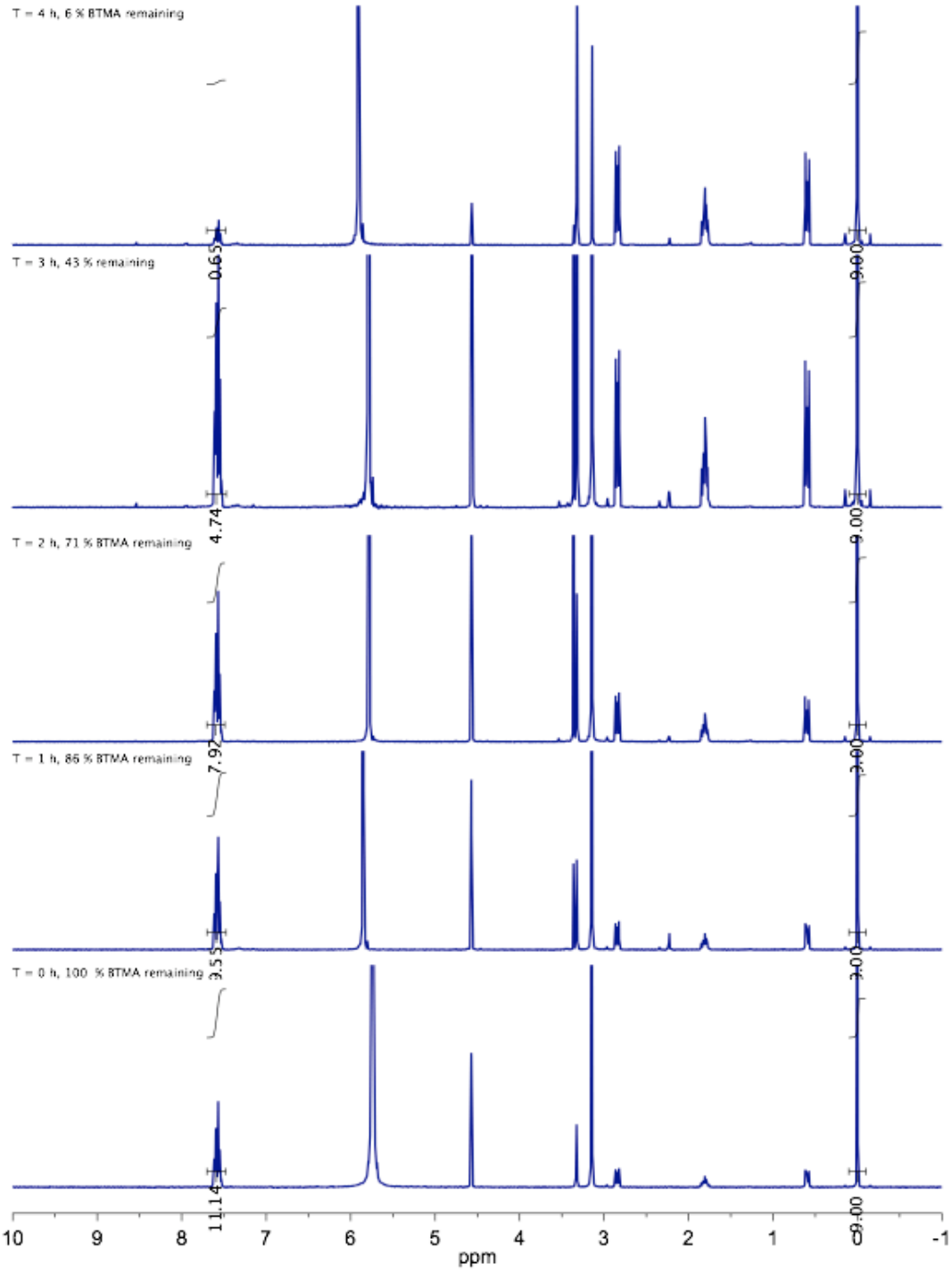

Figure 4.9. [1]H NMR spectra during the course of the experiment under dry conditions.

4.5.6. Monomer and polymer synthesis and characterization

Preparation of (*Z*)-5-((4-(bromomethyl)benzyl)oxy)cyclooct-1-ene (4.2): This compound was prepared using a modified literature procedure from Mirkin and co-workers.[47] In a nitrogen atmosphere 5-Hydroxy-1-cyclooctene (compound **4.1**) (3.53 g, 28.0 mmol) was added to a 500 ml Schlenk flask attached with a reflux condenser. Dry THF (100 ml) was added and the solution was stirred vigorously while sodium hydride (819 mg, 34.1 mmol) was added. The mixture was refluxed for 17 h under a positive stream of nitrogen, and allowed to cool. In a separate 500 ml Schlenk flask, α,α-dibromo-*p*-xylene (8.00 g, 30.2 mmol) was dissolved in dry THF (150 ml), and the flask was capped with a pressure-equalizing dropping funnel. The cooled solution of 5-Hydroxy-1-cyclooctene was then transferred to the pressure-equalizing dropping funnel using a cannula needle and slowly added to the α,α-dibromo-*p*-xylene solution with vigorous stirring over a period of 10 min. The dropping funnel was then replaced with a reflux condenser and the mixture was refluxed for an additional 17 h under a positive stream of nitrogen. Upon cooling, the reaction mixture was filtered and the solvent was removed using a rotary evaporator. The subsequent oil was dissolved in CH_2Cl_2 (100 ml) and washed successively with water (50 ml), 1.0 M NaOH (50 ml), 1.0 M HCl (50 ml), and brine (50 ml). The organic layer was collected, dried over sodium sulfate, and filtered. The solvent was removed using a rotary evaporator. Column chromatography on silica gel with 30% CH_2Cl_2 in hexanes as the eluent gave the desired product 4.1 (3.73 g, 12.1 mmol, 40%) as a clear oil. ^{1}H NMR (400 MHz, $CDCl_3$) δ 7.30-7.36 (4H, m), 5.59-5.70 (2H, m), 4.43-4.53 (4H, m), 3.45-3.48 (1H, m),

2.33-2.43 (1H, m), 1.57-2.24 (8H, s), 1.29-1.48 (1H, m). ^{13}C NMR (100 MHz, $CDCl_3$) δ 139.68, 136.81, 130.18, 129.47, 127.80, 80.27, 69.81, 34.30, 33.57, 33.28, 25.86, 25.66, 22.77. Anal. calc. for $C_{16}H_{21}BrO$: C, 62.14; H, 6.84. Anal. found: C, 62.44; H, 6.86.

Preparation of Compound 4.3: Compound **4.2** was added to a 100 ml round bottom flask. Acetonitrile (20 ml) was added and the solution was stirred while trimethylamine solution (3.46 ml, 14.5 mmol) was added. The mixture was heated to 60 ºC and stirred, after 17 h the solution was allowed to cool. Upon cooling, the solvent was removed using a rotary evaporator. The subsequent solid was washed with tetrahydrofuran (250 ml), filtered and dried under vacuum at 100 ºC for 8 hr giving the desired product (1.22 g, 3.32 mmol, 91%) as a white solid. ^{1}H NMR (400 MHz, $CDCl_3$) δ 7.57-7.60 (2H, m), 7.37-7.40 (2H, m), 5.52-5.69 (2H, m), 5.00-5.11 (2H, s), 4.42-4.53 (2H, m), 3.13-3.93 (10H, m), 2.34-2.36 (1H, m), 1.37-2.17 (9H, m). ^{13}C NMR (100 MHz, $CDCl_3$) δ 142.31, 133.15, 130.05, 129.53, 127.99, 126.41, 80.73, 69.58, 68.59, 52.64, 34.23, 33.33, 25.81, 25.63, 22.64. HRMS EI (*m/z*): calc. for $C_{19}H_{30}NO$, 288.2327 [M+]; found, 288.2328.

Preparation of the Saturated Copolymer with 28 mol % 4.3: Under a nitrogen atmosphere compound **4.3** (150 mg, 0.407 mmol) and **COE** (135 mg, 1.22 mmol) were combined and dissolved in chloroform mixture (1.6 mL). Grubbs' 2nd Generation catalyst (1.8 mg, 0.0023 mmol) was added and the solution allowed to stir vigorously. After 2 hour, the solvent was removed by rotary vacuum. The unsaturated copolymer was dried under vacuum at 100 °C and dissolved in a dichloromethane/methanol

cosolvent (5.0 mL/2.5 mL, respectively) forming a light brown solution. The polymer solution and Crabtree's catalyst (5.3 mg, 0.006 mmol) were combined in a Parr reactor equipped with an overhead stirrer and sealed. It was pressurized to 600 psig hydrogen and then vented down to 50 psig. This process was repeated twice more to purge the reactor of air, then pressurized to 600 psig and heated to 55 °C with rapid stirring. After 17 hours, it was cooled, vented and the swollen polymer gel dried under vacuum at 100 °C, washed with water and dried again under vacuum at 100 °C furnishing a yellow solid (275 mg, 96%). ^{1}H NMR (500 MHz, DMF-d_7, 135 ºC) δ 7.63-7.87 (2H, br m), 7.40-7.57 (2H, br m), 4.81-5.19 (2H, br m), 4.55-4.69 (2H, br m), 3.47-3.56 (1H, br m), 3.27-3.46 (9H, br m), 1.00-1.76 (56H, br m). ^{13}C NMR (125 MHz, CD_3Cl/ D_3COD, 60 ºC) δ 142.6, 132.8, 128.2, 126.3, 80.12, 69.94, 69.38, 52.64, 33.82, 29.77, 29.55, 25.34.

Preparation of AAEM-4.3-28: The saturated copolymer with 28 mol % **4.3** (138 mg) was dissolved in a chloroform/methanol cosolvent mixture (2.5 mL/1.2 mL, respectively) forming a light yellow solution and then transferred to a preheated (45 °C) glass dish (diameter of 5.25 cm and depth of 3.0 cm) on top of a hot plate covered with a metal plate to ensure uniform heating. The dish was covered with a round glass cover with a diameter of 7 cm and volume of 550 mL bearing one Kontes glass valve on top to control the rate of solvent evaporation. After one hour the cover was removed and the temperature was increased to 70 °C for another hour. Following this, water was added and the translucent film freely removed from the dish. The film was then soaked in deionized water for at least 24 hours prior to hydroxide ion exchange.

The AAEM was generated as described above. To make thinner membranes the amount of polymer was scaled back accordingly.

Dry AAEM Experiment: A strip of the thin film in the hydroxide form (ca. 4 cm long × 0.5 mm wide) was removed from 1 M KOH and immediately placed in a plastic bottle and heated at 30 ºC under vacuum. After a given time the reaction was brought to atmospheric pressure at which point the strip was soaked in deionized water for 24 h to ensure complete hydration, re-exchanged with 1 M KOH, washed with water to remove any residual base and the in-plane hydroxide conductivity measured at 20 °C.

References

1. Appleby, A. J.; Foulkes, R. L. *Fuel Cell Handbook*, Van Nostrand Reinhold: New York, **1989**.

2. Diat, O.; Gebel, G. *Nature Mater*. **2008**, *7*, 13-14.

3. Whittingham, M. S.; Savinelli, R. F.; Zawodzinski, T. A. *Chem. Rev*. **2004**, *104*, 4243-4244.

4. Varcoe, J. R.; Slade, R. C. T. *Fuel Cells* **2005**, *5*, 187, and references therein.

5. Schulze, M.; Gülzow, E. *J. Power Sources* **2004**, *127*, 252-263.

6. Couture, G.; Alaaeddine, A.; Boschet, F.; Ameduri, B. *Prog. Polym. Sci*. **2011**, ASAP.

7. Varcoe, J. R.; Slade, R. C. T.; Yee, E. L. H.; Poynton, S. D.; Driscoll, D. J.; Apperley, D. C. *Chem. Mater*. **2007**, *19*, 2686-2693.

8. Hibbs, M. R. Hickner, M. A.; Alam, T. M.; McIntyre, S. K.; Fujimoto, C. H.; Cornelius, C. J. *Chem. Mater*. **2008**, *20*, 2566-2573.

9. Wang, G.; Wenig, Y.; Chu, D.; Chen, R.; Xie, D. J. *J. Membr. Sci*. **2009**, *332*, 63-68.

10. Zhou, J.; Unlu, M.; Vega, J. A.; Kohl, P. A. *J. Power Sources* **2009**, *190*, 285-292.

11. Wang, J.; Zhao, Z.; Gong, F.; Li, S.; Zhang, S. *Macromolecules* **2009**, *42*, 8711-8717.

12. Yan, J.; Hickner, M. A. *Macromolecules* **2010**, *43*, 2349-2356.

13. Wang, J.; Li, S.; Zhang, S. *Macromolecules* **2010**, *43*, 3890-3896.

14. Hibbs, M. R.; Fujimoto, C. H.; Cornelius, C. J. *Macromolecules* **2009**, *42*, 8316-8321.

15. Clark, T. J.; Robertson, N. J.; Kostalik IV, H. A.; Lobkovsky, E. B.; Mutolo, P. F.; Abruña, H. D.; Coates, G. W. *J. Am. Chem. Soc.* **2009**, *131*, 12888-12889.

16. Robertson, N. J.; Kostalik IV, H. A.; Clark, T. J.; Mutolo, P. F.; Abruña, H. D.; Coates, G. W. *J. Am. Chem. Soc.* **2010**, *132*, 3400-3404.

17. Kostalik IV, H. A.; Clark, T. J.; Robertson, N. J.; Longo, J. M.; Mutolo, P. F.; Abruña, H. D.; Coates, G. W. *Macromolecules* **2010**, *43*, 7147-7150.

18. Gu, S.; Cai, R.; Luo, T.; Chen, Z.; Sun, M.; Liu, Y.; He, G.; Yan, Y. *Angew. Chem. Int. Ed.* **2009**, *48*, 6499-6502.

19. Gu, S.; Cai, R.; Luo, T.; Jensen, K.; Contreras, C.; Yan, Y. *ChemSusChem* **2010**, *3*, 555-558.

20. Wang, J.; Li, S.; Zhang, S. *Macromolecules* **2010**, *43*, 3890-3896.

21. Guo, M.; Fang, J.; Xu, H.; Li, W.; Lu, X.; Lan, C.; Li, K.; *J. Membr. Sci.* **2010**, *362*, 97-104.

22. Lin, B.; Qiu, L.; Yan, F. *Chem. Mater.* **2010**, *22*, 6718-6725.

23. Kong, X.; Wadhwa, K.; Verkade, J. G.; Schmidt-Rohr, K. *Macromolecules* **2009**, *42*, 1659-1664.

24. Tanaka, M.; Fukasawa, K.; Nishino, E.; Yamaguchi, S.; Yamada, K.; Tanaka, H.; Bae, B.; Miyatake, K.; Watanabe, M. *J. Am. Chem. Soc.* **2011**, ASAP.

25. Baumann, E. *J. Chem. Eng. Data* **1960**, *5*, 376-382.

26. Hatch, M. J.; Lloyd, W.D. *J. Appl. Polym. Sci.* **1964**, *8*, 1659-1666.

27. Effenberger, F; Strathmann, H; Bauer, B. *Desalination* **1990**, *79*, 125-144.

28. Bauer, B.; Gerner, F. J.; Strathmann, H. *Desalination* **1988**, *68*, 279-292.

29. Sata, T.; Tsujimoto, M.; Yamaguchi, T.; Matsusaki, K. *J. Membr. Sci.* **1996**, *112*, 161-170.

30. Zagorodni, A. A.; Kotova, D. L.; Selemenev, V. F. *React. Funct. Polym.* **2002**, 53, 157-171.

31. Einsla, B. R.; Chempath, S.; Pratt, L. R.; Boncella, J. M.; Rau, J.; Macomber, C.; Pivovar, B. S. *Electrochem. Soc. Trans.* **2007**, *11*, 1173-1180.

32. Macomber C. S.; Boncella, J. M.; Janicke, M.; Pivovar, B. S.; Rau, J. A. *J. Therm. Anal. Calorim.* **2008**, *93,* 225-229.

33. Chempath, S.; Einsla, B. R.; Pratt, L. R.; Macomber, C.; Boncella, J. M.; Rau, J. A.; Pivovar, B. S. *J. Phys. Chem. C* **2008**, *112*, 3179-3182.

34. Chempath, S.; Boncella, J. M.; Pratt, L. R.; Henson, N.; Pivovar, B. S. *J. Phys. Chem. C* **2010**, *114*, 11977-11983.

35. A fluoropolymer lined vessel was used instead of glass in order to eliminate etching concerns.

36. Since the solvation of hydroxide/methoxide by water plays a critical role in mitigating BTMA decomposition, when applying the solution based experiment to other systems, it is important to note the presence of D2O that originates from the sodium deuteroxide solution (40 wt% in D2O).

37. Caution: It is crucial that the *hydroxide* form of BTMA (40 wt% H2O) be used for the test under dry conditions. Experiments using the bromide form (or other anions) of BTMA resulted in significantly slower degradation rates. Furthermore, when applying this procedure to other systems, great care should be taken to ensure that a given model compound is in the *hydroxide or methoxide* form. Failure to completely exchange the anion for hydroxide/methoxide will produce erroneous stability values.

38. Since the solvation of hydroxide/methoxide by water plays a critical role in mitigating BTMA decomposition, when applying the dry experiment to other systems, it is important to note the presence of H2O that originates from the BTMA hydroxide solution (40 wt% in H2O) and sodium hydroxide solution (40 wt% in H2O).

39. Kantor, S. W.; Hauser, C. R. *J. Am. Chem. Soc.* **1951**, *73*, 4122-4131.

40. The dry experiment was principally designed to serve as an accelerated test for alkaline stability in the absence of solvent. While it is difficult to predict if these conditions relate directly to fuel cell operating conditions, we expect that the application of this test should provide fundamental insights and aid in the discovery of AAEMs with increased base stability.

41 . Kneifel, K.; Hattenbach, K. *Desalination* **1980**, *34*, 77-95.

42. Hillmyer, M. A.; Laredo, W. R.; Grubbs, R. H. *Macromolecules* **1995**, *28*, 6311-6316.

43. Lee, C. H; Park, H. B.; Lee, Y. M.; Lee, R. D. *Ind. Eng. Chem. Res.,* **2005,** *44*, 7617-7626.

44. Cai, G.; Fu, Y.; Wan, Z.; Shi, Z. *J. Am. Chem. Soc.,* **2007**, *129*, 7666-7673.

45. Hanada, S.; Tsutsumi, E.; Motoyama, Y.; Nagashima, H. *J. Am. Chem. Soc.,* **2009**, *131*, 15032-15040.

46. Tsai, C.; Sung, R.; Zhuang, B.; Sung, K. *Tetrahedron* **2010**, *66*, 6869-6872.

47. Watson, K. J.; Nguyen, S. T.; Mirkin, C. T. *J. Organomet. Chem.,* **2000,** *606*, 79-83.